Aus der

Universitäts-Hautklinik Tübingen

Sektion Dermatologische Onkologie

Establishment of an in vitro model for melanoma cell dormancy through short-term chemotherapy

Inaugural-Dissertation
zur Erlangung des Doktorgrades
der Medizin

der Medizinischen Fakultät
der Eberhard Karls Universität
zu Tübingen

vorgelegt von

Böhlert, Emanuel

2025

Dekan:	Professor Dr. B. Pichler
1. Berichterstatter:	Professorin Dr. B. Schittek
2. Berichterstatter:	Professor Dr. M. Schindler

Tag der Disputation: 15.06.2020

Für meine Tochter Anouk,

die mich in schwierigen Zeiten auf andere Gedanken bringt.

Table of Contents

Table of Abbreviations v

1 Introduction 1

1.1 Malignant melanoma 1

1.1.1 General information 1

1.1.2 Tumor cell dissemination and metastasis 2

1.2 Tumor dormancy – theoretical models and their reality in melanoma 4

1.2.1 Clinical dormancy 4

1.2.2 Metastatic dormancy 5

1.2.3 Cellular dormancy 7

1.2.4 In vitro models for cellular dormancy 10

1.3 Aim of the study 13

2 Materials and Methods 15

2.1 Materials 15

2.1.1 Devices 15

2.1.2 Consumables 15

2.1.3 Chemicals 16

2.1.4 Kits 17

2.1.5 Buffer, solutions and media 17

2.1.6 Growth factors, proteins and cytotoxic agents 19

2.1.7 Antibodies for Immunofluorescence 19

2.1.8 Cell lines and primary cells 19

2.1.9 Software 20

2.2 Methods 21

2.2.1 Cell culture 21

2.2.2 Scheme for short-term chemotherapy 22

2.2.3 Conditioned media 23

2.2.4 Generation of protein coated plates 23

2.2.5 Primary fibroblast derived extracellular matrix 24

2.2.6 Proliferation Analysis 27

2.2.7 Cell cycle analysis 30

2.2.8 Immunofluorescence 31
2.2.9 Senescence-associated β-galactosidase assay 32
2.2.10 Statistics 34
3 Results 35
3.1 Induction of cell cycle arrest in melanoma cells 35
3.2 Characterization of cell cycle-arrested cells 42
3.2.1 Morphology 42
3.2.2 Cell cycle analysis 44
3.2.3 Immunofluorescence 47
3.2.4 Senescence-associated β-galactosidase staining 50
3.3 Stimulation of cell cycle-arrested cells 52
3.3.1 Seeding on proteins of the extracellular matrix 52
3.3.2 Application of pro-proliferative humoral stimuli 55
4 Discussion 60
4.1 Clinical relevance and usefulness of the established dormancy model 60
4.2 Cellular dormancy versus or together with senescence? 63
4.3 Attempts for waking up dormant cells 71
4.4 Conclusions and Outlook 73
5 Abstract 76
6 Zusammenfassung 77
7 Bibliography 79
8 Erklärung zum Eigenanteil 90
9 Danksagung 91

Table of Abbreviations

°C	degree Celsius
AJCC	American Joint Committee on Cancer
ATCC	American Type Culture Collection
bFGF	basic fibroblast growth factor
BC	breast cancer
BM	bone marrow
CC	colon carcinoma
CD	cluster of differentiation
CDDP	cis-Diammindichloridoplatin; Cisplatin
CDK	cyclin-dependent kinase
d	day
ddH_2O	double-distilled water
DFS	disease-free survival
DMEM	Dulbecco's modified Eagle's medium
DNA	deoxyribonucleic acid
DPBS	Dulbecco's phosphate-buffered saline
DTC	disseminated tumor cell
ECM	extracellular matrix
EGF	epidermal growth factor
FCS	fetal calf serum
FF	primary fibroblasts
FF-ECM	primary fibroblast-derived Extracellular matrix

FGF-2	basic fibroblast growth factor
h	hour
IFN-γ	interferon gamma
IGF-1	insulin-like growth factor 1
mm	millimeter
MM	malignant melanoma
MRI	magnetic resonance imaging
P53	tumor protein 53
PDGF	platelet-derived growth factor
PI	propidium iodide
PC	prostate cancer
RFS	recurrence-free survival
RGP	radial growth phase
RPMI	Roswell Park Memorial Institute
SASP	senescence-associated secretory phenotype
SA-β-gal	senescence-associated β-galactosidase
TGF-β	transforming growth factor beta
TNF-α	tumor necrosis factor alpha
UV	ultraviolet
VGP	vertical growth phase
µM	micromolar

1 Introduction

1.1 Malignant melanoma

1.1.1 General information

Malignant melanoma (MM) is a tumor that primarily arises from tissues containing melanocytes, such as the skin (91.2% of all melanomas), the eye (5.2%), mucosa (1.3%) and from unknown primary sites (2.2%) (American Cancer Society et al., 1998).

Melanoma has an incidence rate of currently around <10-25 new reported cases per 100.000 inhabitants per year in Europe and is thus the seventh most common cancer among all malignancies (non-melanoma skin cancers excluded, age standardized rate). Prognosis in patients with distant metastasis of untreated melanoma is very poor with 6-9 months of median survival which is reflected in a proportion of 90% of all skin cancer related deaths (Garbe et al., 2016, ECIS - European Cancer Information System, from https://ecis.jrc.ec.europa.eu, accessed on 29/7/2019), whilst melanoma accounts only for 5% of all skin cancer cases. The rise of incidence, estimated to 4-6% annually in light-skinned populations, which makes it one of the fastest rising among all malignancies. The incidence of malignant melanoma itself and its rise further vary depending on sex, age, geographical location and ethnicity (Matthews et al., 2017).

The most important exogenous factor leading to the development of MM is ultraviolet (UV) irradiation attributed to the development of up to 85.9% of all melanomas (Parkin et al., 2011). UV light leads to malignant transformation of melanocytes by causing driver mutations and implementing other molecular changes that accumulate over time and enable for melanoma cell proliferation and progression terminating with the event of metastasis (Arlo J. Miller, 2006).

The prognosis for patients with distant metastases is still sobering, given that even when administered to optimal systemic therapy, patients entering stage IV in 2014 faced a 3-year overall survival rate of only 37%. However, the rate more than doubled from 18% in 2011, when the first targeted therapy and

immunotherapy for advanced melanoma were approved (Forschner et al., 2017). Detection of melanoma at early stages is therefore imperative and progress in the identification of melanomas has been made through improved strategies and procedures (Frangos et al., 2012; Apalla et al., 2017).

Still, early detection and excision of localized melanoma does not ultimately mean a definite cure from the disease as the following discourse into early dissemination and tumor dormancy in melanoma outlines (see section 1.1.2).

1.1.2 Tumor cell dissemination and metastasis

The Clark model for melanoma progression was presented in 1984 and postulates a stepwise evolution of neoplasms - in general and of the melanocytic system specifically - through different growth phases: from benign to dysplastic nevus, radial growth phase, vertical growth phase and metastatic melanoma. According to the model, some melanoma cells gain genetical properties during the vertical growth phase that culminates with and enables them for detaching from the primary tumor (dissemination) and migration through the lymphatic system and for forming metastases at different organ sites (Clark et al., 1984).

Although the Clark model of a linear progression is still commonly used to explain the nature of initiation and progression in some forms of malignant melanoma, more recent findings suggest that tumor cell dissemination happens already at earlier time points.

Eyles and colleagues showed in RET.AAD mice (transgenic mouse model for spontaneous melanoma) that metastasis develops relatively late and that only 61.1% of mutations in the primary tumor could be found in cells from metastatic sites supporting the idea of early dissemination and late recurrence from dormant disseminated tumor cells (DTCs) (Eyles et al., 2010). Although frequently cited as proving dormancy mechanisms in MM in general (Röcken, 2010; Senft and Ronai, 2016), it has to be stated, that the RET.AAD model rather recapitulates the onset of spontaneous melanoma of the eye and that there are major differences in kinetics and preferential sites of metastasis development between primary uveal and cutaneous melanoma. In uveal melanoma, a disease-free survival (DFS) of more than 10 years occurs in 40-50% of the patients, which is

tenfold higher than for cutaneous melanoma. The location of the primary tumor (eye vs. skin), the path of disseminating cells (rather hematogenous vs. rather lymphatic) and the favorable tissue for metastasis (liver vs. diverse sites) with their different mechanical, structural and immunological properties might lead to these differences in kinetics, being supportive or detrimental to circulating and disseminated tumor cells. Furthermore, it remains to be elucidated which role the difference in driver mutations (GNAQ vs. B-RAF, N-RAS) attributes to latency in or the outburst of metastasis (Ossowski & Aguirre-Ghiso, 2010). Still, both types of melanoma arise from melanocytes, which theoretically renders investigations on and comparison of divergent molecular mechanisms regarding proliferation and cell cycle arrest in uveal and cutaneous melanoma derived cell lines promising for further understanding of dormancy and recurrence kinetics.

In patients with cutaneous melanoma, tumor cells primarily disseminate through the lymphatic draining system and the further the tumor progresses the more probable it becomes that lymph nodes draining the region of the primary tumor harbor solitary melanoma cells, micro- or even macro-metastases. From the lymph nodes and vessels, melanoma cells can further spread to distinct organ sites and eventually form distant metastases that fundamentally worsen the patient's prognosis. The sentinel lymph node biopsy has therefore become one of the gold standards as a staging procedure for patients with a primary melanoma thicker than 0.75 mm or even thinner when aggravating factors are present such as ulceration or a high mitotic rate in the localized tumor (Garbe et al., 2016; Ferrara et al., 2018).

In a more recent study, Werner-Klein et al. confirmed early dissemination in cutaneous melanoma with spread to the lymphatic system already from very thin primary tumors (median of ~0.5 mm). Interestingly, in these patients, gene alterations in B-RAF, MET and CDKN2A, necessary for metastasis development, are acquired not only in the primary tumor - which would fit to the Clark model of linear progression - but additionally in the lymph nodes (Werner-Klein et al., 2018). These findings strengthen the idea of the existence of parallel progression as previously presented and reviewed (Klein, 2009).

Dissemination at early stages of progression has also been described in breast and prostate cancer (Schardt et al., 2005; Hüsemann et al., 2008; Klein, 2009), malignancies that are strongly associated with survival of dormant DTCs in the bone marrow and late recurrence (Aguirre-Ghiso, 2007).

1.2 Tumor dormancy – theoretical models and their reality in melanoma

1.2.1 Clinical dormancy

The term clinical dormancy refers to a state with absence of any clinically detectable disease between removal of the tumor and first manifestation or recurrence of metastasis. Epidemiologically, this would be best described with the term disease-free survival (DFS). In melanoma, this could be applied to patients with stage I or II primary tumors that can exceed 4.00 mm of vertical thickness without histopathological appearance of regional or distant metastasis. Stage I and II primary tumors, which contribute to about 90% of all melanomas are connected to 75-85% disease-specific 10-year survival which means that about 15-25% melanoma patients with localized disease die within 10 years because of melanoma recurrence (Garbe et al., 2016). Patients can have a risk of very late recurrence even beyond 10 years of DFS. As reviewed by Ossowski and Aguirre-Ghiso, depending on the cohort's composition, 2.4-11% of melanoma patients experienced late recurrence after a 10-year disease-free interval (Ossowski and Aguirre-Ghiso, 2010)

One of the most striking examples supporting the existence of dormancy mechanisms in cutaneous melanoma is reported in a case study about two recipients of renal transplants from the same donor developing secondary melanoma without a sign of a primary tumor. 16 years after removal of a 2.6 mm-thick melanoma, the donor died from subarachnoid hemorrhage, declared tumor-free through regular Follow-up examinations (MacKie et al., 2003). The transplants must have contained disseminated, quiescent melanoma cells that were reactivated in the immunosuppressed environment of transplantation. Similar cases have repeatedly been described. In fact, melanoma is among the most common malignancies developing as donor-derived, either because the existence of a primary tumor was unknown or patients had a long disease-free

history and were therefore considered as being cured (Strauss and Thomas, 2010).

Melanoma patients can also experience clinical dormancy after complete resection of regional and distant metastases (stages III and IV), which is not always feasible. Nowadays, melanoma patients at these stages are commonly administered to systemic therapy, which makes it difficult to compare inherent kinetics of clinical dormancy throughout the stages after resection. However, when assigned to the placebo group in the setting of a clinical trial, only 56-61% of the patients survive the first 12 months without recurrence of the tumor (Kwak et al., 2019). Obviously, the high “obscure” tumor burden of undetected dormant or slowly growing but still established micro-metastases in these patients of higher stages increases the risks for immune evasion and acquisition of or selection for inherent resistance to adjuvant therapy thus enabling the pounce from micro-metastases to overt, incontrollable macro-metastases. Mechanisms of drug resistance in melanoma are extensively discussed elsewhere (Winder and Virós, 2018). All in all, next to aggressively proliferating melanoma metastases, dormant DTCs surely do not have a considerable impact on the patient’s prognosis at higher stages.

The two widely accepted biological models of metastatic (tumor mass) and cellular dormancy, reviewed in various publications (Aguirre-Ghiso, 2007; Sosa et al., 2014; Yeh and Ramaswamy, 2015) also in regard to melanoma (Ossowski and Aguirre-Ghiso, 2010; Senft and Ronai, 2016) can be consulted to explain the mechanisms underlying clinical dormancy. Both conditions of surviving yet non-invasively undetectable cancer cells (minimal residual disease) might co-exist and even evolve from one to the other in melanoma patients and shall be presented in the following (see section 1.2.2 and 1.2.3).

1.2.2 Metastatic dormancy

One possible explanation for recurrence of melanoma in patients initially declared tumor-free is the overcoming of metastatic dormancy through outgrowth of previously existing micro-metastases. Two conditions, angiogenic and immunogenic dormancy, may limit the transformation of small cell clusters to

detectable, overtly proliferating macro-metastases. In both cases, an equilibrium state between proliferation and cell death results in a stable size of the clusters.

Growing cancer cell clusters are intrinsically restricted in size since the efficacy of simple diffusion of molecules, needed for cell growth and proliferation, such as nutrients and oxygen, is limited to a certain distance. This limitation may be overcome upon the so-called angiogenic switch, when cancer cells manage to recruit blood vessels, essential for a sufficient supply above a particular cluster size. Until then, micro-metastases remain in angiogenic dormancy (Naumov et al., 2006). In melanoma, poor vascularization of lymph node micro-metastases in comparison to macro-metastases has been shown in humans and a low number of microvessels per area was associated with a significantly lower proliferation rate (2.4% of the melanoma cells in micro-metastases and 18% in higher vascularized macro-metastases) (Barnhill et al., 1998). This hints not only to cytotoxic but also cytostatic mechanisms in angiogenic dormancy.

As a second possible scenario, proliferation and cell death in cancer cell agglomerates might be balanced through active control by the immune system, resulting in immunogenic dormancy until cancer cells either evade this control and macro-metastasis occurs or they are ultimately removed by the immune cells. In melanoma, metastasis outgrowth control through the immune system has been shown in several mouse and *in vitro* models (Senft and Ronai, 2016). Besides clearing tumor cells through cytotoxic activity, immune cells restrain outgrowth of melanoma metastases through cytostatic mechanisms reducing the number of proliferating melanoma cells. This was shown to be accomplished by $CD8^+$ T-cells, significantly reducing Ki-67^+ melanoma cells (Eyles et al., 2010) and $CD4^+$ T-cells, driving melanoma cells into p16-mediated senescence through tumor necrosis factor alpha (TNF-α) and Interferon gamma (IFN-γ) secretion (Braumüller et al, 2013). However, as reviewed by Senft and Ronai, the role of some immune cell-derived factors in cytostasis of melanoma cells is paradoxical and cytokines might even fuel dormancy evasion depending on complex interplay between these factors or the mutational status of the tumor cells (Senft and Ronai, 2016).

Both models indicate possible therapeutic approaches, but whereas immunotherapies have become one of the pillars in melanoma therapy, introduction of (adjuvant) antiangiogenic therapies for melanoma has not yet been successful (Garbe et al., 2016; Jayson et al., 2016).

1.2.3 Cellular dormancy

After removal of the primary tumor in former breast and prostate cancer patients with no sign of metastasis, single cancer cells are frequently found in aspirates from bone marrow biopsies. These cells are often cell cycle-arrested in G0-phase, a state that is called quiescence. Apparently, these quiescent cells originate from a small fraction of DTCs that survive the process of dissemination and settle at favorable organ sites, the “dormant niches”, before they eventually re-awake and form metastases (Ghajar, 2015).

In melanoma patients and animal models, similar processes in metastatic inefficiency and survival of DTCs can be observed. In a mouse model for reproduction of hematogenous dissemination, B16F1 murine melanoma cells were injected into the Portal vein to evaluate metastasis development in the liver. 80% of the cells survived and extravasated the blood stream but more than a third of the injected cells (36%) stayed solitary on day 13 and most of these were dormant, as only 2% showed proliferation (Ki-67) and 3% apoptosis (TUNEL). Metastasis formation was far from being effective: only 2.5% of the extravasated cells proliferated into micro-metastases and only 1% of these developed into macro-metastases (Luzzi et al., 1998). These findings underline the harsh selection process that cancer cells, which already managed to successfully detach from the primary tumor and intravasated, encounter before entering a supportive environment. Furthermore, the authors prove that under certain conditions melanoma cells can survive in protective niches at extraneous sites such as the liver, staying dormant for a prolonged period of time. In another mouse model of this group, B16F10 murine melanoma cells were assessed for their ability to form metastases in the lung. Here, only 3.5% cells stayed solitary on days 12-14 and only about 3% of these showed Ki-67 positivity (thus proliferating) whereas none were apoptotic. From calculations of the location

specific development in tumor burden, the authors deduced that metastases would grow preferentially close to arteries, veins and pleural surface but switch from dormancy to proliferation would be location independent, (Cameron et al., 2000). This information put together, suggest a limited distribution of inhibitory niches for disseminated melanoma cells in the lung in comparison to the liver but the differences in metastasis initiation by tissue might also be explained by the inherent properties of the two cell lines. The B16F10 cell line is generally seen as being more metastatic than its preceding B16F1 cell line, which is due to a high selection process for the ability of metastasis formation *in vivo* (Fidler, 1975).

As mentioned above, tumor cells from cutaneous melanoma primarily disseminate trough the lymphatic system. Indeed, they can already be detected as solitary cells in sentinel nodes of patients histopathologically staged for localized disease (stages I and II) (Ulmer et al., 2005). A more recent study by the group shows that 78.0-88.6% of disseminated melanoma cells in lymph nodes are located in G0-phase, thus being dormant. The locations within the lymphatic tissue of these dormant cells in comparison to the proliferating ones were unfortunately not evaluated (Werner-Klein et al., 2018). Others found an unequal distribution of proliferating melanoma cells within the lymph node of intradermally B16F10-LacZ melanoma cells injected syngeneic C57BL/6 mice. Moreover, they identified the subcapsular sinus and the stroma of lymph nodes as preferential sites for metastasis formation and excluded melanoma cell proliferation within lymphatic vessels. Anyway, this study did not link solitary dormant cells to a specific location within the analyzed tissues (Morris et al., 2013). Therefore, the existence of possibly distinct dormant and metastatic niches in the lymphatic system for melanoma cells, as it has been found for other cancer cells in the endosteal niche of the bone and the bone marrow (Lawson et al., 2015), can only be hypothesized.

As already mentioned, another organ that is widely discussed and accepted as a niche for homing and survival of dormant DTCs is the bone marrow (BM) (Byrne et al., 2018). Molecular mechanisms of ligands present in the BM, that might induce growth arrest in cells from different tumor entities such as from breast and

prostate cancer are extensively discussed elsewhere (Ghajar, 2015; Byrne et al., 2018).

To what extent the skeletal system plays a role in dormancy mechanisms of melanoma, remains unclear. This is mainly because the bone marrow - for instance - is not regularly examined in melanoma patients with histopathological evaluation of primary tumors and sentinel lymph nodes as well as imaging techniques being the gold standards for staging (Garbe et al., 2016). A recently published study (Chernysheva et al., 2019) addressed this question by analyzing samples from the bone marrow of 47 melanoma patients. Disseminated tumor cells and the deviance in myelogram parameters of DTC positive and DTC negative patients were characterized by flow cytometry. Surprisingly, disseminated melanoma cells were identified in 57.4% of the bone marrow samples and throughout all stages - even in two of the seven patients with stage I. Put into relation with the rareness of macro-metastasis development in the bone marrow (Jain et al., 2007), these observations suggest the BM as a possible niche for dormant melanoma cells.

In breast cancer patients, adjuvant chemotherapy fails to eliminate dormant disseminated cells in the bone marrow (Braun et al., 2000). Once settled in the protective niche and cell cycle-arrested, most cancer cells seem to be refractory to different types of treatments in general and in different niches. The molecular mechanisms behind onset and reversal of cellular dormancy are needed to be understood to target tumor cells surviving in that quiescent state, to maintain their dormant state or eradicate them and thus prolong recurrence free survival (Ghajar, 2015).

As general mechanisms behind cellular dormancy induction and reversal can only be elucidated on the molecular level, an overview of existing *in vitro* models for cellular dormancy that influenced (or were further elaborated in) this study, shall be presented hereinafter (see section 1.2.4).

1.2.4 In vitro models for cellular dormancy

1.2.4.1 Carcinomas and myelomas

Based on findings of quiescent DTCs from different cancers in distinct compartments of the bone, the creation of supportive (pro-proliferative) and inhibitory (dormancy inducing) niches was introduced in a breast cancer (BC) dormancy model using co-cultures of cells derived from the bone marrow with BC cell lines (Marlow et al., 2013).

The above-mentioned study (see section 1.2.3) investigating on the endosteal niche in myeloma depictures both onset and reversal of dormancy in two distinct niches of either endosteum or bone marrow. Former quiescent cells can be stimulated to re-proliferate upon cultivation ex vivo. Re-inoculated in naive mice, a subset of these re-proliferating myeloma cells becomes dormant again when being in direct contact to the endosteal bone surface. The authors connect induction of dormancy to osteoblasts and reactivation to osteoclast activity (Lawson et al., 2015)

More basic is the approach of recapitulating dormancy induction by the microenvironment through seeding breast cancer cell lines on proteins from the extracellular matrix (ECM). Mammary-carcinoma-derived cell lines, staying cell cycle-arrested *in vivo* (D2.0R) but starting proliferation when grown on plastic, keep their dormant phenotype when transferred on basal membrane extract. Here, cellular dormancy is linked to an elevated nuclear expression of p16 and p27. In this model, the authors attribute the switch from dormancy to proliferation to fibronectin via integrin β1 signaling and stress fiber formation (Barkan et al., 2008). On the other hand, fibronectin combined with the upregulation of integrin α5β1 through stimulation with FGF-2 is reported to rather induce dormancy in an otherwise proliferating MCF-7 breast cancer cell line and factors secreted by senescent bone marrow cells, namely IL-6, IL-8 and TGF-β1 reverse this effect (Tivari et al., 2018).

These - even though partially contradictory - findings further introduce the ECM and soluble (growth) factors as decisive parts for the dormant niche of tumor cells.

In addition to its composition, mechanical properties of the ECM in the microenvironment of DTCs might constitute the critical cue in the induction of a reversible cell cycle arrest. Breast, colon and pancreatic cancer cell lines embedded into a stiff Col-Tgel (a 3D collagen-based hydrogel system) had a significantly prolonged doubling time which was further enhanced by cross-linking of collagen and thereby stiffening of the matrix. The authors further propose dormant cells to exit the cell cycle arrest through modulation of the matrix properties (Fang et al., 2016).

As mentioned above, cell cycle-arrested DTCs are more resistant to therapy, but treatments and other cellular stress-inducing factors might as well initially trigger the onset of dormancy. *In vitro* models, recapitulating therapy-induced dormancy and recurrence, exist in simple and sophisticated ways for prostate cancer (PC), BC and colon carcinoma (CC) (Li et al., 2014; Wu et al., 2017; Saleh et al., 2019). All three studies report that cancer cells originating from different entities were subjected to short-term chemotherapy of 24-96 h and were homogenously cell cycle-arrested under specific conditions until a subpopulation of cells took up proliferation and formed colonies with a latency of up to 18 days, depending on the cell line and condition.

1.2.4.2 Cutaneous malignant melanoma

In vitro dormancy models for melanoma are rare and those existing are limited in various aspects. Mostly, the time frame for observation of the cell cycle-arrested cells is very short, not reflecting kinetics in tumor dormancy and recurrence. Others do not evaluate kinetics and mechanisms of re-proliferation or a direct lineage of re-proliferating cells to formerly cell cycle-arrested ones is not traceable.

Henriet et al. established a method by which proliferation of M24met melanoma cells was inhibited by contact with fibrillary collagen I which forms a large part of the ECM and is known to influence cell survival and proliferation through integrin signaling, connected to downstream cellular pathways (Henriet et al., 2000). Melanoma cells were incubated overnight on different proteins of the ECM, such as fibronectin and its fragments vitronectin and laminin as well as non-neutralized

and neutralized (fibrillary) collagen I. When analyzed for cell cycle distribution and other proliferation associated characteristics, M24met cells showed a significant cell cycle arrest when initially seeded on fibrillary collagen I.

In previous experiments, we were interested in reproducing this model but with the goal to induce a growth arrest in melanoma cells over a longer period of time to better depicture the temporal dimension of tumor dormancy. Unfortunately, we did not find a long-term difference in proliferation of any of the tested melanoma cell lines when incubated on collagen I (unpublished data).

The composition and organization of fibers such as collagen I modulates the ECM stiffness, which is crucial in tumor dormancy induction, as mentioned above for other cancers and such a role might as well account for melanoma. Indeed, remodeling of the collagen matrix through processes of aging promotes melanoma metastasis (Kaur et al., 2019). The authors state that the effects on tumor growth are not at all attributable to proliferation but uniquely to invasiveness of melanoma cells. Increased invasiveness is connected to and mediated through a phenotype switch in tumor cells, the so called Epithelial-Mesenchymal Transition (EMT), that goes along with specifically altered gene expression patterns. High plasticity in or only partial display of EMT characteristics in turn is increasingly appreciated as one mean of dormant DTCs to cope with changing conditions in different microenvironments (Weidenfeld and Barkan, 2018; Yang et al., 2018). These findings suggest a role of mechanical properties and alterations of the dermal ECM in induction and reversal of melanoma cell dormancy.

Other *in vitro* melanoma models focus on mechanisms behind the establishment of senescence (a cell cycle arrest in G1 that is supposed to be irreversible) by therapies or soluble factors and the influence of secreted factors associated to the phenotype on cells in vicinity (Braumüller et al, 2013; Haferkamp et al., 2013; Sun et al., 2018). In the studies presenting these methods, observation and measurement of proliferation of the cell cycle-arrested cells generally stops after a week or two passages with an end-point analysis for senescence-associated β-galactosidase (SA-β-gal) activity or other markers for senescence. At these

time points, cell cycle arrest seems relatively homogenous and 70-99% of the cells show SA-ß-gal positivity depending on experiments condition and cell line. Sun et al. mention that under specific conditions, chemotherapy treated cells escape cell cycle arrest and form colonies six days after removal of the treatment. It is plausible that also in the other models some cells occasionally escape the cell cycle arrest and resume proliferation. Still, kinetics, characteristics and intrinsic or extrinsic factors related to these escapes remain to be elucidated but understanding will be critical for preventing disease recurrence in melanoma.

A recent study introduces an *in vitro* model for melanoma where different cell lines are driven into a cell cycle arrest similar to senescence trough maintenance at a low pH (Böhme and Bosserhoff, 2019). The authors couple their findings to the prevalence of acidic milieus in primary melanomas and show that prior to re-adjustment to a neutral pH, formerly cell cycle-arrested cells re-proliferated and divided even more readily than parental cells. Unfortunately, a direct connection between senescent cells and the re-proliferating cells is not elaborated. A role of acidosis in the disseminated tumor cell niche in melanoma has previously been discussed (Peppicelli et al., 2017), though not fully elucidated, thus limiting this model in explaining cellular dormancy.

1.3 Aim of the study

The preceding assembled information about rising incidence in malignant melanoma (section 1.1.1), the existence of dormant DTCs in melanoma (section 1.2.3), their involvement in cancer recurrence (section 1.2.3) and the lack of an elaborated *in vitro* dormancy model in melanoma (section 1.2.4.2) indicates an urgent need for the development of the latter. Therefore, the aim of this study was to establish a model with a stable (homogenous) but reversible, long-term induction of cell cycle arrest in different melanoma cell lines, building upon and developing further an existing dormancy model for breast and prostate cancer based on short-term chemotherapy (Li et al., 2014).

In melanoma, chemotherapy has been shown to be effective in inhibiting growth of metastases but could not decrease the number of dormant cells in a melanoma mouse model using labeled B16F1 melanoma cells and magnetic resonance

imaging (MRI) tracking (Townson et al., 2009). It is known, that in proliferating cells of melanoma cell culture, Cisplatin (CDDP) treatment leads to apoptosis and cell cycle arrest, with proportions of fates depending on different experimental settings such as drug concentration, treatment duration or cell density (Makino et al., 2018; Sun et al., 2018). In the management of advanced melanoma, chemotherapy was the only treatment option for a long time and is nowadays administered upon failure of first-line therapies (Luke et al., 2017) (see also section 4.1). We hypothesized for the *in vitro* setting that short-term chemotherapy with Cisplatin induces a stable and homogenous but reversible cell cycle arrest in a subgroup of cells in different melanoma cell lines.

The establishment of an *in vitro* model for cellular dormancy through short-term chemotherapy in cutaneous melanoma included the optimization of different experimental conditions such as the initial cell number, the treatment dose and the availability of pro-proliferative/anti-apoptotic factors in the cell culture medium. To avoid the establishment of drug resistance, chemotherapy was uniquely applied on parental cells once, for a relatively short time. After assessing the kinetics in cell death, growth arrest and proliferation under the different conditions through simple cell and colony counting over time, the best fitting set-up for each cell line, leading to a stable and homogenous cell cycle arrest, was chosen for further analysis. As a second step, cells surviving under this optimized treatment conditions were analyzed for growth arrest related characteristics such as the cell cycle status by cell cycle analysis and the expression of the Proliferating Cell Nuclear Antigen (PCNA) by immunofluorescence as well as the possible fate of the cell cycle-arrested cells by SA-β-gal staining. The third and last step aimed for finding cues that reliably reverse the therapy induced cell cycle arrest and thereby might - among others - lead to late recurrence of melanoma in patients. This was carried out by mimicking a change towards a supportive niche by either seeding the surviving, cell cycle-arrested cells on different extracellular matrix proteins or application of pro-proliferative humoral factors on the growth-arrested cells.

2 Materials and Methods

2.1 Materials

2.1.1 Devices

Table 2.1.1 Devices

Device	Company and type
Camera	Shenzhen Yangwang Technology Co., Ltd RS-500C HD camera
Cell counting chamber	Neubauer (Assistant)
Centrifuges	Eppendorf 5810 R; Hettich Mikro 200
CO_2 incubator	New Brunswick Galaxy 170S
Flow cytometer	BD LSRII (BD Bioscience)
Heat block	Techne Dri-Block DB20
Laminar flow cabinet	Thermo Scientific MSC-Advantage 1.8
Microplate reader	Berthold technologies TriStar LB 941
Microscope	Zeiss Axiovert 35
pH-meter	XS Instruments pH50 + DHS
Pipetus	Hirschmann
Refrigerator	OK. DFR100
Roller mixer	Cat RM 5.40 Zipperer
Vacuum pump	Schuett biotech EcoVac Vakuumpumpe
Vortexer	neo lab Vortex mixer 7.2020
Waterbath	Thermolab GFL 1083

2.1.2 Consumables

Table 2.1.2 Consumables

Consumable	Company
Cell scraper	Corning
Coverslips 12 mm	R. Langenbrinck GmbH
Cryopreservation vials	Greiner Bio-One
Feather disposable scalpel	Feather
Parafilm M	Sigma-Aldrich
T25, T75 cell culture flasks	Sarstedt
0.2 µm sterile filter Minisart	Sartorius Stedim
1.5 ml and 2 ml reaction tubes	Eppendorf
15 ml and 50 ml reaction tubes	Greiner Bio-One
12 and 24 well plates	Corning Costar
6 and 96 well plates	Sarstedt

2.1.3 Chemicals

Table 2.1.3 Chemicals

Chemical	Company
Ammonium solution (NH_4OH) (25%)	Merck
Bovine serum albumin (BSA)	Roth
Crystal Violet stock solution (2.3%)	Sigma-Aldrich
DABCO	Merck
Dimethylformamide ≥ 99%	Sigma
Dithiothreitol	Applichem Panreac
DMEM medium	Sigma-Aldrich
DMSO	Sigma-Aldrich
Donkey serum	Dianova
Ethanol	VWR Chemicals
Ethanolamine	Sigma-Aldrich
Fetal calf serum (FCS)	Biochrom/Thermo Fisher
Fungizone (Amphotericin B)	Gibco Life Technologies
Gelatin	Applichem Panreac
Glutaraldehyde (50%)	Roth
Glycerin	Sigma-Aldrich
Guanidin	Roth
Magnesium chloride	Merck
Methanol	VWR Chemicals
Mowiol	Calbiochem
N,N-Dimethylformamide, Uvasol	Merck
Para-Formaldehyde	Sigma-Aldrich
Penicillin-Streptomycin	Gibco
Potassium ferricyanide ($K_3[Fe(CN)_6]$)	Merck
Potassium ferrocyanide ($K_4[Fe(CN)_6]$)	Merck
Propidium iodide	Sigma-Aldrich
RNAse A	Thermo Scientific
RPMI Medium	Gibco
Sodium hydroxide (NaOH)	Merck
Triton X-100	Sigma-Aldrich
Trypsin/EDTA solution (0.05%/0.02%)	Gibco
Vitamin C	Fluka BioChemika
X-Gal	Appligene Oncor SA
Yo-Pro-1	Thermo Scientific

2.1.4 Kits

Table 2.1.4 Kits

Kit	Company
Pierce BCA Protein Assay Kit	Thermo Scientific

2.1.5 Buffer, solutions and media

Table 2.1.5-1 Buffer for cell cycle analysis

Substance	End concentration
Propidium iodide	50 µg/ml
RNAse A	100 µg/ml
DPBS	100-1000 µl per sample

Table 2.1.5-2 Gelatin solution for primary fibroblast derived ECM deposition

Substance	End concentration
Gelatin	0.2%
DPBS	0.5 ml (24 well) or 2 ml (6 well plate)

Table 2.1.5-3 Extraction buffer for primary fibroblast derived ECM preparation

Substance	End concentration
Triton X-100	0.5% (v/v)
NH_4OH	20 mM
DPBS	0.5 ml (24 well) or 2 ml (6 well plate)

Table 2.1.5-4 Solubilization buffer for primary fibroblast derived ECM preparation

Substance	End concentration
Guanidin	5 M
Dithiothreitol	10 mM
ddH_2O	0.5 ml (24 well) or 2 ml (6 well plate)

Table 2.1.5-5 Blocking buffer for immunofluorescence

Substance	End concentration
Donkey serum	5%
Triton X-100	0.3%
DPBS	250 µl

Table 2.1.5-6 Antibody dilution buffer for immunofluorescence

Substance	End concentration
Bovine serum albumin	1%
Triton X-100	0.3%
DBPS	250 µl

Table 2.1.5-7 X-gal solution

Substance	End concentration
X-gal (5-bromo-4-chloro-3-indolyl-beta-D-galactopyranoside) dissolved in dimethylformamide	0.1% (v/v)
$MgCl_2$	1 mM
$K_3[Fe(CN)_6]$	5 mM
$K_4[Fe(CN)_6]$	5 mM
DPBS	300 µl

Table 2.1.5-8 Melanoma cell growth medium

Substance	End concentration
RPMI 1640 medium	500 ml
Fetal bovine serum	10%
Penicillin-Streptomycin	100 U/ml

Table 2.1.5-9 Primary fibroblast growth medium

Substance	End concentration
DMEM medium	500 ml
Fetal calf serum	10%
Penicillin-Streptomycin	100 U/ml

Table 2.1.5-10 Freezing medium

Substance	End concentration
Fetal calf serum	90%
DMSO	10%

2.1.6 Growth factors, proteins and cytotoxic agents

Table 2.1.6 Growth factors, proteins and cytotoxic agents

Substance	Type/Target	Company
bFGF	Growth factor	R&D Systems, Biotechne
Cisplatin, 1st and 2nd stock	Cytostatic agent	Hexal
Collagen	ECM protein	Corning
EGF	Growth factor	Sigma
Fibronectin	ECM protein	R&D systems
IGF-1	Growth factor	Peprotech
Insulin	Hormone	Sigma
PDGF	Growth factor	Peprotech
Ribociclib (LEE011)	CDK4/6 inhibitor	Hycultec
TGF-β	Growth factor	Peprotech

2.1.7 Antibodies for Immunofluorescence

Table 2.1.7 Antibodies for Immunofluorescence

Antigen	Dilution	Species	Type	Company	Product/ Catalogue	Clone/ lot
PCNA	1:2500	Mouse	mono-clonal	Sigma-Aldrich	P 8825	Clone: PC10
Anti-mouse IgG Cy3 conjuga-ted	1:250	Donkey	poly-clonal	Dianova	715-166-150	lot# 99782

2.1.8 Cell lines and primary cells

Table 2.1.8 Cell lines and primary cells

Cell line	Entity of origin	Stage	Mutational status	Origin
A375	Melanoma	metastatic	V600E B-RAF mutated	[1]
SBCL2	Melanoma	RGP	Q61K N-RAS mutated	[2]
WM115	Melanoma	VGP	V600D B-RAF mutated	[1]
[1]purchased from the ATCC				

[2]kindly gifted by M. Herlyn from Wistar Institute (Philadelphia, USA)
Primary Fibroblasts (FF) were isolated from human foreskins after circumcision and generously provided by Birgit Sauer, biotechnical assistant in the group of Prof. Dr. Birgit Schittek, file reference number for ethics committee approval: 093/2019B02. Isolation followed previously described methods (Lasithiotakis et al., 2008; Sinnberg et al., 2009).

2.1.9 Software

Table 2.1.9 Software

Software	Company
Acrobat Reader	Adobe
BD FACS Diva	BD Biosciences
Excel 2016	Microsoft
Gimp 2.10.6	The GIMP Development Team
Graphpad Prism 6.0 and 8	Graphpad
ImageJ	Rasband, W.S., ImageJ, U. S. National Institutes of Health
Mendeley Desktop	Elsevier
Paint	Microsoft
PowerPoint 2016	Microsoft
S-Eye 1.2.6.154	Shenzhen Yangwang Technology Co., Ltd
Word 2016	Microsoft

2.2 Methods

2.2.1 Cell culture

Melanoma cell lines were maintained in RPMI 1640 medium supplemented with 10% FCS and 1% Penicillin/Streptomycin (see table 2.1.5-8)

Primary fibroblasts were isolated and kindly provided by biotechnical assistant Birgit Sauer (laboratory of Prof. Dr. Birgit Schittek) as previously described (Lasithiotakis et al., 2008; Sinnberg et al., 2009) and maintained in DMEM medium containing 10% FCS and 1% Penicillin/Streptomycin (see table 2.1.5-9). For all experiments, primary fibroblasts with passage number <6 were used.

In all experiments, where reduced-serum RPMI medium was used, melanoma cells were seeded, maintained and treated in RPMI medium supplemented with 2% FCS and 1% Penicillin/Streptomycin, if not indicated otherwise.

For cell culture maintenance, all media were changed every 2 days. All media, DPBS and Trypsin/EDTA solution (0.05%/0.02%) used on viable cells were prewarmed to 37°C in a water bath. Cells were passaged when they reached 70-80% confluence. Therefore, cells were washed with DPBS to remove cellular debris as well as remaining cell growth medium. The cells were harvested through incubation with Trypsin/EDTA solution (0.05%/0.02%) for 2-3 minutes. After stopping the reaction with cell growth medium, the cell suspension was centrifuged at 290 x g for 4 minutes. After removing the supernatant, the precipitate with the cells was re-suspended in cell growth medium and 1/10 – 1/6 of the single cell suspension reseeded.

For cryopreservation, the steps for passage were followed but the precipitate with ca $2*10^6$ viable cells was resuspended in 1 ml freezing medium consisting of 90% FCS and 10% DMSO (see table 2.1.5-10), transferred into a cryopreservation tube and directly frozen at -20°C. After 24 h, the cryopreservation vials were transferred to -80°C. Frozen cells were stored up to 12 months and could be re-introduced into culture by adding 1 ml prewarmed cell growth medium to the frozen cells and resuspending the obtained 2 ml cell suspension in 8 ml cell growth medium. After a centrifugation step (290 x g, 4 minutes) the precipitate with the cells was resuspended in 10 – 15 ml cell growth medium and incubated

overnight in the CO_2 incubator. The next day, the cell growth medium was changed to remove remaining DMSO.

2.2.2 Scheme for short-term chemotherapy

If not indicated otherwise, short-term chemotherapy treated cells underwent therapy under the following scheme (see Figure 2.2.2).

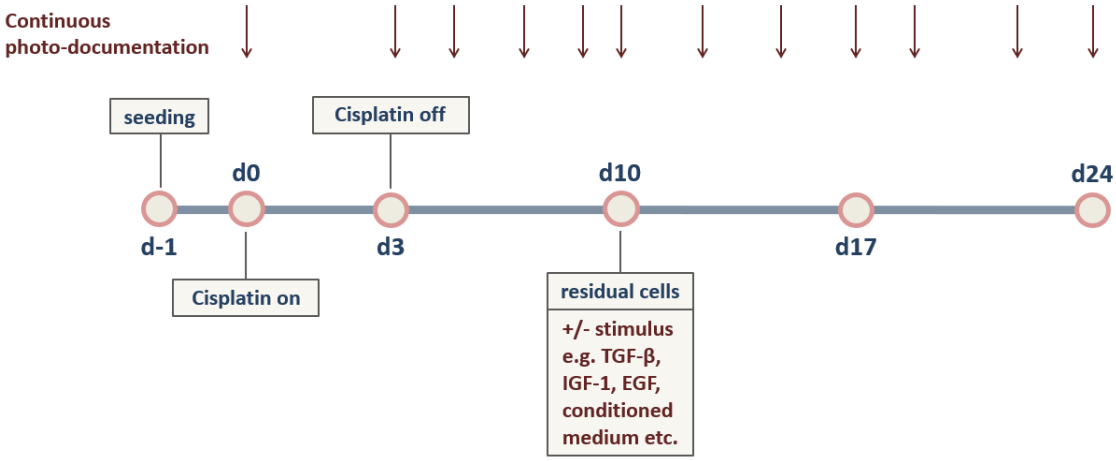

Figure 2.2.2 ***Scheme for short-term chemotherapy.*** *Melanoma cells are seeded at a specific density in reduced-serum RPMI medium. The next day the medium is changed with or without Cisplatin (as a control). After 72 h the therapy is taken off, the wells are washed twice with 2ml DPBS per well and fresh reduced-serum RPMI medium is added. On day 10 and day 17, medium is changed after washing once with serum-free RPMI medium. On day 10 and day 13 (then without medium change), different humoral stimuli can be added to the medium to test their pro-proliferative effect on surviving, growth-arrested cells.*

On day 0 and, from day 3 on, every 1-2 days, images of specific areas within the well of each condition are taken for monitoring changes in cell death, proliferation and morphology following Cisplatin treatment or stimulation.

On day -1, 10^5 – $3*10^5$ melanoma cells were seeded in reduced-serum RPMI medium per well in 6 well plates and let attach for 24 hours. For better distribution of the cells within the wells, plates were wet by washing with DPBS once. After removing the medium on day 0, 2 ml fresh reduced-serum RPMI medium with up to 15 µM Cisplatin was added to each well. Throughout the experiments, two different Cisplatin stock solutions (1^{st} stock and 2^{nd} stock) were used, as a precipitate appeared in the 1^{st} stock solution after some time and therefore its unrestricted effectivity had to be questioned. The treatment was taken off after 72 hours (day 3) and the plates were washed three times with DPBS. New reduced-

serum RPMI medium was added and subsequently changed every 7 days (on day 10, day 17 and up to day 24) after washing once with serum-free RPMI medium.

To prove cell death and growth arrest is not a result of starvation due to the reduction of serum, three wells with reduced-serum RPMI medium without Cisplatin added on day 0 were taken as controls. On day 3 and after that every 2-3 days the control cells were passaged in all three wells separately at 1/4-1/3.

2.2.3 Conditioned media

A375, SBCL2 and primary fibroblasts were cultured in their respective media in T75 flasks until they reached 70-80% confluence. Melanoma cells were washed twice with DPBS and incubated for 48 h with 15 ml of new, non-supplemented RPMI medium to obtain melanoma conditioned medium (MCM). Primary fibroblasts were washed twice with DPBS and incubated for 48 h with 15 ml of new, non-supplemented RPMI medium containing 10% MCM of the respective melanoma cell lines to generate melanoma-stimulated fibroblast conditioned media (MSFCM). Generation of MCM and MSFCM was performed based on methods described by others (Li et al., 2009).

For repopulating cells supernatant in experiment A375.10/SBCL2.10, medium was taken off on day 10 from plates showing proliferation on day 9 of the scheme for short-term chemotherapy.

All conditioned media were centrifuged at 1200 x g for 5 min and sterile filtered through a 0.2 µm filter before use and stored at -20°C.

2.2.4 Generation of protein coated plates

96 and 24 well plates were coated with different protein components of the extracellular matrix (ECM) prior to seeding cells for different proliferation assays. The different ECM components were either purchased (collagen I, fibronectin) or derived from primary fibroblasts (solubilized FF-ECM, see section 2.2.5)

The proteins were diluted and incubated on the respective plates as indicated below (see table 2.2.4) After incubation, the plates were rinsed twice with DPBS

to remove all possibly remaining solvents and could be either directly used for proliferation analysis or stored at 4°C for up to one week.

Table 2.2.4 Details on protein coating of tissue culture dishes

Protein		Collagen I		Fibronectin	FF-ECM
origin		rat tail		bovine plasma-derived	primary fibroblasts
company		Corning		R&D systems	house production
condition upon use		diluted in DPBS	Neutralized to pH 7.2 – 7.4, ~0.8 ml Collagen I with ~0.2 ml 0.1 M NaOH, diluted in DPBS	diluted in DPBS	diluted in DPBS
density in µg/cm²		100.00	100.00	17.66	56.50
amount per well in µg	24 well plate	177.00	177.00	31.25	100.00
	96 well plate	29.00	29.00	5.12	16.39
incubation		overnight, 4°C	1 h, 37°C	overnight, 4°C	1 h, 37°C
reference		(Henriet et al., 2000)		(Henriet et al., 2000)	(Franco-Barraza et al., 2017)

2.2.5 Primary fibroblast derived extracellular matrix

The procedure of primary fibroblast derived extracellular matrix (FF-ECM) production was adapted from Franco-Barraza et al. (Franco-Barraza et al., 2017)

All following, freshly prepared liquids were sterile filtered through a 0.2 µm filter and used at 2 ml per well (6 well plate) or 0.5 ml per well (24 well plate), if not indicated otherwise.

2.2.5.1 Deposition

For better attachment of the FF-ECM to the tissue culture dishes, 6 and 24 well plates were coated with gelatin and the gelatin was cross-linked prior to seeding the primary fibroblasts. This step emerged to be essential to avoid detachment of the FF-ECM layer, especially if solubilization of the FF-ECM was not intended. Therefore, the wells were covered with a freshly prepared 0.2% gelatin solution (see table 2.1.5-2) and incubated for one hour in the cell incubator. After rinsing carefully with DPBS, 1% glutaraldehyde solution (dissolved in DPBS) was added, and the plates were incubated for 30 min at room temperature. The plates were then washed three times with DPBS for 5 min and covered with 1 M Ethanolamine solution (dissolved in sterile water) before incubating again for 30 min at room temperature. After washing again three times for 5 min, the plates could directly be used or stored up to one week, covered with DPBS, at 4°C under sterile conditions.

For FF-ECM production, $3*10^5$ (or $5.4*10^4$) primary fibroblasts from a 70-80% confluent flask were seeded per well in a previously coated 6 well plate (or 24 well plate respectively) in primary fibroblast growth medium (see table 2.1.5-9). One day after seeding, the old medium was replaced by primary fibroblast growth medium supplemented with 50 µg/ml Vitamin C. Supplemented medium was then changed every two days.

2.2.5.2 Extraction

Nine days (six days in the case of 24 well plates) after seeding, fibroblasts were lysed. For this purpose, the medium was removed, the well carefully rinsed once with DPBS and 1 ml (250 µl respectively) of pre-warmed Extraction buffer (see table 2.1.5-3) was added. Cell lysis could be observed and monitored under the microscope. Depending on the thickness of the FF-ECM layer, lysis was complete after 3-5 min and stopped by dilution with 2-3 ml (500 µl respectively) DPBS. After incubation over night at 4°C the buffer with cellular debris was removed and the FF-ECM gently washed with DPBS.

FF-ECM could then either be solubilized (6 well plates only) or let in its native state for further experiments. If not directly used, plates with the native FF-ECM

could be covered with DPBS supplemented with 1% Penicillin/Streptomycin and 0.25 µg/ml Fungizone, sealed with parafilm and stored at 4°C up to 6 weeks.

2.2.5.3 Solubilization

For solubilization, excess DPBS was accumulated by carefully tapping the plates at an angle of approximately 30°C to the bench for 1 min and taking off the liquid. The plates were placed on ice and 300 µl Solubilization buffer (see table 2.1.5-4) was added per well for 5 min. The FF-ECM could then be scraped with a cell scraper to one side of the well and transferred into a 1.5 ml microcentrifuge tube containing 200 µl of additional Solubilization buffer. After rotating for 1 h on a roller mixer, the tubes were micro-centrifuged at $1.5*10^4$ x g and 4°C for 15 min. The supernatant containing the solubilized FF-ECM could then be transferred to a new tube and stored indefinitely at 4°C.

The protein concentration of the solubilized FF-ECM was determined by the BCA assay, using the Pierce BCA Protein Assay Kit and following the manufacturer's protocol. For the calculation of the standard curve, bovine serum albumin (BSA) was diluted in solubilization buffer in a dilution series from 20 mg/ml. Standards and solubilized FF-ECM were diluted 1:1 with DPBS to reduce background signals from the solubilization buffer. Into triplicate wells of a 96 well plate were added 2.5 µl of either the diluted standard or the diluted, solubilized FF-ECM. After mixing Reagent A and B of the BCA kit, 100 µl of the Reagent solution were added to each cavity, the plate was shaken for 1 min and then incubated for 30 min at 37°C. The absorption values of the standard dilution series at 540 nm in the microplate reader lead was used to calculate a logarithmic regression curve.

2.2.5.4 Increasing the stiffness of the extracellular matrix

According to Franco-Barraza et al. (Franco-Barraza et al., 2017), the FF-ECM remains intact throughout the extraction process and closely resembles *in vivo* conditions in the stroma. The authors also present the possibility to rigidify the FF-ECM through chemical cross-linking.

To study the influence of different stiffness levels of the extracellular matrix on melanoma cells regarding proliferation, either native FF-ECM or previously solubilized FF-ECM used for coating of 24 well plates was thus rigidified.

For chemical cross-linking, the FF-ECM covered wells were carefully rinsed twice with DPBS. 1% glutaraldehyde solution (dissolved in DPBS) was gently added to the wells and the plates were incubated for 30 min at room temperature. After removing the cross-linking solution and washing three times with DPBS, 1 M ethanolamine solution (dissolved in sterile water) was added and the plates incubated for another 30 min at room temperature. The ethanolamine solution was removed, and the washing procedure was repeated.

2.2.6 Proliferation Analysis

2.2.6.1 Visual and optical analysis

Several studies reported a chemotherapy-induced change in metabolic activity in *in vitro* experiments (Li et al., 2014; Shirmanova et al., 2017). Therefore, assays measuring metabolic activity as a correlate for cell vitality and proliferation, such as the non-toxic Alamar Blue assay, based on the activity of cellular reductases, were not used for determining cell number development in experiments following the scheme for short-term chemotherapy or in experiments using cells that survived the latter. Instead, cell death and proliferation were monitored over time by continuous photo-documentation. This approach enabled not only for assessment of kinetics but also of changes in size and morphology of single cells as well as colonies.

Fixpoints within the wells were essential to ensure orientation within the well under the microscope and monitoring of the exact same area at all times. Hence, tissue culture plates of different sizes were provided with a grid in an easily recognizable design by scratching it on the back of the plate (see Figure 2.2.6).

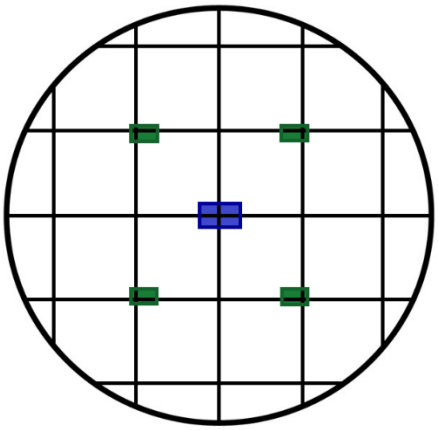

Figure 2.2.6-1 ***Exemplary grid for tissue culture dishes.*** *Scratching a grid on the back of the plates allowed (re-)orientation for simple cell counting and continuous photo-documentation. Adjacent (blue) and non-adjacent (green) images were taken from the same specific areas over time throughout the entire experiment.*

Images were taken from specific areas through the microscope on different specific days, at least on day 0, day 3, day 10, day 17 of the scheme for short-term chemotherapy as well as when obvious changes in cell number or morphology occurred. These specific areas could be adjacent or non-adjacent. In the first case, images of the area would be taken in a way that there would always be a segment overlapped by two adjacent images to enable for aligning the sections of the big area (image matrix) afterwards.

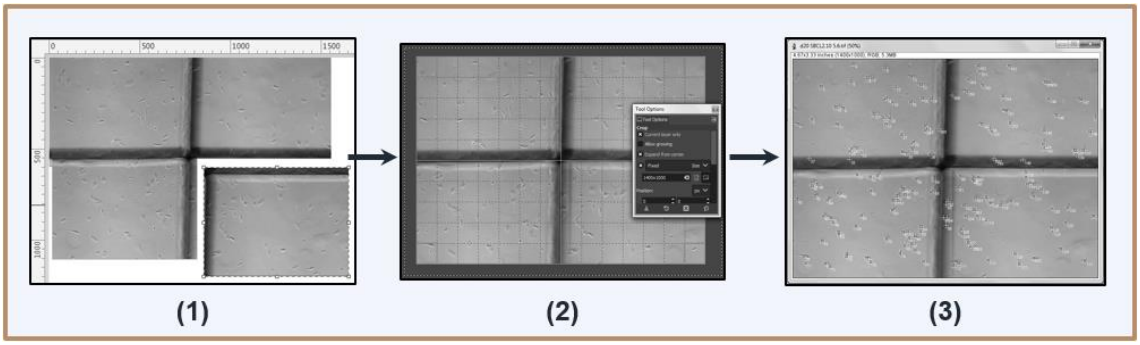

Figure 2.2.6-2 ***Exemplary scheme for work-flow in quantitative analysis of images taken through continuous photo-documentation with the steps of alignment (1), cropping (2) and counting (3).***

Segmental images were aligned with Microsoft Paint and cropped to specific areas in Gimp 2.10.6. For quantification, images were counted out manually in ImageJ with the help of the options “Multi-point tool” and “Measure”. To ensure comparability between the image matrices the latter were vigorously checked for

congruence over time and cropped to the same size throughout all conditions, if not indicated otherwise (see table 2.2.6-1). Due to differences in cell density and numbers of photos taken, the biggest common area, that congruent image matrices were cropped to, was not always of the same size between different experiments. Absolute numbers of cells under different conditions would only be compared, if matrices had the same size. Relative numbers of cells with a specific characteristic among a population (as in quantitative analysis from SA-β gal staining, see Figure 3.2.4-3) under various conditions would be compared even though derived from matrices of different sizes.

Table 2.2.6-1 ***Details on settings of evaluation of continuous photo-documentation from different experiments***

Experiment	Condition	Final size in pixel	Element presenting data from evaluation
SBCL2.9/A375.10	Treated and untreated	700x550	Figures 2.2.10-3 – 2.2.10-5; 3.2.1-1
SA-β gal staining	Treated, pH6	3500x3600	Figure 3.2.4-3
	Untreated (pH4,pH6,pH7); Ribociclib treated (pH6)	800x600	
Seeding on proteins of the extracellular matrix	Cell cycle-arrested cells	1000x1000	Figure 3.3.1-1
	Parental cells	900x1000	Figure 3.3.1-2
Application of pro-proliferative stimuli 1	All conditions	1400x1000	Table 3.3.2-1
Application of pro-proliferative stimuli 2	All conditions	1500x1100	Figure 3.3.2-4

2.2.6.2 Colony formation assay

Untreated A375, SBCL2 and WM115 melanoma cells seeded in melanoma cell growth medium (see table 2.1.5-8) on different proteins of the ECM (see figures 3.3.1-2 and 3.3.1-3; for coating modalities see section and table 2.2.4) at a density of 500 cells per well in a 24 well plate were fixed 5 days after seeding

inside the wells and by that their proliferation status preserved as well as stained to increase contrast for manual counting or photo-documentation at different end points. Therefore, plates were washed once with DPBS and then fixed in 4% paraformaldehyde for 15 min before being washed once again with DPBS. The cells were then stained with 3% Crystal Violet (of 2.3% Crystal Violet stock solution) in 50% Methanol and 47% ddH_2O for one hour at room temperature. After being washed with purified water until the wells seemed clear, the plates were left to dry overnight.

2.2.7 Cell cycle analysis

For cell cycle analysis, $7.8*10^5$ or $15.6*10^5$ cells were seeded in reduced-serum RPMI medium into T75 cell culture flasks and followed the scheme for short-term chemotherapy. Three flasks per condition were pooled to achieve a cell number high enough for flow cytometry.

For further investigation on SBCL2 cell line, $7.8*10^5$ cells were treated in six T75 cell culture flasks and three of the flasks were fixed on day 10 whereas the cells in the other three flasks got the medium changed on day 10 and were fixed on day 17. On day 10, cells in all six flasks appeared equally healthy and homogenous in cell number and morphology. Hence, the two populations treated differently from day 10 on were presumed to be congruent in their distribution in the cell cycle.

On day 3 (control cells), day 10 or day 17 (treated cells) the old medium was taken off, the cells washed once with DPBS and both liquids centrifuged at 290 x g for 5 min, whilst attached cells were harvested through incubation with Trypsin/EDTA for 2-3 min. The single cell suspension was diluted with complete RPMI medium and added to the precipitate obtained from the previous centrifugation step. After resuspending the precipitate in the single cell suspension, the tubes were centrifuged at 290 x g and 22°C for 5 min. Afterwards, the supernatant was removed, the precipitate washed with DPBS and centrifuged again at 290 x g and 22°C for 5 min. The pellet was solved in 0.5 - 1 ml ice-cold 70%-ethanol and thoroughly pipetted up and down until no particles could be seen in the suspension. The cells were then let to be permeabilized and fixed at 4°C over-night.

Within a week, the fixed cells were stained and analyzed through flow cytometry. To this extend, the cells were washed twice by filling up the tube with DPBS to 12 ml and centrifuging at 1500 x g and 22°C for 10 min. After the second washing step, the DPBS was removed and the precipitate resuspended in 100-1000µl of buffer for cell cycle analysis (see table 2.1.5-1)
In order to apply the staining dye proportionally to the approximate DNA amount, the exact volume of the staining solution used for the control cells was calculated for each cell line and experiment as the following:

$$volume = 100\mu l * \frac{number\ of\ untreated\ control\ cells}{number\ of\ treated\ cells}$$

The cell number was determined in 10 µl of the suspended, fixed cells during the second washing step before centrifugation through simple cell counting in a Neubauer chamber.
The cells were incubated with the staining solution for 30 min in the dark before performing a cell cycle analysis using LSRII FACS (BD) and FACSDiva software (BD). As the PI stained DNA varies in its content per cell throughout the cell cycle, the measurement of the fluorescence intensity per each single cell count leads to the absolute and relative distribution of the population in the cell cycle phases.

2.2.8 Immunofluorescence

The immunofluorescence was performed following the Cell Signaling Technologies "Immunofluorescence Protocol with Methanol Fixation (IF Methanol-fixed) (https://www.cellsignal.com/contents/resources-protocols/immunofluorescence-protocol-with-methanol-fixation-(if-methanol-fixed)/if-methanol-fixation, accessed on 03/21/2019, 18h40)

All solutions were applied at 250 µl per well in a 24 well plate. For immunofluorescence, melanoma cells SBCL2, A375 and WM115 were seeded in reduced-serum RPMI medium on coverslips at $3.6*10^4$ cells per well at triplicates in a 24 well plate and followed the scheme for short-term chemotherapy. On day 3 (control cells) or day 10 (treated cells) the used medium was removed, and the coverslips were washed once with DPBS. The cells were then fixed with 4%

paraformaldehyde for 15 min. After fixation, the coverslips were washed three times with DPBS for 5 min each, covered with fresh DPBS, sealed with parafilm and stored at 4°C for up to two weeks.

For further analysis, the DPBS was aspirated and cells were permeabilized with ice-cold 100% methanol at -20°C for 15 min. The coverslips were then washed with DPBS three times for 5 min each. Whilst blocking non-specific binding sites with the blocking buffer (see table 2.1.5-5) for 1 h, the primary antibody anti-PCNA was diluted 1:2500 in the antibody dilution buffer (see table 2.1.5-6). After aspirating the blocking buffer, the diluted primary antibody was applied over night at 4°C. The following day, the coverslips were washed three times with DPBS for 5 min and incubated for 2 hours with the Cy3-linked anti-mouse secondary antibody diluted 1:250 in antibody dilution buffer. The coverslips were washed with DPBS three times for 5 min each, incubated for 5 min in Yo-Pro-1 (diluted 1:1000 in DPBS) for nuclei staining and washed again with DPBS three times for 5 min.

For fluorescence microscopy and analysis, coverslips were taken out of the tissue culture plates and transferred on microscope slides by sticking the inverted coverslips on 2-3 drops of Polyvinyl alcohol (MOWIOL) pre-warmed to 60°C and supplemented with one crystal of 1,4-diazabicyclo[2.2.2]octane (DABCO).

Photos were kindly taken from representative areas of the different conditions and provided by Birgit Fehrenbacher (Electron microscopy section of Prof. Dr. Schaller, Department of Dermatology, University of Tübingen).

2.2.9 Senescence-associated β-galactosidase assay

The senescence-associated β-galactosidase (SA-β-gal) staining was performed as previously described (Griessinger et al., 2018).

B-galactosidase activity can be detected as lysosomal β-gal which is expressed by most of the cells and has its optimum at pH 4.0, as senescence-associated β-gal at an optimum of pH 6.0 and as bacterial β-gal at an optimum of pH 7.0 (7.5) (Dimri et al., 2006; Griessinger et al., 2018).

SBCL2 melanoma cells were seeded at 10^5 cells per well in a 6 well plate in reduced-serum RPMI medium and were treated with 3.75 µM Cisplatin following the scheme for short-term chemotherapy. At day 18 of the scheme, cells were fixed, washed and stained as described below at pH 6.0 to explore SA-β-gal activity in growth-arrested cells.

For controls, SBCL2 melanoma cells were seeded at 10^5 cells per well in a 6 well plate in reduced-serum RPMI medium. 96 hours after seeding, cells were fixed, washed and stained at pH 4.0 (control for lysosomal non-SA-β-gal activity) or at pH 7.0 (control for bacterial β-gal activity). The CDK4/6-inhibitor Ribociclib (LEE011) has been shown to drive cell lines of neuroblastoma and leukemia into senescence (Martinez et al., 2013; Tao et al., 2017). SBCL2 melanoma cells treated for 24 hours (72-96 hours after seeding) with 0.5 µM Ribociclib (commonly used setting in our laboratory) in 2 ml reduced-serum RPMI medium, then fixed and stained at pH 6.0 were therefore used as a positive control for senescence-associated β-galactosidase activity.

All solutions were prepared and titrated to the different pH on the same day of the staining. On the day of staining, cells were fixed inside of the 6 well plates with 0.25% glutaraldehyde/2% paraformaldehyde at pH 4.0, 6.0 or 7.0 for 12 min at room temperature. The cells were then washed twice with freshly prepared DPBS/$MgCl_2$ 1 mM solution at the respective pH for 5 min at room temperature. After washing, freshly prepared X-gal solution (see table 2.1.5-7) at pH 4.0, 6.0 and 7.0 was added to the wells and the plates were incubated in the cell incubator (37°C). The SBCL2 cells under the different conditions were examined for blue staining every hour and a blue appearance in untreated SBCL2 cells under pH 4.0 condition as well as in the Ribociclib treated SBCL2 cells (positive control) under pH 6.0 was considered as a successful staining and as the endpoint of the experiment. After 8 hours incubation, the staining solution was removed, and the wells were washed once with DPBS/$MgCl_2$ 1 mM solution at the respective pH for 10 min. After removing the washing solution, fresh DPBS/$MgCl_2$ 1 mM solution was added. Photos were taken from representative areas of the different conditions immediately afterwards. Wells were further covered with glycerol, sealed with Parafilm and stored at 4°C. Three months later, blue staining was still

prominent and adjacent photos were taken from triplicates of all conditions for quantitative analysis (see figure 3.2.4-3).

2.2.10 Statistics

Graphs and bars were created using GraphPad Prism 6.0 and 8 as well as Excel from Microsoft Office 2016. When conditions were applied in and data was generated from triplicates, statistical analysis was performed with both programs and figures show the means and - if calculated - their standard deviation. The statistical test Ordinary one-way ANOVA corrected by the Tukey's test for multiple comparisons was used for evaluating statistical significance. Differences between mean values were considered significant when $p<0.05$, and indicated by asterisk (*P<0.05; **P<0.01; ns – non-significant)

3 Results

3.1 Induction of cell cycle arrest in melanoma cells

The first aim was to determine the optimal conditions, under which cells of different melanoma cell lines are reproducibly driven into a stable growth arrest. The best suitable outcome was defined as the generation of a relatively homogenous population of viable cells, staying scattered and non-dividing over at least seven days.

Therefore, following the scheme for short-term chemotherapy (see section 2.2.2), SBCL2, A375 and WM115 melanoma cells were seeded at 10^5 – $3*10^5$ in 6 well plates and treated with 2 – 15 µM Cisplatin for 72 hours. Two different lots (1st and 2nd lot) of Cisplatin stock solutions were used, as a precipitate appeared in the 1st lot stock solution after some time. New CDDP (2nd lot) was ordered and both stock solutions were compared which indeed revealed differences in effectivity of the different stocks (data not shown). Seeding and treatment was performed using reduced-serum RPMI medium as previous experiments showed that a reduction of fetal calf serum in the medium enhanced the susceptibility of melanoma cells to Cisplatin. Every day, from day 3 until at least day 17, all wells were checked for the occurrence of colonies under the microscope and images were taken from specific areas over time (for methodology see section 2.2.6.1). Colony formation was documented for time point of first occurrence, the number of colonies (Figures 3.1-1, 3.1-2) and their location within the well (data not shown). All experiments were carried out with each condition applied and analyzed in triplicates.

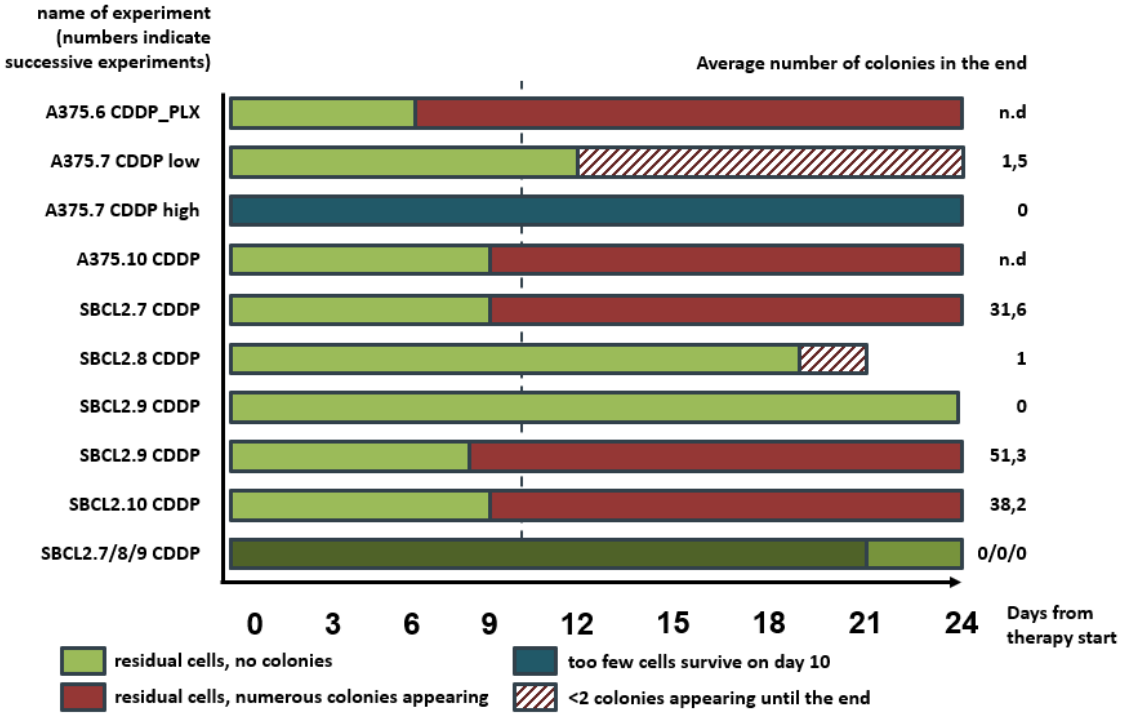

Figure 3.1-1 ***Experimental scheme for short-term chemotherapy under different conditions, 1st lot Cisplatin (CDDP).*** *To determine the optimal setting for generating stably arrested melanoma cells through short-term chemotherapy, cells were seeded in different densities per well in 6 well plates at triplicates (n=3, mean), treated with different concentrations of CDDP following the scheme, observed and photographed every 1-2 days for re-proliferation. Colonies were counted manually through the microscope. The last bar summarizes three independent experiments (darker color) that were carried out under the same condition (see table 3.1-1) and led to the same result (no colony formation until the end). The experiment SBCL2.8 CDDP was stopped on day 21 from therapy start already. CDDP– Cisplatin; PLX – Vemurafenib; n.d. – not determined*

Table 2.2.10-1 ***Conditions of the experiments in figure 3.1-1*** *The conditions are listed in the same order of experiments as they are represented graphically in figure 3.1-1; CDDP – Cisplatin; PLX - Vemurafenib*

Name of the experiment	Cell line	Cell number per well	Concentration and treatment
A375.6 CDDP_PLX	A375	$1*10^5$	10 µM PLX
A375.7 CDDP low	A375	$1*10^5$	7.5 µM CDDP (1^{st} lot)
A375.7 CDDP high	A375	$1*10^5$	15 µM CDDP (1^{st} lot)
A375.10 CDDP	A375	$1*10^5$	7.5 µM CDDP (1^{st} lot)
SBCL2.7 CDDP	SBCL2	$1*10^5$	7.5 µM CDDP (1^{st} lot)
SBCL2.8 CDDP	SBCL2	$1*10^5$	10 µM CDDP (1^{st} lot)
SBCL2.9 CDDP	SBCL2	$2*10^5$	15 µM CDDP (1^{st} lot)
SBCL2.9 CDDP	SBCL2	$3*10^5$	15 µM CDDP (1^{st} lot)
SBCL2.10 CDDP	SBCL2	$2*10^5$	15 µM CDDP (1^{st} lot)

SBCL2.7/8/9 CDDP	SBCL2	$1*10^5$	15 µM CDDP (1st lot)

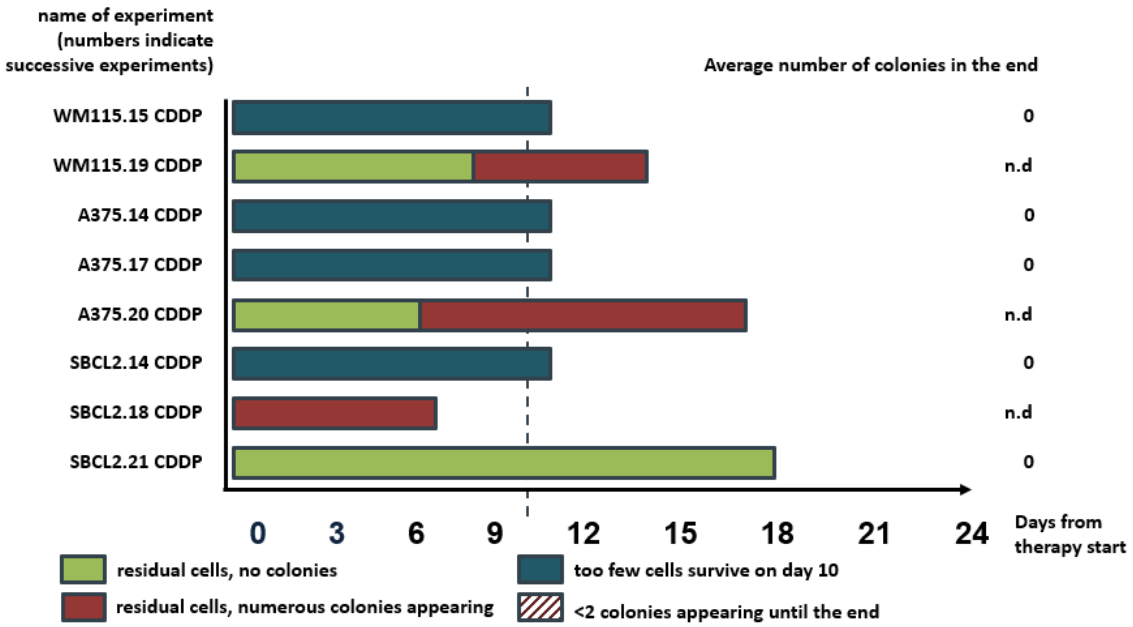

Figure 3.1-2 ***Experiments following scheme for short-term chemotherapy under different conditions, 2nd lot Cisplatin (CDDP).*** *To determine the optimal setting for generating stably arrested melanoma cells through short-term chemotherapy, cells were seeded in different densities per well in 6 well plates at triplicates (n=3, mean), treated with different concentrations of CDDP following the scheme, observed and photographed every 1-2 days for re-proliferation. Colonies were counted manually through the microscope. After a precipitate appeared in 1st lot CDDP stock solution, new, 2nd lot CDDP was purchased and used for experiments as correct concentration in 1st lot CDDP stock solution could not be guaranteed anymore. n.d – not determined; CDDP– Cisplatin*

Table 2.2.10-2 ***Conditions of the experiments in figure 3.1-2*** *The conditions are listed in the same order of experiments as they are represented graphically in figure 3.1-2; CDDP – Cisplatin*

Name of the experiment	Cell line	Cell number per well	Concentration and treatment
WM115.15 CDDP	WM115	$1*10^5$	15 µM CDDP (2nd lot)
WM115.19 CDDP	WM115	$1*10^5$	3.75 µM CDDP (2nd lot)
A375.14 CDDP	A375	$2*10^5$	7.5 µM CDDP (2nd lot)
A375.17 CDDP	A375	$1*10^5$	3.75 µM CDDP (2nd lot)
A375.20 CDDP	A375	$2*10^5$	2 µM CDDP (2nd lot)
SBCL2.14 CDDP	SBCL2	$2*10^5$	7.5 µM CDDP (2nd lot)
SBCL2.18 CDDP	SBCL2	$2*10^5$	3.75 µM CDDP (2nd lot)
SBCL2.21 CDDP	SBCL2	$1*10^5$	3.75 µM CDDP (2nd lot)

Manual counting and comparison of images taken over time (see figure 3.1-3) revealed that melanoma cells would die off before and after removal of the chemotherapy. When cells survived the Cisplatin treatment, they would take up proliferation before day 10 of the scheme and form numerous colonies until day 24 or stay growth-arrested until the end of the experiment. The day 10 was therefore set as a fix date for further characterization or stimulation. When seeded at a density of 10^5 cells per well and treated with 15 µM CDDP (1st lot) or 3.75 µM CDDP (2nd lot), cells of SBCL2 melanoma cell line would reach the best suitable outcome and stay growth-arrested until at least day 17 (see figure 3.3-1, SBCL2.7/8/9 and figure 3.3-2, SBCL2.21). A375 seeded at a density of 10^5 cells per well and treated with 7.5 µM CDDP (1st lot) mostly stayed growth-arrested and only a mean number of 1.5 colonies appeared until day 24. With the introduction of the 2nd lot of CDDP, this result could not be reproduced. Likewise, an optimal setting for cell line WM115 could not be definitely determined (Figure 3.1-2, compare WM115.15 and WM115.19).

Among the five plates with CDDP treated cells in the experiment A375.10 (10^5 cells/well, 7.5 µM CDDP, 72 h)/SBCL2.10 ($2*10^5$ cells/well, 15 µM CDDP, 72 h), some wells showed spontaneous re-proliferation on day 9 but localized on one plate whereas the other plates did not show any re-proliferation. Under the same conditions, in SBCL2.9 no colonies appeared, which is why the unrestricted effectivity of the CDDP (1st lot) stock solution was questioned and a new CDDP stock solution (2nd lot) was ordered and used in following experiments, as mentioned above.
Nevertheless, the experiment A375.10/SBCL2.10 offered the unique opportunity to examine two populations from the same cell culture stock and treated under the same conditions but reacting differently concerning growth-arrest and proliferation. How these populations were further analyzed and manipulated is described in the sections 3.2 and 3.3.

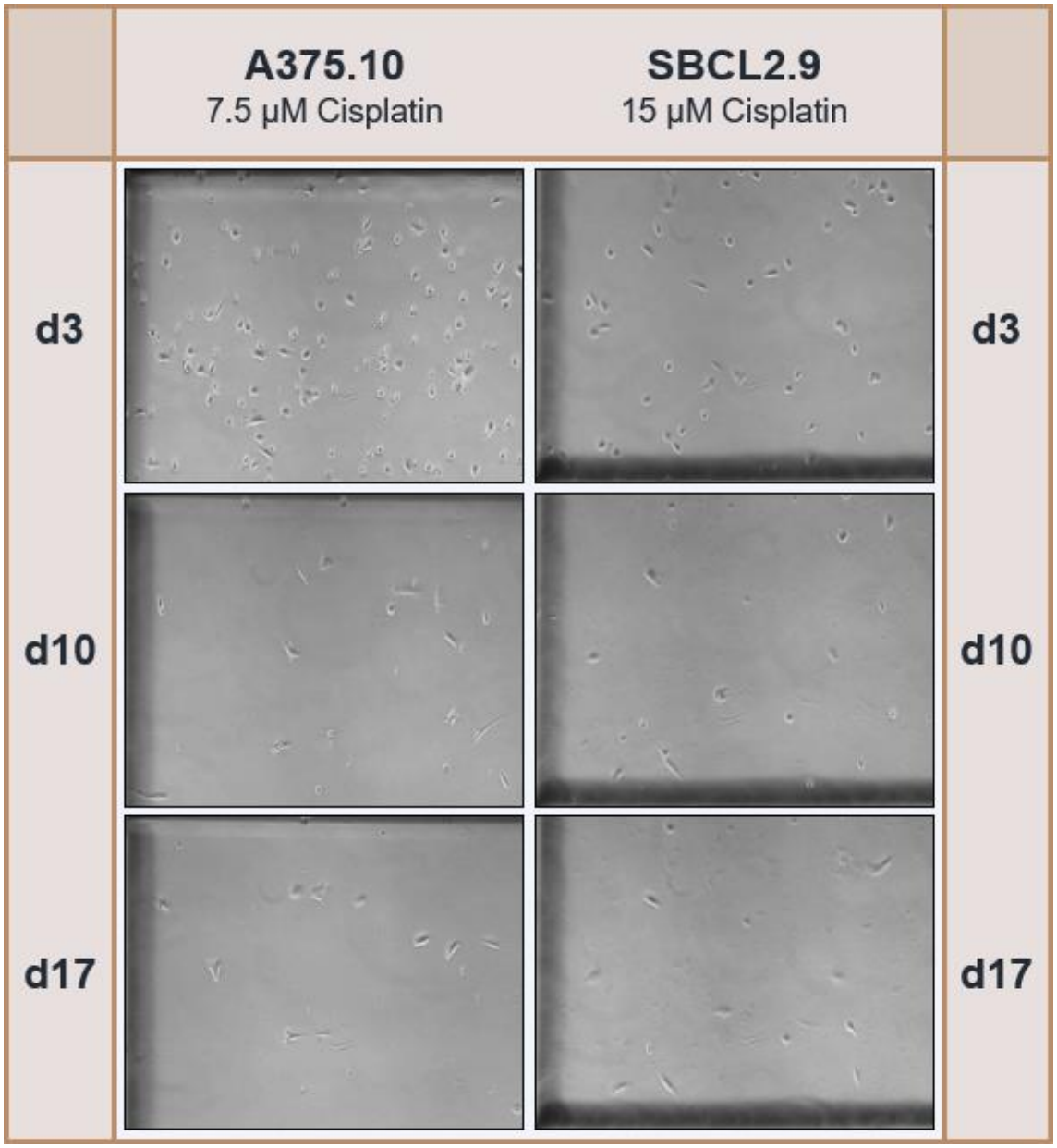

Figure 3.1-3 ***Example for continuous photo-documentation showing stably growth-arrested melanoma cells over time following the scheme for short-term chemotherapy****. SBCl2 and A375 melanoma cells followed the scheme for short-term chemotherapy (SBCL2.9 and A375.10, seeded at 10^5 cells per well, for details on conditions see Figure 3.1-1). All conditions were applied in triplicates. Images above were taken at 4x magnification and cropped to an area congruent over time of 700x550 pixels. SBCL2.9, A375.10 – names of the experiments; d – day within the scheme for short-term chemotherapy*

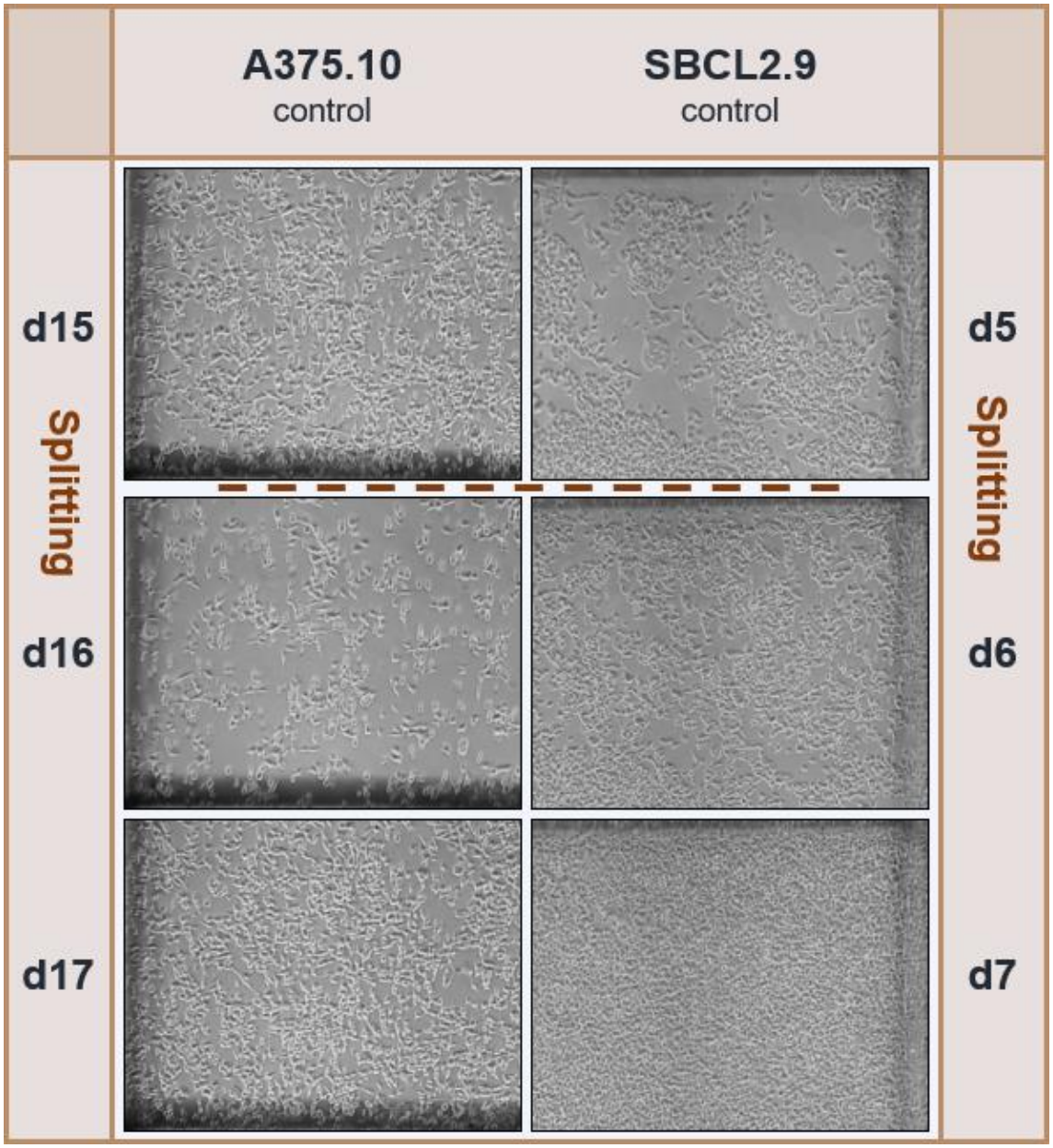

Figure 3.1-4 ***Example for continuous photo-documentation showing stably proliferating melanoma cells over time after seeding and splitting in reduced-serum RPMI medium.*** *As controls, SBCl2 and A375 melanoma cells were seeded at 10^5 cells per well in reduced-serum RPMI medium. Control cells were passaged on day 3 and after that every 2-3 days in all three wells separately at 1/4-1/3. All conditions were applied in triplicates. Images above were taken at 4x magnification and cropped to an area congruent over time of 700x550 pixels. SBCL2.9, A375.10 – names of the experiments; d – day within the scheme for short-term chemotherapy.*

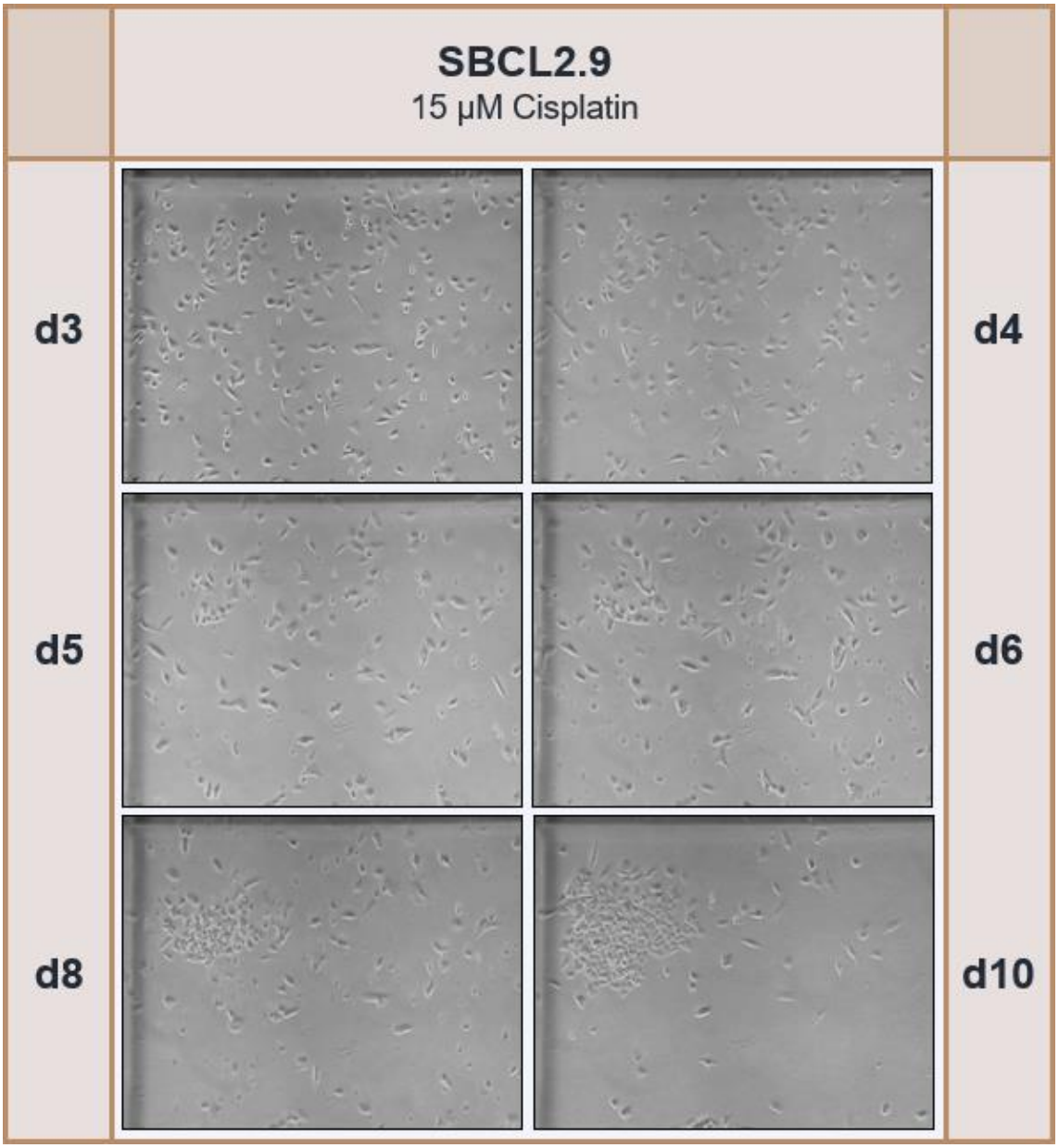

Figure 3.1-5 ***Example for continuous photo-documentation showing the formation of a colony by repopulating melanoma cells over time.*** *SBCl2 melanoma cells followed the scheme for short-term chemotherapy (SBCL2.9, 3*10^5 cells per well, for details on conditions see Figure 3.1-1). All conditions were applied in triplicates. Images above were taken at 4x magnification and cropped to an area congruent over time of 700x550 pixels. SBCL2.9 – name of the experiments; d – day within the scheme for short-term chemotherapy*

3.2 Characterization of cell cycle-arrested cells

3.2.1 Morphology

Following treatment with CDDP within the scheme for short-term chemotherapy, the morphology of surviving melanoma cells changed in comparison to parental control cells.

The most concise transformation could be observed in the cell size as it can be exemplary seen on day 17 (SBCL2) or day 15 (A375) (see Figure 3.2.1-1). When treated with CDDP (1st lot) for 72 hours, most of the cells obviously cover an enlarged area per cell in comparison to parental untreated cells at the same late time points.

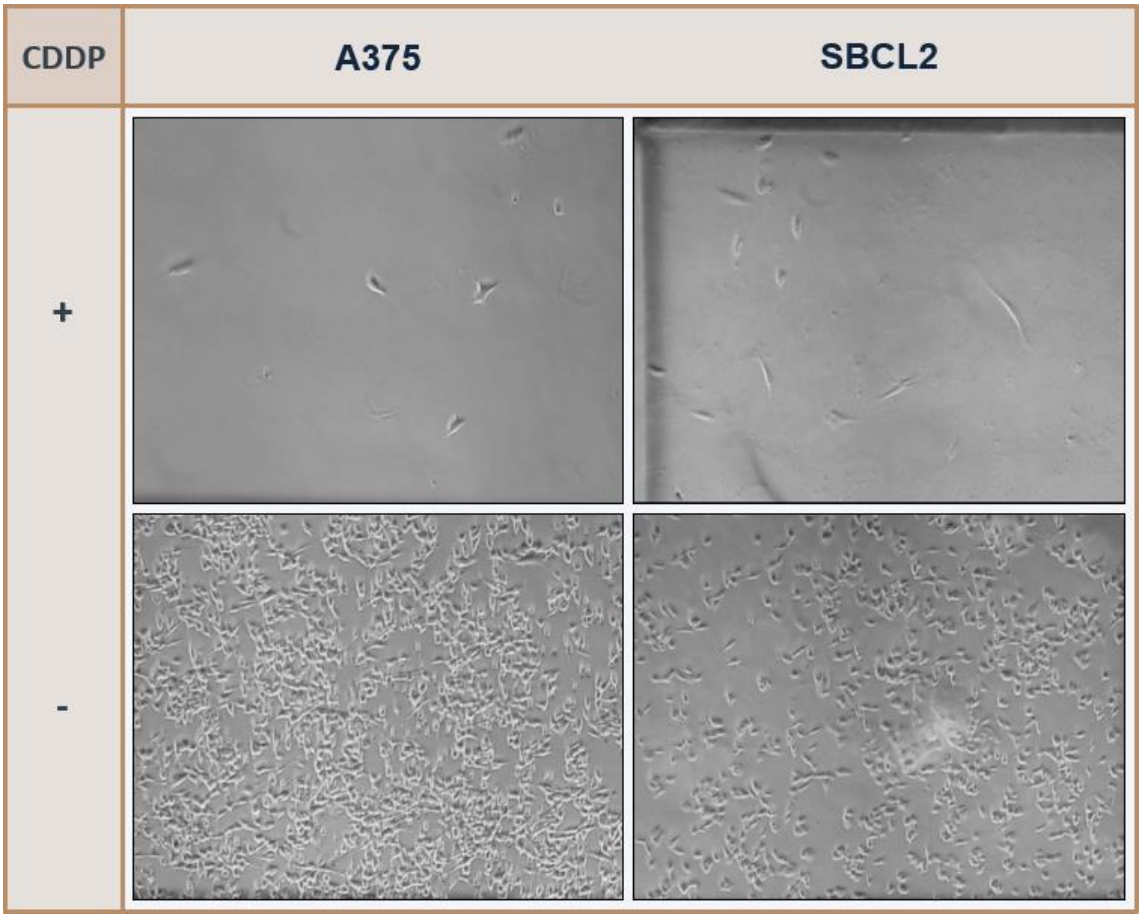

Figure 3.2.1-1 ***Representative images of melanoma cell lines SBCL2 and A375 following the scheme for short-term chemotherapy.*** *SBCl2 and A375 melanoma cells followed the scheme for short-term chemotherapy (SBCL2.9 and A375.10, seeded at 10^5 cells per well, for details on treatment conditions see table 3.1-1). All conditions were applied in triplicates. Images above were taken at 4x magnification on the following days of the scheme: SBCL2 growth-arrested and SBCL2 control cells 2% FCS - both on day 17; A375 growth-arrested cells and A375 control cells 2% FCS – both on day 15, CDDP - Cisplatin*

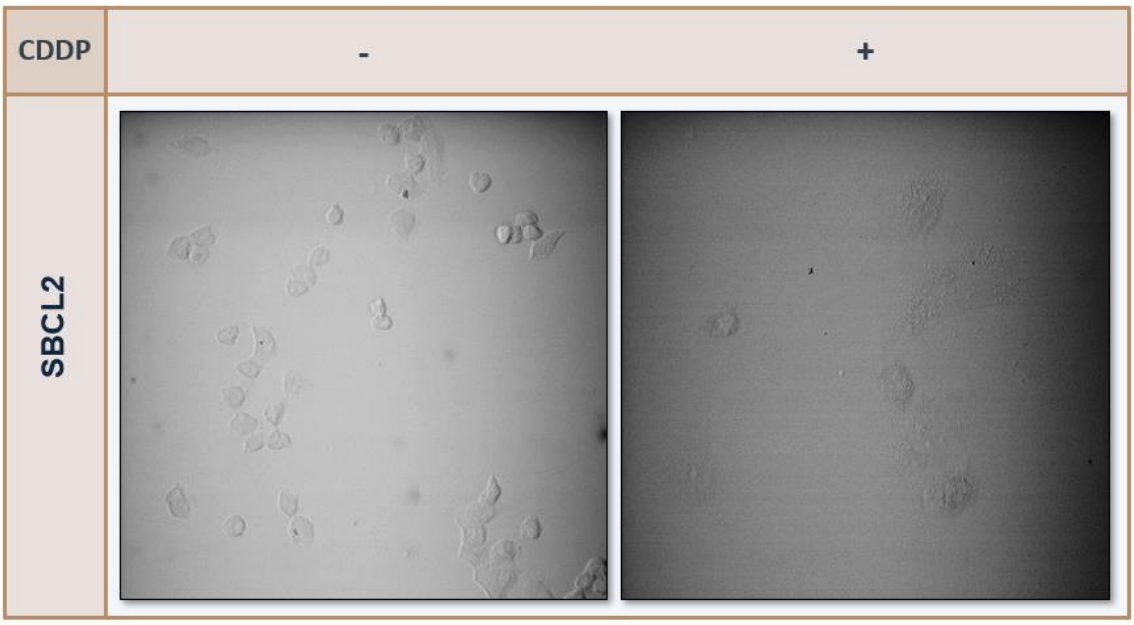

Figure 3.2.1-2 ***Representative images of melanoma cell line SBCL2 following the scheme for short-term chemotherapy.*** *Brightfield images from series of immunofluorescence pictures showing melanoma cell line SBCL2 (CDDP, 72h, 3.75 µM (2nd lot), fixed 11 days after seeding). All conditions were applied in triplicates. Both images were taken at 25x magnification. CDDP – Cisplatin*

Furthermore, the nucleus of CDDP (2nd lot) treated SBCL2 cells shows a broader expansion on day 10 under the immunofluorescence microscope than the parental cells (see Yo-Pro-1 channel for nucleus, Brightfield for cytoplasm in figure 3.2.3-1).

In addition, a sharp cell border is missing especially in treated SBCL2 cells, as brightfield imaging already suggests at 4x magnification (see figure 3.2.1-1) but becomes obvious at higher magnifications of 20x or 25x (figures 3.2.4-1 and 3.2.1-2).

3.2.2 Cell cycle analysis

Cells go through different phases of the cell cycle within which the DNA content, that can be stained with the fluorescent dye propidium iodide (PI), varies from 1 DNA copy number (G1-phase and when cells are arrested in G0-phase), over 1-2 DNA copy numbers (in S-Phase the DNA is replicated) to 2 DNA copy numbers in G2- and M-phase. A deviation in the distribution of a treated cell population in the cell cycle in comparison to the distribution of untreated cells hints at a cell cycle arrest following the therapy. Through simple DNA content analysis, G0- and G1- as well as G2- and M-phase can not be identified separately from each other.

To obtain more information about the cell population surviving short-term chemotherapy and staying quiescent, particularly about their location in the cell cycle at later time points, melanoma cells were treated with Cisplatin following the scheme for short-term chemotherapy and underwent cell cycle analysis by flow cytometry (for methodology see section 2.2.7). SBCl2 melanoma cells were treated with 7.5 µM (1st lot) and analyzed on day 10 as well as treated with 3.75 µM CDDP (2nd lot) and analyzed on day 10 and day 17 of the scheme. A375 cells treated with 7.5 µM CDDP (1st lot) and WM115 cells treated with 15 µM (1st lot) were analyzed on day 10 of the scheme. Gating of all events for single cells and for the subpopulations in the different cell cycle phases according to their fluorescence intensity determined the distribution of the cells in the cell cycle (figure 3.2.2-1).

Seven days after taking off the therapy, cells still undergo apoptosis as can be seen in the subG1 fraction of the different cell lines (A375 – 39.47%; SBCL2 – 20.86%; WM115 – 30.69%) in comparison to the control cells (A375 – 14,92%; SBCL2 – 17,78%). The WM115 control cell population was apparently unhealthy as 86.96% of the cells were apoptotic.

Excluding apoptotic cells from analysis leads to the distribution of all viable cells in the cell cycle (figure 3.2.2-2). Cells viable on day 10 in the scheme mostly stay growth-arrested in G2/M-phase (A375 – 48.29%; SBCL2 – 66.55%).

Further analysis of SBCL2 cell line showed that cells surviving short-term chemotherapy on day 10 are mainly growth-arrested in G2/M-phase (61.34% in

G2/M; 7.69% in G1; 4.69% in S; 26.27% polyploid) and most of them undergo apoptosis until day 17 (73.83% in subG1-phase). Most of the SBCL2 cells viable on day 17 were still growth-arrested in G2/M-phase (53.49%). Though, there is a shift towards G0/G1-phase (7.69% on day 10 to 28.06% on day 17) accompanied by a relative reduction of polyploid cells (26.27% on day 10 to 14.74% on day 17).

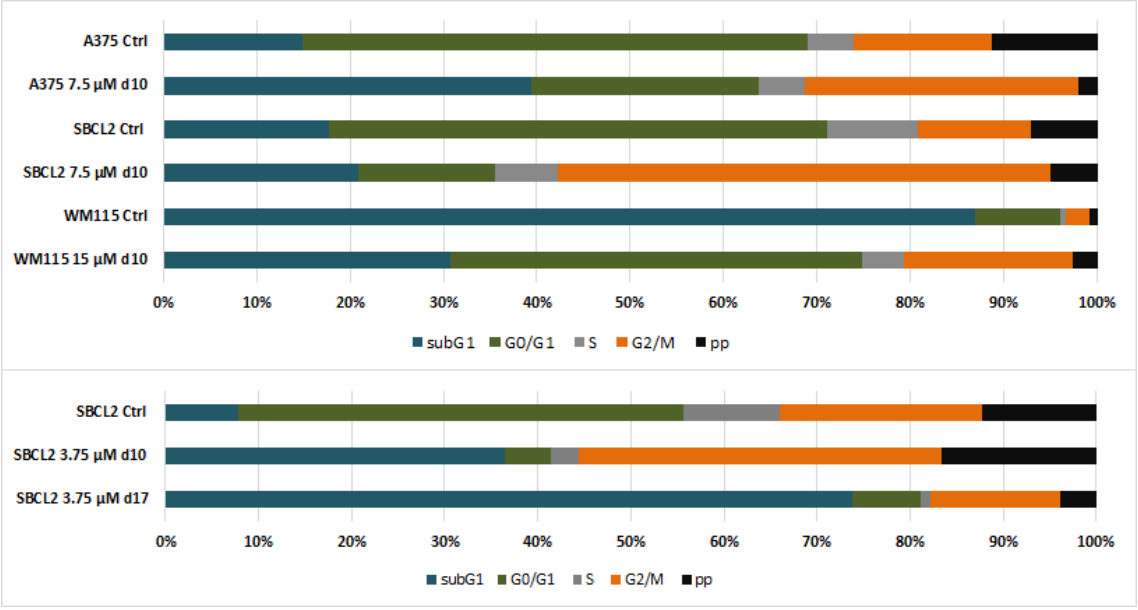

Figure 3.2.2-1 ***Distribution of all melanoma cells in the different phases of the cell cycle in percent following short-term chemotherapy.*** *For cell cycle analysis, parental melanoma cells of the cell lines A375, SBCL2 and WM115 followed the scheme for short-term chemotherapy (treated with 7.5 µM or 15 µM CDDP, 1st lot, or with 3.75 µM CDDP, 2nd lot, for 72 hours) and were fixed on day 10 (d10) or day 17 (d17) of the scheme. For control populations (Ctrl), untreated parental cells were fixed on day 3 of the scheme at 70-80% confluence. The DNA was stained with propidium iodide and cell cycle analysis by flow cytometry was performed directly afterwards.*
The "single cell population" depicted here includes all single cells harvested from tissue culture flasks as well as non-attached cells in the medium. pp – polyploid cells

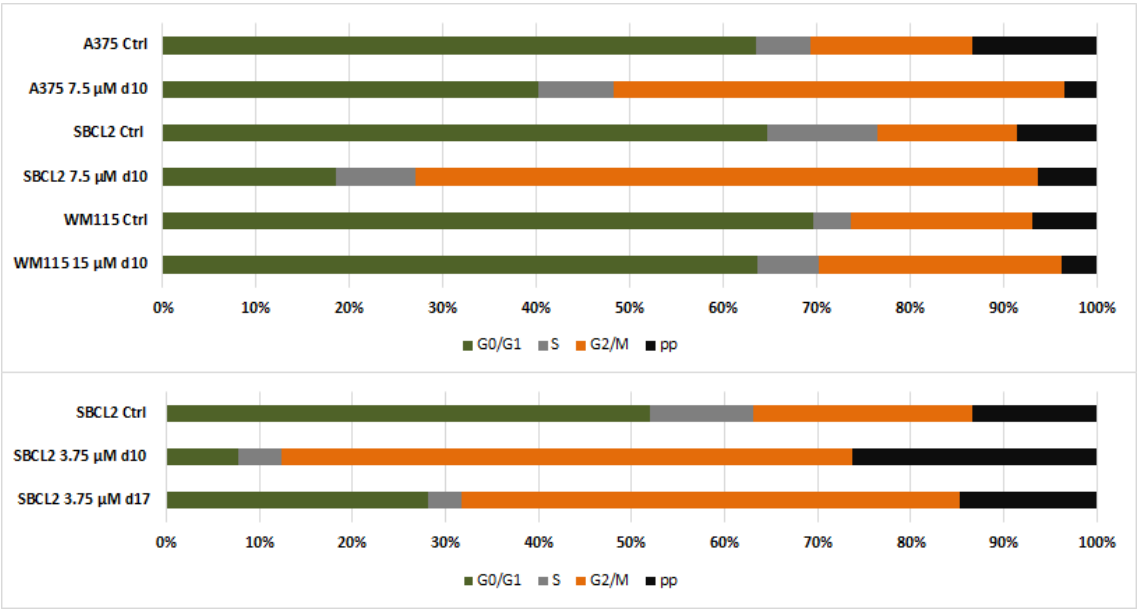

Figure 3.2.2-2 ***Distribution of the viable cells within the single cell population in the different phases of the cell cycle in percent.*** *The "viable single cells population" includes all surviving, single cells harvested from T75 flasks as well as non-attached cells in the medium (changed day 3) excluding the subG1 subpopulation. For details in generation of the different populations see Figure 3.2.2-1. pp – polyploid cells*

Table 3.2.2-1 ***Table of percentages for distribution of melanoma cells in the different phases of the cell cycle in figure 3.2.2-1*** pp – polyploid cells; s.c.p. – single cell population

Cell cycle phase in % of s.c.p.	subG1	G0/G1	S	G2/M	pp
A375 Ctrl	14.92	54.08	4.97	14.68	11.35
A375 7.5 µM d10	39.48	24.31	4.94	29.23	2.05
SBCL2 Ctrl	17.80	53.22	9.74	12.21	7.03
SBCL2 7.5 µM d10	20.86	14.62	6.84	52.67	5.01
WM115 Ctrl	86.96	9.09	0.51	2.55	0.89
WM115 15 µM d10	30.69	44.16	4.49	18.01	2.65
SBCL2 Ctrl	7.75	47.91	10.30	21.70	12.34
SBCL2 3.75 µM d10	36.51	4.89	2.98	38.95	16.68
SBCL2 3.75 µM d17	73.83	7.34	0.97	14.00	3.86

Table 3.2.2-2 ***Table of percentages for distribution of melanoma cells in the different phases of the cell cycle in figure 3.2.2-2*** pp – polyploid cells; v.s.c.p. – viable cells of single cell population

Cell cycle phase in % of v.s.c.p.	G0/G1	S	G2/M	pp
A375 Ctrl	63.57	5.84	17.25	13.34
A375 7.5 µM d10	40.17	8.16	48.29	3.38
SBCL2 Ctrl	64.75	11.85	14.85	8.55
SBCL2 7.5 µM d10	18.48	8.64	66.55	6.33
WM115 Ctrl	69.72	3.91	19.52	6.85
WM115 15 µM d10	63.72	6.48	25.98	3.82
SBCL2 Ctrl	51.94	11.16	23.52	13.38
SBCL2 3.75 µM d10	7.69	4.69	61.34	26.27
SBCL2 3.75 µM d17	28.06	3.70	53.49	14.75

3.2.3 Immunofluorescence

Cell cycle arrest can further be confirmed by an immunofluorescence staining of proteins that are expressed in actively cycling cells and downregulated in growth-arrested cells. Most commonly labelled proteins for that approach are Ki-67 and Proliferating Cell Nuclear Antigen (PCNA) that are seen as equally reliable. In this study, PCNA was chosen for practical reasons. For further confirmation of cell cycle arrest in melanoma cells following the scheme for short-term

chemotherapy, A375, SBCL2 and WM115 cells, treated with 3.75 µM CDDP (2nd lot) and untreated parental cells underwent immunofluorescence staining against PCNA and nuclei were stained with Yo-Pro-1. Representative images were taken (figures 3.2.3-1 to 3.2.3-2). Nuclei staining for melanoma cell lines A375 and WM115 was unsuccessful, contours of the cells are therefore depictured in brightfield mode.

Treated A375, SBCL2 and WM115 cells on day 10 and untreated cells on day 3 are positive for PCNA but most of the Cisplatin treated cells show a slight reduction of fluorescence intensity in comparison to untreated parental cells.

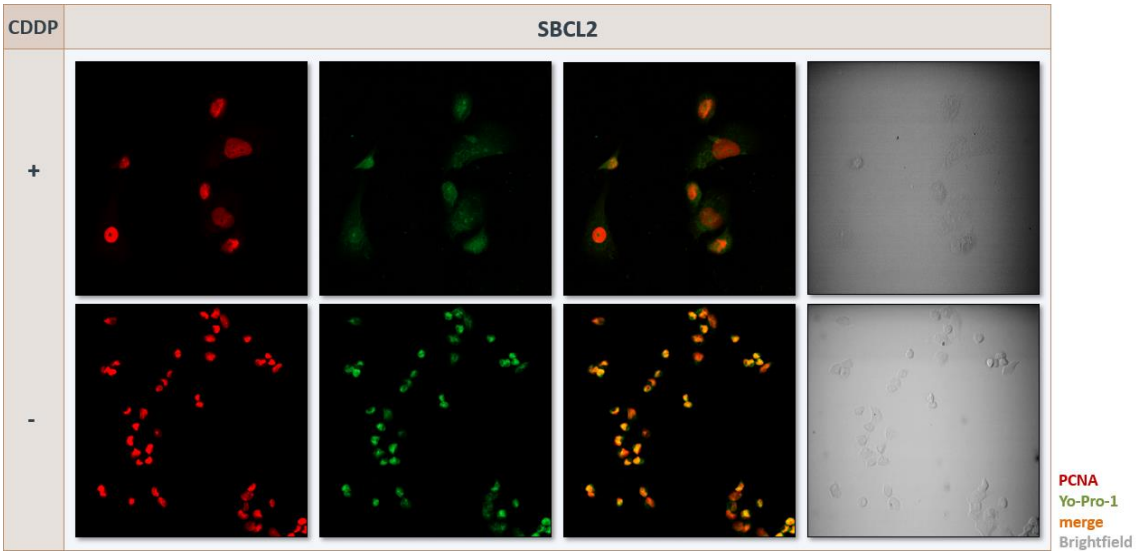

Figure 3.2.3-1 ***Representative pictures of immunofluorescence analysis.*** *Images show Proliferating Cell Nuclear Antigen (PCNA)(in red) and Yo-Pro-1 (in green) staining, both channels merged as well as the brightfield image (grey), in melanoma cell line SBCL2 following scheme for short-term chemotherapy, being treated (CDDP, 72 h, 3.75 µM (2nd lot), fixed 11 days after seeding) or left untreated (fixed 4 days after seeding, when cells were subconfluent). All images were taken at 25x magnification.*

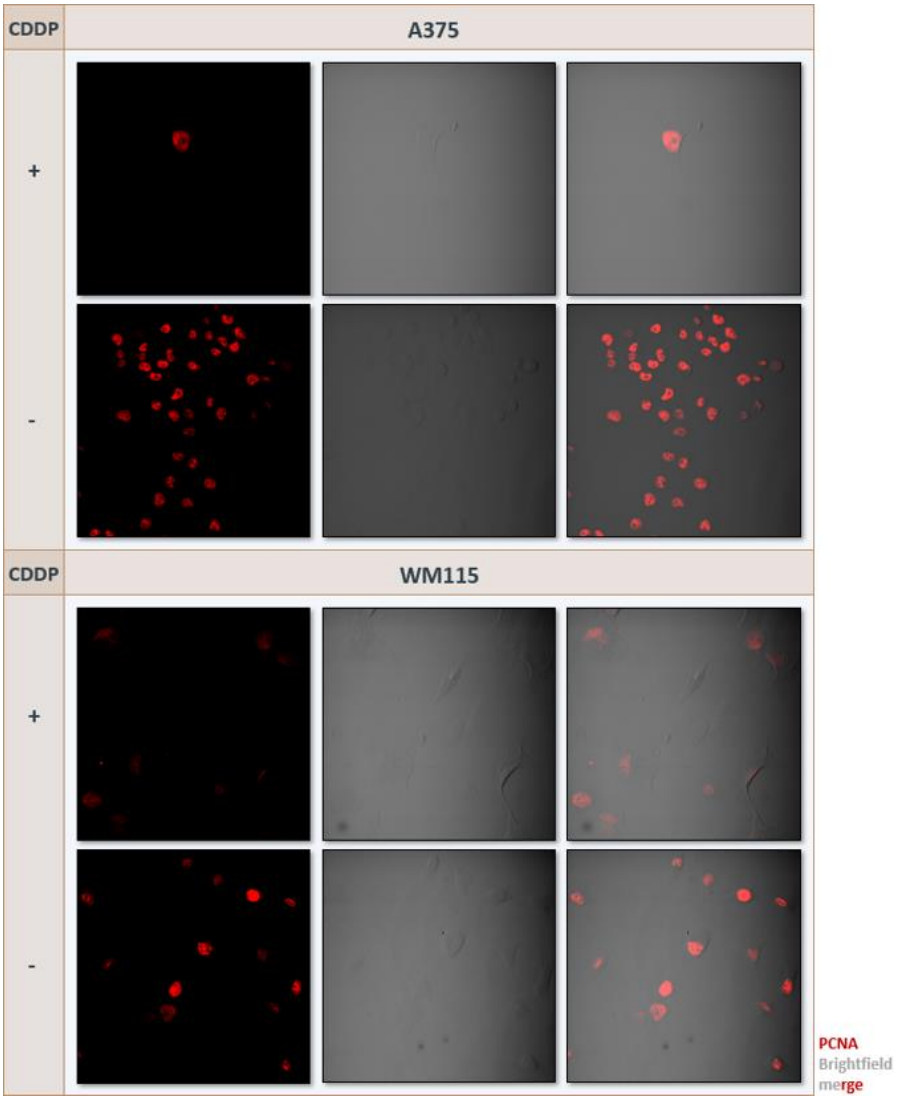

Figure 3.2.3-2 ***Representative pictures of immunofluorescence analysis.***
Images show Proliferating Cell Nuclear Antigen (PCNA) staining (in red) and brightfield (in grey) as well as both channels merged, in melanoma cell lines A375 and WM115 following scheme for short-term chemotherapy, being treated (CDDP, 72 h, 3.75 µM (2nd lot), fixed 11 days after seeding) or left untreated (fixed 4 days after seeding, when cells were subconfluent). All images were taken at 25x magnification.

3.2.4 Senescence-associated β-galactosidase staining

In response to cellular stress, for example of oncogenic and oxidative nature or through DNA damage, tumor cells can become senescent. This form of cell cycle arrest in G1-phase is, as to the consensus, irreversible.

Senescence goes along with a change in metabolic activity, namely the increase in expression and secretion of characteristic factors (senescence-associated secretory phenotype, SASP) as well as an elevated lysosomal β-galactosidase activity. This enzyme, ubiquitously present at a basal level in most somatic cells, can be detected through an enzymatic reaction where it cleaves the colorless substrate X-gal (5-bromo-4-chloro-3-indolyl-β-D-galactopyranoside) into galactose and an intermediate product that, through spontaneous dimerization and oxidation, becomes the insoluble and deep blue product 5,5'-dibromo-4,4'-dichloro-indigo. When lysosomal activity is elevated as in senescent cells, β-galactosidase can be detected at pH 6.0 whereas at basal lysosomal activity β-galactosidase would cleave X-gal preferably at its optimum of pH 4.0.

For a better characterization and understanding of the possible mechanisms behind the growth arrest in melanoma cells surviving short-term chemotherapy at a later time point, treated (but non-stimulated) SBCL2 cells in experiment SBCL2.21 (for experiment conditions see figure and table 3.1-2) underwent senescence-associated β-galactosidase staining (SA-β-gal) on day 18. Images of representative areas of all conditions were taken immediately after stopping the reaction (figures 3.2.4-1 and 3.2.4-2)

The majority of CDDP treated SBCL2 melanoma cells (62.95% ±10.54 SD) showed a clearly blue area close to their nucleus (see figure 3.2.4-3). Only very few Ribociclib treated SBCL2 cells (0.2%), used as the SA-β-gal positive control, developed a blue appearance but the blue staining of the untreated SBCL2 cells fixed and stained at pH 4.0 for basal lysosomal β-gal activity confirmed the success of the staining. Untreated SBCL2 stained at pH 7.0 stayed colorless and thereby confirm that positive blue staining of treated and untreated SBCL2 cells is not related to bacterial β-galactosidase activity.

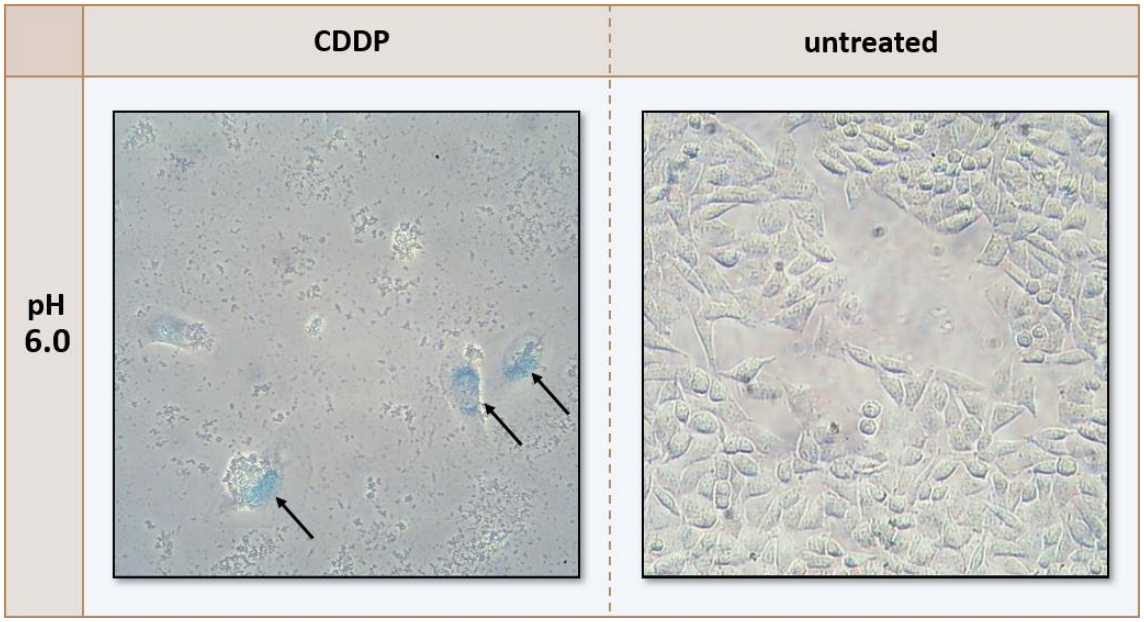

Figure 3.2.4-1 ***Representative pictures of senescence-associated β-galactosidase staining in melanoma cell line SBCL2.*** *Cisplatin treated cells (3.75 µM CDDP, 72 h, 2nd lot) followed the scheme for short-term chemotherapy and were fixed and stained at day 18 of the scheme at pH 6.0. For untreated control, untreated SBCL2 cells were fixed and stained at pH 6.0 96 hours after seeding. All images were taken at 20x magnification. Arrows indicate examples of clearly blue cells.*

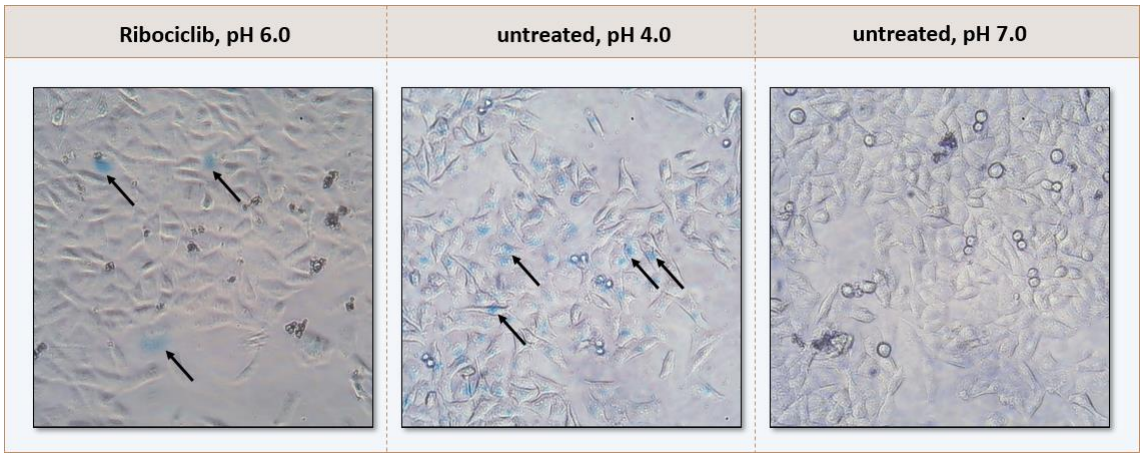

Figure 3.2.4-2 ***Representative pictures of senescence-associated β-galactosidase staining in melanoma cell line SBCL2 – control conditions.*** *For SA-β-gal positive control, cells were fixed and stained at pH 6.0, after 24 hours incubation with Ribociclib. For non-SA, lysosomal β-galactosidase control, parental SBCL2 cells were fixed and stained at pH 4.0. For bacterial β-galactosidase control, parental SBCL2 cells were fixed and stained at pH 7.0. All cells were fixed 96 hours after seeding. All images were taken at 20x magnification. Arrows indicate examples of clearly blue cells.*

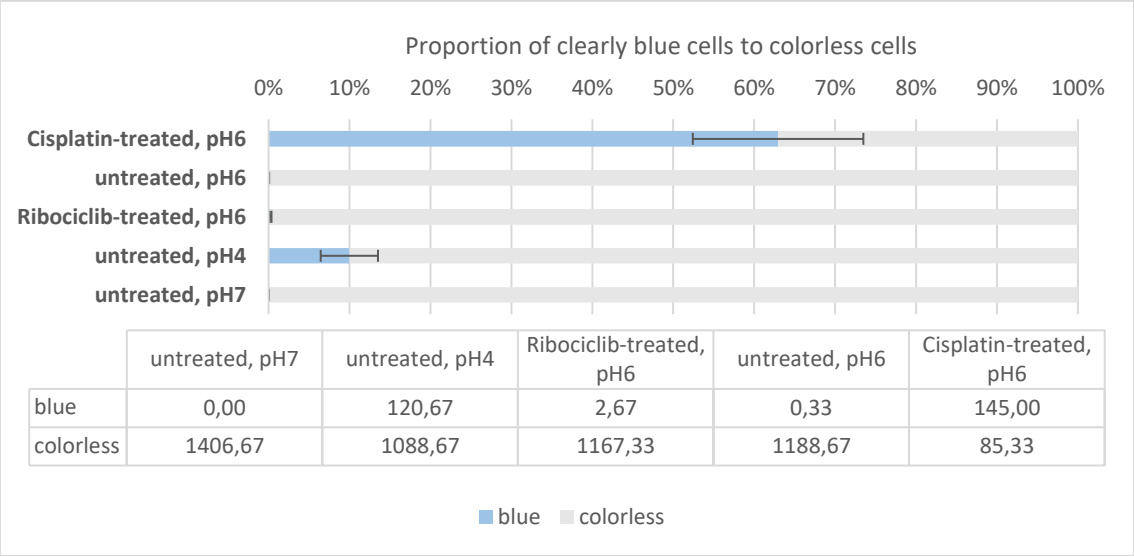

	untreated, pH7	untreated, pH4	Ribociclib-treated, pH6	untreated, pH6	Cisplatin-treated, pH6
blue	0,00	120,67	2,67	0,33	145,00
colorless	1406,67	1088,67	1167,33	1188,67	85,33

Figure 3.2.4-3 ***Quantitative analysis of senescence-associated β-galactosidase activity in melanoma cell line SBCL2.*** *Adjacent images, taken from representative areas of SBCL2 melanoma cells surviving under the different conditions, were aligned and counted out manually for blue and colorless cells. The stacked column bar represents the relative amount of β-gal positive (blue) and negative cells (colorless) in percent per condition. The table shows the means of the absolute cell numbers per area. For details on methods of quantification, see section 2.2.6. Conditions were applied and analyzed in triplicates (n=3; mean ± SD).*

3.3 Stimulation of cell cycle-arrested cells

3.3.1 Seeding on proteins of the extracellular matrix

The extracellular matrix (ECM) plays an important role in the microenvironment of a tumor cell, and interacts with the latter through complex connective structures, consisting mainly of proteins. Changes in the ECM, such as physiological remodeling by fibroblasts or stiffening due to pathological processes can be cues for tumor cells, resulting in a modulation of signaling pathways that can be related to the regulation of the cell cycle. Thereby, depending on its properties, the ECM can form a tumor cell niche, supportive or inhibitory to proliferation.

To find out, if the interaction of growth-arrested melanoma cells with proteins of the ECM could reverse the cell cycle arrest and trigger proliferation by simulating a supportive niche, CDDP treated SBCl2 melanoma cells from day 13 of the scheme and untreated SBCL2 cells were seeded on different proteins or protein

compositions constituting or resembling the ECM. The cells were observed, and proliferation was documented through continuous photo-documentation over four days from seeding and images were manually counted for cells after the experiment (see figure 3.3.1-1).

In contrast to untreated parental SBCL2 cells which proliferated readily, growth-arrested melanoma cells did not take up proliferation under any condition until day 4 from seeding. There seem to be differences in the success of adherence between the different coatings (compare mean number of cells on day 1 between growth-arrested on non-neutralized collagen I and on plastic). None of the proteins or protein compositions seems to be a putative stimulus for growth-arrested SBCL2 cells.

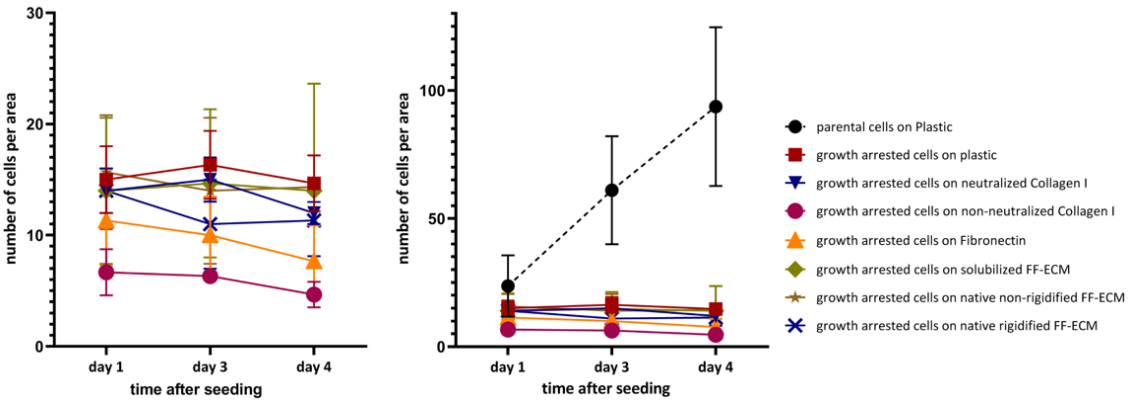

Figure 3.3.1-1 ***Mean numbers of SBCL2 cells per area over time after seeding on different proteins of the ECM in detail (left graph) and in comparison to cells seeded on plastic (right graph).*** *Untreated (parental) and treated SBCL2 cells were seeded in melanoma cell growth medium at 500 cells per well in 24 well plates on plastic (uncoated tissue culture dishes) or on tissue culture dishes coated with different proteins of the extracellular matrix (ECM). For details on coating and generation of primary fibroblast-derived ECM (FF-ECM), see section 2.2.4 and 2.2.5. For details on methods of quantification, see section 2.2.6. Conditions were applied and analyzed in triplicates (n=3; mean ± SD).*

Extracellular matrix proteins might present growth inhibitory cues to untreated melanoma cells and thus induce cellular dormancy. Parental cells of three different melanoma cell lines A375, SBCL2 and WM115 were seeded on gridded tissue culture dishes, coated with native or solubilized FF-ECM, or uncoated as control. Images of specific areas in the well were taken on day 2 and 3 after seeding, were counted out manually for cells and the results were compared (see figure 3.3.1-2).

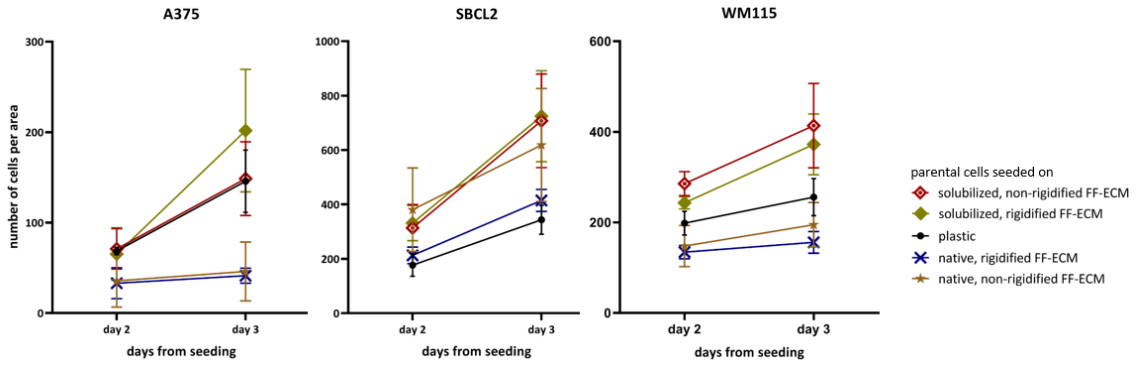

Figure 3.3.1-2 ***Quantitative analysis of untreated melanoma cells per area over time after seeding on different proteins of the ECM.*** *Untreated (parental) A375, SBCL2 or WM115 cells were seeded in melanoma cell growth medium at 500 cells per well in 24 well plates on plastic (uncoated tissue culture dishes) or on different forms of primary fibroblasts derived extracellular matrix (FF-ECM). For details on coating and generation of FF-ECM see section 2.2.4 and 2.2.5. Some of the tested melanoma cell lines grow in scattered colonies on some of the proteins of the ECM, which renders quantitative analysis of colony formation incomparable, therefore single cells were counted. For details on methods of quantification, see section 2.2.6. Conditions were applied and analyzed in triplicates (n=3; mean ± SD).*

All three cell lines show differences in cell number between the different conditions. In A375 and WM115, the increase in number of cells per area is higher when seeded on solubilized, rigidified or non-rigidified FF-ECM than when growing on plastic but lower when seeded on non-solubilized (native) either rigidified or non-rigidified FF-ECM. Proliferation of these cell lines seems to be inhibited when growing on FF-ECM in its native form, but enhanced, when seeded on coating of solubilized FF-ECM.

SBCL2 cell line shows a similar tendency. Seeded on solubilized, rigidified or non-rigidified FF-ECM, the increase in cell number from day 2 to day 3 is higher than when seeded on Plastic or native FF-ECM.

In general, the radial growth phase-derived melanoma cell line SBCL2 shows high plasticity when seeded on different proteins of the ECM which is reflected in different patterns of colony formation (see figure 3.3.1-3).

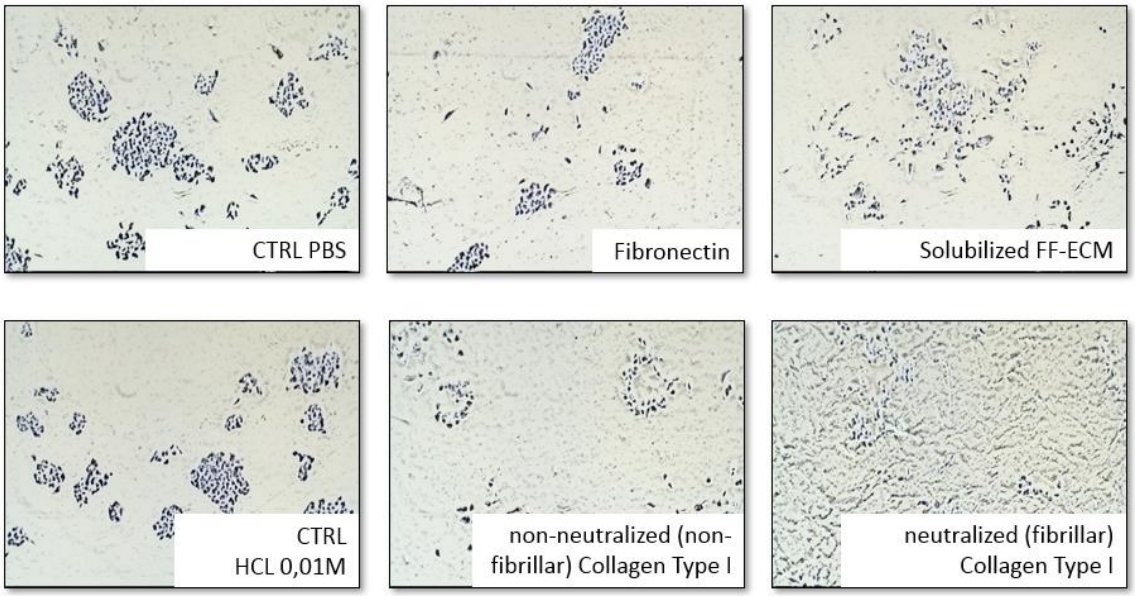

Figure 3.3.1-3 ***Representative images of melanoma cell line SBCL2 forming diverse types of colonies on different proteins of the ECM.*** *Untreated SBCL2 cells were harvested and seeded at 500 cells per well in 24 well plates on plastic (uncoated tissue culture dishes) incubated with DPBS or 0.01 M hydrochloride acid as controls or on different proteins of the extracellular matrix. Staining of native FF-ECM lead to strong background, images of colony formation on it are therefore not shown. For details on coating and generation of FF-ECM, see section 2.2.4 and 2.2.5. For details on staining of colonies with Crystal Violet, see section 2.2.6.*

3.3.2 Application of pro-proliferative humoral stimuli

Besides through physical contact, cells interact with their environment via secretion of soluble factors in an autocrine, paracrine or endocrine way. One group is the family of growth factors mediating initiation and limits of proliferation. Often tumor cells evade this regulation by becoming independent on growth factors resulting in an autonomous state as one mechanism of tumorigenicity. Rising evidence suggests induction and reversal of cellular dormancy being a complex integration of growth-inhibiting and growth promoting signals.

To investigate on possible cues potent enough to reverse cell cycle arrest in cells surviving short-term chemotherapy seeded in reduced-serum RPMI medium, populations showing no active proliferation on day 9 and 10 were exposed to a rise in fetal calf serum which is a mixture of different growth promoting factors to 10% of the medium as well as to single putatively growth-promoting humoral factors at high, but physiologic concentrations.

A375 and SBCL2 melanoma cells were seeded at 10^5 cells per well (A375) or $2*10^5$ cells per well (SBCL2) in 6 well plates and treated with 7.5 µM (A375) or 15 µM (SBCL2) Cisplatin (1st lot) following scheme for short-term chemotherapy in A375/SBCL2.10. On day 9 and day 10, plates were checked for colonies. When showing no proliferation on day 9 and 10, different humoral stimuli were added, and wells were observed every 2-3 days until day 20, appearing colonies were counted (Figure 3.3.2-1) and their location was documented (data not shown).

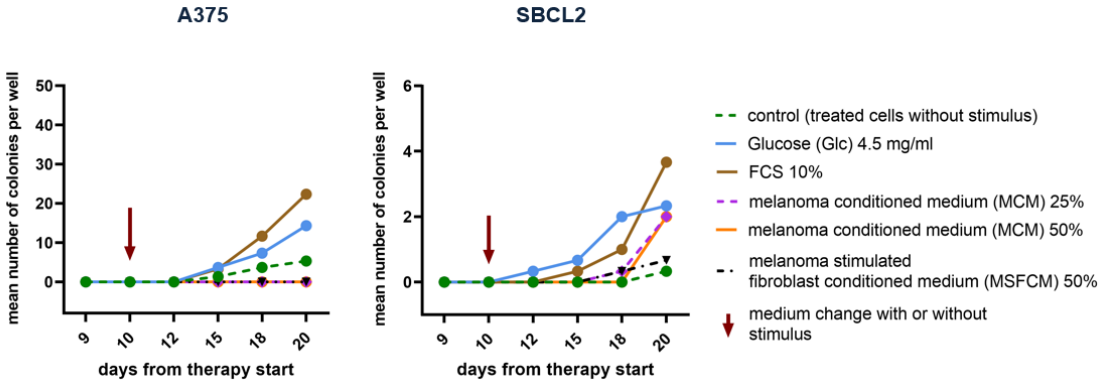

Figure 3.3.2-1 ***Mean numbers of colonies occurring over time after application of different humoral stimuli.*** *For clarity, standard deviation as well as statistical significance is not shown here, but in figure 3.3.2-2 for day 20. On plates without colonies appearing until day 10, cells were washed with serum-free RPMI medium and new reduced-serum RPMI medium non-supplemented or supplemented with stimuli as indicated in the legend was added. For details on generation of conditioned media see section 2.2.3. All conditions were applied in triplicates. Appearing colonies were counted in each condition and triplicate every 2-3 days until day 20 (n=3, mean)*

Within ten days from addition of different stimuli, colonies appeared under different conditions in this experiment. In general, A375 cells took up proliferation more readily than SBCL2 cells. Until day 20, a mean number of 5.33 A375 colonies per well and a mean number of 0.33 SBCL2 colonies appeared, where no stimulus was added to the medium (control). This suggests intrinsic mechanisms playing a role in overcoming short-term chemotherapy induced growth-arrest. There seem to be differences in the mean numbers of occurring colonies between the conditions, but on day 20 these are not significant in A375 (Figure 3.3.2-2). Though differences in mean numbers of colonies between elevation of fetal calf serum concentration (FCS 10%) in comparison to the control

population are significant in SBCL2 on day 20, mean numbers of colonies per well are relatively small (3.67 for FCS high; 0.33 for control).

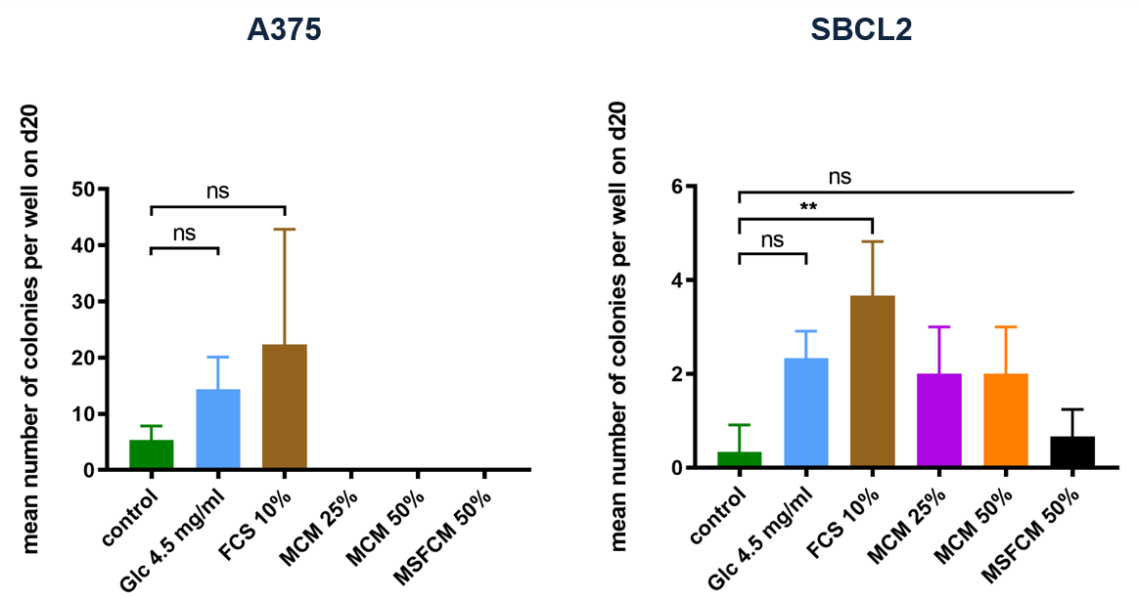

Figure 3.3.2-2 ***Mean number of colonies on day 20 after application of different humoral stimuli on day 10.*** *For experiments conditions, see Figure 3.3.2-1. Glucose high – 4.5 mg/ml D-Glucose, FCS high - 10% fetal calf serum, MCM - melanoma conditioned medium, MSFCM - melanoma stimulated fibroblast conditioned medium. For details on generation of conditioned media see section 2.2.3. Appearing colonies were counted in each condition and triplicates every 2-3 days until day 20 (n=3, mean ± SD). Significance was determined through an ordinary one-way ANOVA corrected through Tukey's test for multiple comparisons, differences were considered as significant with a p-value <0.05 (*), p<0.01 (**), ns – non-significant*

To put this into relation to the total number of surviving cells per well, staying growth-arrested at that time point, existing image matrices from day 20 were counted out manually for single cells. In average, among all conditions, 188.17 cells were counted per an area of 7.02 mm^2 (=1.4*10^6 $pixels^2$) (see table 3.3.2-1). This would be equivalent to 23,775.9 cells per well of a 6 well plate (8.87*10^2 mm^2 growth area according to the manufacturer).

Table 3.3.2-1 ***Quantitative analysis of total surviving cell number on day 20 under different conditions.***

Condition	Image name	Cell number
Control	d20 SBCL2.10 5.6	165
Glucose high	d20 SBCL2.10 5.3	199
FCS high	d20 SBCL2.10 5.4	244
MCM 25%	d20 SBCL2.10 5.5	213
MCM 50%	d20 SBCL2.10 5.2	144
MSFCM 50%	d20 SBCL2.10 5.1	164
Mean of all conditions		**188,17**

In both A375.10 and SBCL2.10, one whole plate per cell line showed colonies on day 9/10. In this plate, if feasible, colonies were counted over time until day 20 (figure 3.1-1) and medium taken off on day 10 was used as conditioned medium "repopulating cells supernatant", diluted 1:1 with fresh medium and added to growth-arrested cells on plates without colonies on day 9/10. Plates were observed and appearing colonies were counted (figure 3.3.2-3). Again, the mean numbers of appearing colonies was relatively small.

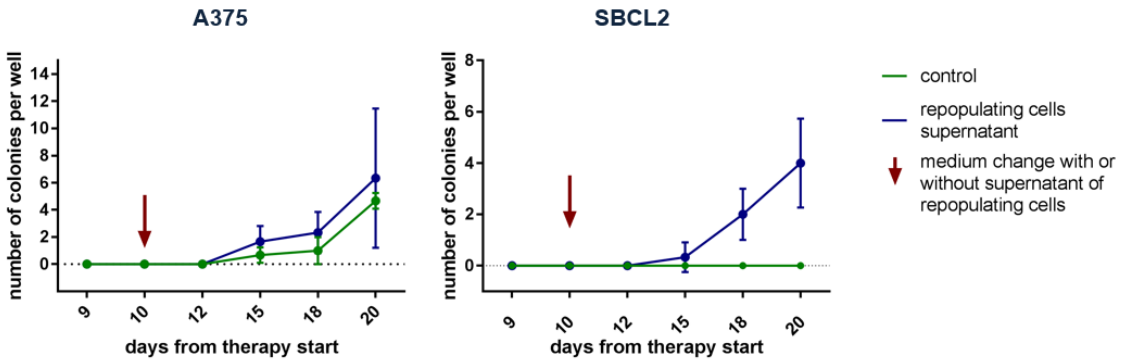

Figure 3.3.2-3 ***Mean number of colonies occurring over time after application of repopulating cells supernatant.*** *On plates without colonies appearing until day 10, cells were washed with serum-free RPMI medium and new reduced-serum RPMI medium non-supplemented or supplemented with 50% of repopulating cells supernatant (RCS) was added. For details on generation of RCS see section 2.2.3 (conditioned media). All conditions were applied in triplicates. Appearing colonies were counted in each condition and triplicate every 2-3 days until day 20 (n=3, mean ± SD)*

In further experiments, populations of growth-arrested cells did not take up proliferation and no colonies appeared after day 9/10 of the scheme neither with nor without addition of distinct stimuli such as growth factors and insulin. Furthermore, comparison of mean cell numbers of SBCL2 over time under different conditions, with either single, putatively pro-proliferative growth factors or no stimuli (control) added to the medium, did not reveal a significant difference between the conditions and cell numbers decreased consistently over time (figure 3.3.2-4).

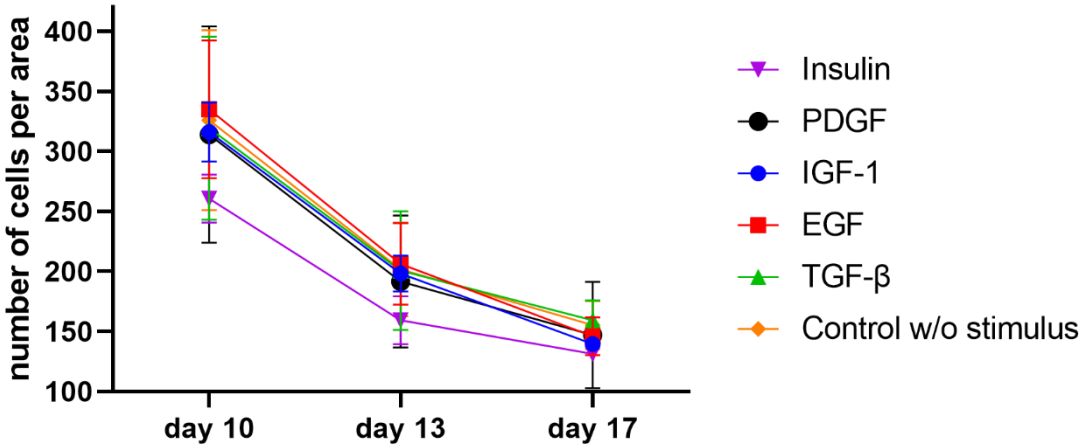

Figure 3.3.2-4 ***Quantitative analysis of cell number per area after application of different humoral stimuli on growth-arrested SBCL2 cells.*** *Melanoma cells SBCL2 followed the scheme for short-term chemotherapy in experiment SBCL2.21. On day 10 and 13, cells were washed once with serum-free RPMI medium and new reduced-serum RPMI medium supplemented with 10 µg/ml Insulin, 100 ng/ml PDGF, 100 ng/ml IGF-1, 20 ng/ml EGF, 5 ng/ml TGF-β or non-supplemented reduced-serum RPMI medium (Control without [w/o] stimulus) was added. No colonies appeared until day 21 under any of the applied conditions, therefore single cells were counted. For details on methods of quantification, see section 2.2.6. All conditions were applied and analyzed in triplicates (n=3; mean ± SD)*

4 Discussion

4.1 Clinical relevance and usefulness of the established dormancy model

The last decade brought development and approval of new therapeutic options for melanoma in advanced stages, namely targeted therapy (inhibitors of mutated B-RAF and wild-type MEK) and immunotherapy (anti-CTLA4, anti-PD1 and anti-PD-L1 antibodies). In advanced stages, these new treatments introduced an impressively prolonged survival from a median overall survival of 9 months to 2 years and even higher (Luke et al., 2017).

Despite the numerous adverse effects that melanoma patients can encounter following these new treatments, the latter signify an immense improvement compared to conventional chemotherapy, radiotherapy, Interleukin-2 and Interferon α-2b, which were the only and yet poor hope to most of the patients with advanced melanoma and doctors for a long time (Domingues et al., 2018).

Nevertheless, melanoma is far from being defeated as recurrence or non-responsiveness occurs in a high number of patients. New therapeutic options such as Ipilimumab (anti-CTLA4) or Dabrafenib (mutated B-RAF inhibitor) in combination with Trametinib (MEK inhibitor) prolong recurrence-free survival (Kwak et al., 2019) and thus, by definition, the period of clinical dormancy. With the development of new, effective treatments, tumor dormancy and the understanding of its underlying biological mechanisms is critical and gets more and more important. At the moment, adjuvant therapy is indicated for high risk patients after complete resection of the primary tumor and local or regional metastasis which accounts for stage III and some stage II or IV melanoma patients. So far, there is no data on benefits in RFS for Immune Checkpoint-blockade or BRAF-targeted therapy in “low risk” stage II melanoma patients (Sullivan et al., 2018). Ongoing clinical trials intend to investigate on the question, if adjuvant therapy might even offer a benefit in localized melanoma as for example for Immunotherapy (“Nivolumab in treating patients with stage IIB-IIC melanoma that can be removed by surgery” phase 2 study at Sidney Kimmel Cancer Center, NCT03405155). Its outcome will be interesting for research in

minimal residual disease and tumor dormancy. Together with improved follow-up screenings it will show if current adjuvant therapy is enabling for complete eradication of DTCs and micro-metastases and/or prolongs recurrence-free survival and increases the risks for late and ultra-late recurrence.

The mechanisms of melanoma therapies inducing cell cycle arrest are still poorly understood, and studies focus mainly on senescence induction, resulting in SASP and its influence on malignant and non-malignant cells in vicinity.

As senescence is more extensively characterized than quiescence when it comes to associated changes in protein expression and secretion as well as morphology that are linked to the phenotype, identification of and investigation on senescent cells is a lot easier than it is for quiescent cells. But senescence is - by definition - an irreversible cell cycle arrest and would therefore not fully explain multifactorial late recurrence of melanoma. Besides acquired resistance mechanisms, quiescence as the - by definition - reversible form of cell cycle arrest is a feature that might contribute to tumor dormancy and late recurrence in melanoma. Until now, there are no such markers associated with the reversibly growth-arrested quiescent cells as there are for senescence. This lack hinders straight-forward *in vitro* studies which is reflected by the limited number of specifically dormancy-related publications in melanoma. Hence, the few reviews thematizing cellular dormancy in melanoma are limited to a comparison of molecular mechanisms of cellular dormancy in other cancer entities and characteristics of melanoma cells fitting into the former (Ossowski and Aguirre-Ghiso, 2010; Senft and Ronai, 2016).

The aim of this study was to establish an in-vitro model for cellular dormancy in cutaneous malignant melanoma. Applying Cisplatin as short-term chemotherapy in combination with a reduction of serum in the cell culture medium, the melanoma cell line SBCL2 was reproducibly and stably growth-arrested under specific conditions, whereas in cell lines WM115 and A375 growth arrest could not be reproducibly induced. The combination of optimized treatment conditions as well as observation and continuous photo-documentation of the growth-

arrested cells in specific areas over time enabled for a simple real-time imaging-like analysis.

The advantages of this model are diverse. First of all, the same population of melanoma cells is followed over a long period of time, better reflecting the clinical reality, where disseminated cells may stay growth-arrested for months and years before they eventually re-proliferate or die. Furthermore, the development of the cells in terms of morphology can be tracked over time. Depending on the interval chosen for continuous photo-documentation and migratory ability of the specific cell line, colonies and even single cells can be followed. Cell number within representative areas of the tissue culture dish can be determined without harvesting and reseeding the cells, thus guaranteeing the observation and analysis of the exact same population at all time. Another advantage is the possibility to observe the reaction of a subpopulation to a specific stimulus at different time points regarding viability and cell death as well as proliferation through cell and colony number development. Metabolism of chemotherapy-treated cells is often altered (Li et al., 2014; Shirmanova et al., 2017). Most of the current proliferation assays, usable in a high throughput setting, reflect relative cell number development through measurement of enzyme activity or energy accessibility (NADH etc.). As these metabolic parameters might be changed after short-term chemotherapy, we established this model to ensure independence from such factors.

The use of tissue culture dishes gridded in an easy recognizable manner enables for exact orientation within the well and observation of the same area at all time points. Still, as plates were moved and images taken manually, congruence of the photographed images could only be guaranteed through cropping of congruently assembled image stacks to the biggest common area. Furthermore, cells had to be counted manually, as an automated process of cell counting by a trainable program (such as WEKA trainable segmentation) turned out to require powerful hardware equipment and thorough validation.

These two aspects make our method rather time consuming and less suitable for a high throughput in daily routine and should be pointed out as disadvantages of our model.

One point of critique regarding the clinical relevance of this model could be the choice of Cisplatin as the cell cycle arrest inducing agent. Nowadays, chemotherapy is recommended as a second-line therapy of metastatic melanoma in case of resistance to immunotherapy or targeted therapy or as first-line therapy in countries without access to the new treatments, but not in an adjuvant setting for stage II or III melanoma patients (Garbe et al., 2016), where tumor dormancy might have a higher impact on the patient's prognosis (see section 1.2.1). In our experiments, Cisplatin reproducibly induced a stable and homogenous cell cycle arrest in melanoma cell line SBCL2 under optimized conditions, which renders it a reliable methodological tool for investigation on cellular dormancy and recurrence. Melanoma cells treated with inhibitors against mutated B-RAF, namely A375 melanoma cells treated with Vemurafenib, re-proliferated shortly after therapy removal (data not shown). For even higher clinical relevance of our model, optimization including targeted therapy would be appropriate - a concrete suggestion for such an experiment is depictured below (see section 4.4).

However, the currently minor role of chemotherapy in treatment of malignant melanoma might also evolve into treatment regimens combining first-line, targeted therapies with chemotherapy, as melanoma cells resistant towards mutant B-RAF inhibitors (Vemurafenib) and MEK inhibitors (Trametinib) show a higher susceptibility to Cisplatin and Carboplatin (Makino et al., 2018). In the case of prolonged recurrence-free survival following these combined therapies, chemotherapy-mediated tumor dormancy would then gain in importance in melanoma.

4.2 Cellular dormancy versus or together with senescence?

In contrast to breast and prostate cancer, the debate about tumor dormancy in melanoma is very controversial. With the establishment of the SA-β-gal assay in replicative-senescent fibroblasts, more and more features, among others the senescence-associated secretory phenotype (SASP), altered patterns in

expression of Cyclin-dependent kinase inhibitor proteins (p16, p21), appearance of γH2AX foci and loss of Lamin B1 could be linked to the phenotype of classical senescence (Zhao et al., 2017). Hence, several tools to identify putatively senescent tumor cells, which are by definition irreversibly cell cycle-arrested, exist.

The SBCL2 cell line was the only one among three tested, were a stable growth-arrest in surviving cells under optimized conditions could be reproducibly induced and it was therefore chosen for further investigation on kinetics and characteristics at later time points by cell cycle analysis on day 17 and senescence-associated β-galactosidase staining on day 18 of the scheme for short-term chemotherapy (see section 2.2.2). The outcome of these further experiments actually raises even more questions since the results do not directly fit into the classical understanding of senescence in melanoma.

Cell cycle analysis through DNA content measurement in flow cytometry revealed that melanoma cells of the different cell lines undergo apoptosis at all time points of the scheme for short-term chemotherapy. As the used medium (day 3 to day 10 and day 10 to day 17 (in SBCL2 only) is also analyzed for cellular events, floating yet not disintegrated cells are considered as well as attached cells. Thus, all cells undergoing apoptosis are determined as belonging to the fraction of subG1-phase hence being apoptotic. Here, it should be noted that also the subG1-fraction in A375 (14.92%) and SBCL2 (17.80%) of the untreated control cells (see figure 3.2.2-1 and table 3.2-1) is elevated in comparison to usual apoptotic rates of <5% in these cell lines under control conditions in our laboratory (Sinnberg et al., 2016; Makino et al., 2018), which might be due to the transition from maintenance in melanoma cell growth medium containing 10% FCS to reduced-serum RPMI medium containing 2% FCS. Proliferation, however, was not impaired upon this transition (see figure 3.1-4)
SBCL2 cells surviving on day 10 (dead cells are washed away through medium change) are growth-arrested in G2/M-phase and mainly undergo apoptosis until day 17. The majority of the viable population on day 17 is still growth-arrested in

G2/M-phase but there is a considerable shift versus G0/G1-phase. If this shift, which would explain the relatively high number of SA-β-gal-positive cells (see below) on day 18, is a regular phenomenon could only be confirmed by further experiments. In this current, limited state of knowledge, there is only one possible explanation for a shift in the determined distribution of the population in the cell cycle. G0/G1-arrested cells might be less predisposed for enrolling the apoptosis program than G2/M-arrested cells and the G0/G1-arrested cell fraction would be more likely to survive until day 17. Indeed, *in vitro* models suggest senescence as an alternative mechanism to apoptosis in cancer cells (Yang et al., 2017) and that senescent cells are refractory to pro-apoptotic signals under some conditions (Wang, 1995).

But how to explain the discrepancy between cell cycle analysis and SA-β-gal staining? Manual cell counting of blue and colorless cells on representatively taken images of treated SBCL2 cells showed that 62.95% (±10.54% SD) of the cells were clearly blue, suggesting that more than half of the growth-arrested cells are senescent. Senescence is commonly described as an irreversible cell cycle arrest in G1-phase. Though others indeed confirm the induction of senescence in melanoma cell lines such as A375 and B16F10 by chemotherapy (Sun et al., 2018), cell cycle analysis of SBCL2 cell line on day 17 of the scheme for short-term chemotherapy shows only 28.06% of the viable cells in G1-phase, whereas more than half of the viable cells (53.49%) is still located in G2/M-phase.

Cell cycle exit and senescence induction from G2/M might be the answer. In fact, despite the predominant understanding of senescence as a G1-phase arrest, this other scenario is also plausible and supported by several findings in benign and malignant cells as reviewed by others (Gire and Dulic, 2015). As the molecular mechanisms behind the elevated β-galactosidase activity in senescent cells are still unknown, a possible display of this senescence-associated feature in G2/M cannot be excluded.
If increased SA-β-galactosidase activity was only feasible when coupled to G1-phase specific gene expression, a progression in the cell cycle from G2/M-phase

through bypassing the mitotic phase and staying growth-arrested in a 4N-G1-phase, where the checkpoint is supposed to be more efficient than the one hindering mitosis enrolment, could be conceivable (Gire and Dulic, 2015). The DNA content determining PI staining intensity of such a cell would be equivalent to one in G2/M-phase and thus appear in the gate among cells of the latter, thus leading to the discrepancy in our results between cell cycle analysis and SA-β-gal staining.

It is conceivable that in CDDP treated melanoma cells, such as SBCL2, senescence would be induced through DNA damage response (DDR) mechanisms and in consequence through p53, which upregulates the expression of p21, PML, PAI-1, DEC1 and numerous other effectors connected to the senescent phenotype (Qian and Chen, 2013). As in the G1-phase arrest, p21 would activate pRB through inhibition of cyclin D1-Cdk4/6 complexes. Instead of executing its major role in coupling E2F1 for G1-phase arrest, for enrolling the G2-phase arrest senescence program, pRB would mainly repress genes enabling G2/M progression. For both scenarios, p16 is mentioned as stabilizing and thus maintaining the cell cycle arrest (Gire and Dulic, 2015).

Indeed, as shown by others, A375 melanoma cell line, expressing p16 and treated with 2 μM CDDP for 24 hours, is driven into senescence via p53 activation and p21 upregulation (Sun et al., 2018). In this model, p21 expression is upregulated by ~14-fold on mRNA level three days after taking off the therapy, whilst the upregulation shrinks to ~7-fold within three other days. p53 and p16 mRNA expression is not significantly altered at the two time points in comparison to the basic level in untreated cells. Whilst p53 activity is regulated mainly post-transcriptionally and therefore its mRNA level is not of such immediate importance, p16 mRNA expression beyond regression of p21 on day six after therapy removal would have been interesting. The authors admit that at 2 μM CDDP treatment for 24 hours some cells escape senescence and form colonies 6 days after taking off the treatment and for p21 in A375 cells treated with the higher concentrations of CDDP, the authors unfortunately do not present mRNA expression data.

In the SBCL2 melanoma cell line, the CDKN2A gene, encoding for Cyclin dependent kinase inhibitor (CKI) protein p16, carries deletions at the three exon sites 1α, 2 and 3 (Sini et al., 2018). As mentioned above, p16 is a protein that plays a major role in stabilization and maintenance of cellular senescence (Gire and Dulic, 2015).
These facts taken together raise the question, if the function of p16 is impaired in this cell line and if so, how cellular senescence is maintained for such a long period of 14 days in our model.
Our study does not elucidate how the growth arrest, the distribution in the cell cycle and SA-β-gal-activity are orchestrated on mRNA and protein level. All three cell lines tested, A375, WM115 and SBCL2, carry the wild-type form of the gene TP53, encoding for p53 (Catalogue of somatic mutations in cancer 2019, Sanger Institute, https://cancer.sanger.ac.uk/cosmic, accessed 11/10/2019). Hence, it would be interesting, upon which path SBCL2 cells following the scheme for short-term chemotherapy would embark after inactivating p21 or p53, if they would undergo apoptosis or re-proliferate. Intriguingly, it has been shown that irreversibility of replicative senescence in fibroblasts is depending on p16 expression, as cells with low levels of p16 reproliferated upon p53 inactivation (Beauséjour et al., 2003).

Another feature of senescent cells is their changed morphology in comparison to parental cells. They are described as having a flattened appearance and an increased cell size (Zhao et al., 2017).
Images of CDDP treated cells on day 17 (SBCL2) or day 15 (A375) show cells with an enlarged cytoplasm in comparison to untreated parental cells on the same days under a brightfield microscope (see figure 3.2.1-1). Under the fluorescence microscope, CDDP treated cells on day 10 show enlarged nuclei (Yo-Pro-1 in SBCL2) and cytoplasms (brightfield in WM115, A375) in comparison to parental cells on day 3, which would also underline a senescence-like morphology (see figures 3.2.3-1 and 3.2.3-2). Some CDDP treated SBCL2 cells on day 18, stained for SA-β-gal and being clearly blue look like passing over directly into the

background, missing a sharp cell border in comparison to untreated cells, which suggests a flattened appearance and thereby a senescent phenotype.

Representative images of anti-PCNA immunofluorescence staining and Yo-Pro-1 staining show that most of CDDP treated cells on day 10 still express PCNA in comparison to parental cells, but the limited number of cells on the images taken, hinders a meaningful quantification and comparison. Still, given the representability of the images taken, a discussion of the results seems appropriate.

PCNA expression varies throughout the cell cycle. Whilst it is highly expressed during S-phase, G0/G1-arrested cells do not express PCNA on a significant level. G2/M-cells show a reduced level of PCNA in comparison to cells in S-phase but a higher one than G0/G1-arrested cells (Kurki et al., 1986).

PCNA is also involved in repair mechanisms in response to DNA damage mediated by Cisplatin (Canman et al., 2014). Therefore, its expression in CDDP-treated cells on day 10 of our model cannot be linked exclusively to either location of the cells in the cell cycle or repair mechanisms that might still be active at this relatively late time point.

Further investigation on repair mechanism kinetics throughout the scheme would be necessary. Though, it should be pointed out that CDDP treated cells, which are PCNA positive also show an enlarged nucleus and cytoplasm and an indistinct cell border that in turn is linked to the senescent phenotype, where cells would be - traditionally seen - arrested in G0/G1. However, PCNA-associated partner KIAA0101 and PCNA-interacting partner PARPBP and PCNA itself are repressed in senescent cells (Collin et al., 2018).

If an active involvement of PCNA in repair mechanisms at the late time point could be excluded, measurable PCNA expression would support the idea of cell cycle exit and senescence induction in G2/M-phase in melanoma cells following short-term chemotherapy with Cisplatin.

One could express the doubt that chemotherapy is known to induce senescence in melanoma cells (Sun et al., 2018) and pro-proliferative stimulation of growth-

arrested cells is therefore groundless with respect to the irreversibility of senescence. Nonetheless, two basic reflections justify our approach.

Firstly, the irreversibility of the cell cycle arrest in senescent cells and thus of senescence itself is repeatedly questioned among experts in the field. Some studies showed that subpopulations of tumor cells can actually escape therapy-induced senescence (Yang et al., 2017; Saleh et al., 2019). Using etoposide treated small lung cancer and colon carcinoma cell lines enriched for SA-β-gal highly positive cells, Saleh and colleagues prove recovery of proliferative capacity and loss of the senescent phenotype in a subset of cells *in vitro*. Furthermore, cell populations enriched for SA-β-gal highly positive cells were able to form tumors in immunodeficient as well as immunocompetent mice (Saleh et al., 2019).

Secondly, assuming senescence to be irreversible, cell populations showing a homogeneous growth arrest might still be heterogeneous in the matter of the type of their cellular dormancy. Around two fifth of SBCL2 cells following the scheme for short-term chemotherapy and stained for SA-β-gal activity were colorless yet non-cycling, suggesting them to be quiescent and ready to reproliferate upon the appearance of a potent stimulus.

Senescence is a dynamic state with different depths such as pre- or early senescence and deep senescence (Lee and Schmitt, 2019). Recovery from DNA damage and escape from senescence program enrolment might be possible at an early time point of the program but not anymore when cells are in deep senescence. As described above, expression of functional p16 is critical for maintenance of G2/M-senescence but not necessary for its induction where p53 and p21 play major roles (Gire and Dulic, 2015).

Similarly, in benign nevi, oncogene-induced senescence has been proposed to be a major mechanism for tumor suppression (Michaloglou et al., 2005) and senescent melanocytes often show increased p16 expression which is lost in nevi upon malignant transformation (Gray-Schopfer et al., 2006). However, p16 seems not to be required for senescence induction or maintenance in melanocytes, but irreversibility of the cell cycle arrest might be questionable, as

presence of heterochromatin foci was lower in p16 negative, senescent melanocytes (Haferkamp et al., 2009).
All in all, further investigation into expression patterns of these actors throughout the scheme for short-term chemotherapy could reveal a better timepoint for stimuli application, where a senescent cell might be more susceptible for pro-proliferative stimulation and would eventually re-enter cell cycle prior to the appearance of a potent stimulus.

Not only the unclear functional status of p16, but various other reasons that will shortly be presented in the following, render the low-aggressive, RGP-derived melanoma cell line SBCL2 most interesting for further investigation on dormancy mechanisms. SBCL2 is a cell line carrying an N-RAS mutation, which is present in 15-20% of melanomas and connected to a poor prognosis whilst therapeutical options are limited (Muñoz-Couselo et al., 2017). Elucidation of the mechanisms behind the induction and maintenance of cell cycle arrests independent on the mutational status might offer new treatment options even for this sub-group of patients.
SBCL2, among other cell lines derived from localized melanomas, was shown to have a lower pro-proliferative effect on hepatic stellate cells (HSC) than cell lines from metastasized melanoma. HSC are considered as forming a pro-metastatic niche in the liver (Meyer et al., 2017). This suggests that DTCs from an early cutaneous melanoma, which the SBCL2 cell line could be representative for, might fail in priming the microenvironment and, as a mechanism of survival, become quiescent. If here the acquisition of growth promoting mutations at secondary sites, as described for malignant cells in the lymph node (Werner-Klein et al., 2018), could play a role in dormancy escape, remains to be elucidated.
An external factor that could be critical for the switch from cellular dormancy to metastatic growth for early DTCs might be hypoxia, that is usually associated with limitation for metastasis outgrowth prior to angiogenic switch and thus rather (metastatic) dormancy inducing. In SBCL2 cells and melanocytes, hypoxia was shown to be negatively regulating Pigment epithelium-derived factor (PEDF), which is in turn associated with proliferation inhibiting behavior (Fernández-Barral

et al., 2012). Thus, hypoxia could be used as a putatively pro-proliferative stimulus in our *in vitro* model (see figure 2.2.2).
To summarize, the SBCL2 melanoma cell line seems to be promising for further experiments to get new insights into cellular dormancy in melanoma, which should then be confirmed in further melanoma cell lines.

4.3 Attempts for waking up dormant cells

Simulation of a favorable niche did not lead to a prompt re-proliferation of the growth-arrested cells, neither by reseeding growth-arrested SBCL2 melanoma cells on different proteins of the extracellular matrix nor by addition of soluble, putatively pro-proliferative factors such as growth factors or insulin to growth-arrested A375 or SBCL2 melanoma cells.

At the transition of and as a reason for replacing the CDDP stock solution, A375 as well as SBCL2 populations treated under the same conditions acted differently regarding the aspect of re-proliferation as described above (see section 3.1). The existence of heterogeneity within the population of a cell line is generally accepted and to what extend it should be considered when assessing specific properties of a certain cell line and applying it to its primary origin is discussed elsewhere (Altschuler and Wu, 2010). We took advantage of this display of heterogeneity and used conditioned medium from populations with re-proliferating cells and added it to homogenously growth-arrested populations of the same cell line. Comparison with wells, where simple reduced-serum RPMI medium was added, revealed re-proliferation in both control and stimulated populations in A375 without a significant difference but in SBCL2 melanoma cell line only stimulated populations re-proliferated, though moderately. It is beyond question that these experiments need to be repeated in order to validate the results, but these first observations suggest that reproliferating cells might secrete soluble factors that “wake up” other dormant cells.
During the same experiment, different basic putatively pro-proliferative stimuli such as a higher concentration of FCS, glucose, different conditioned media from parental cells and fibroblasts were added to homogenously growth-arrested melanoma cells. Only FCS significantly increased the mean number of new

colonies appearing until day 20 of the scheme and the significant influence was restricted to cell line SBCL2. With an average of only 3.67 newly forming colonies, FCS (in comparison to 0.33 when no stimulus was added) cannot be declared as a potent stimulus, especially as the time frame of ten days after application of the different stimuli is relatively long. The significant difference appears particularly negligible when the number of colonies per well on day 20 is put into relation to the number of more than 20,000 solitarily staying cells in average per well, at the same time point.

Fetal calf serum contains various growth factors, rendering it an appreciated supplement to cell culture medium enhancing both viability and proliferation of mammalian cell lines. The moderately but significantly increased colony number in homogenously growth-arrested populations when the amount of FCS in the medium was increased, suggested that the serum might contain a specific growth factor at low concentrations which would be a potent stimulus at higher concentrations. Therefore, different growth factors were added at concentrations commonly used in *in vitro* studies to homogenously growth-arrested SBCL2 melanoma cells. Unfortunately, none of the applied growth factors led to re-proliferation in the population in terms of colony formation, and absolute cell number per area decreased under all conditions without a significant difference between them showing that none of the applied growth factors had an anti-apoptotic effect on CDDP treated SBCL2 cells.

Reseeding of CDDP treated growth-arrested SBCL2 melanoma cells on day 13 of the scheme on various proteins of the ECM and fibroblast derived extracellular matrix (FF-ECM) did not initiate progression in the cell cycle, which was reflected in the absence of a significant increase in cell number.

Interestingly, seeding of untreated parental cells of melanoma cell lines A375 and WM115 on non-solubilized (native) FF-ECM lead to a decreased number of cells counted per representative area, two and three days after seeding in comparison to cells seeded on uncoated tissue culture dishes (control setting) or coated dishes with solubilized FF-ECM. Furthermore, the increase in cell number from day 2 to day 3 was equal or higher when A375 or WM115 melanoma cells were

seeded on solubilized FF-ECM and lower when seeded on native FF-ECM in comparison to the control setting (seeding on uncoated growth area). This might reflect an at least partial growth inhibitory effect of fibroblast derived extracellular matrix in its native form and a possible induction of dormancy in melanoma cell lines A375 and WM115. As FF-ECM is mainly composed of fibronectin (Franco-Barraza et al., 2017), this would underline a role of fibronectin in tumor dormancy induction as stated by others (Tivari et al., 2015).

Of course, these results are only of preliminary nature and further investigation is required, especially because the experiment was carried out only once and the time frame within which assessment of proliferation took place was too short to prove a fundamental dormancy mechanism. Cells were seeded and maintained in complete RPMI medium supplemented with 10% FCS. A reduction to 2% FCS supplementation might strengthen the manifestation of a possible growth inhibitory effect of native FF-ECM on melanoma cell lines and recapitulate a harsh microenvironment of dormant DTCs.

4.4 Conclusions and Outlook

All in all, our established *in vitro* model enables for multifactorial investigation on cellular dormancy over several weeks (up to 21 days), reflecting more closely than others the clinical reality of late recurrence. The established model can be used to study the effect of different agents and stressors on melanoma cells with a focus on the ability of single cells to cope with and surmount cytotoxic effects.

Whilst a potent pro-proliferative stimulus reversing Cisplatin-induced cell cycle arrest in our *in vitro* model remains to be found, the diverse results of this study encourage questioning widely accepted theories of cellular dormancy regarding quiescence and senescence in cutaneous melanoma. This accounts especially for mechanisms of senescence induction and maintenance in melanoma cell line SBCL2 were expression of genes on a protein level, critical for the senescent state remain to be elucidated. Patterns in expression of cyclin-dependent kinase inhibitor proteins, such as p21 and p16, might differ between a reversible quiescent and an irreversible senescent state as well as vary depending on the depth of senescence in short-term chemotherapy treated melanoma cells. This

is only one of many missing pieces in the puzzle of tumor dormancy that open the opportunity for further investigation. Some others might be suggested to continue this study, such as the following.

Firstly, the scheme for short-term chemotherapy could be optimized for other therapeutical therapies, such as mutated B-RAF- and MEK-inhibitors (targeted therapy) to better depicture clinical relevance. Haferkamp et al. already showed effectiveness of Vemurafenib (selective inhibitor of mutated B-RAF) treatment to induce senescence in melanoma cells at low concentrations (Haferkamp et al., 2013). In their later work, this group focused on the pro-proliferative influence of the SASP of senescent cells, identifying FGF-1 as a fueling factor to proliferation of parental cells (Grimm et al., 2018).

This approach could be combined with SA-β-gal staining with lipophilic stain C12FDG rendering the fixation step obsolete and enabling for measurement of galactosidase activity of a viable population over time and detection of senescence escape as described for colon carcinoma, breast and small-cell lung cancer (Saleh et al., 2019).

Secondly, capacities of FF-ECM in its native form to induce cellular dormancy in different melanoma cell lines are going to be assessed and compared with solubilized FF-ECM and other proteins of the extracellular matrix used for coating. These melanoma cell populations will then be analyzed for their distribution in the cell cycle and other dormancy related characteristics.

Furthermore, growth inhibitory niches harboring dormant melanoma cells could be partially digested by different (metallo-)proteinases that are physiologically secreted by fibroblasts for ECM remodeling or pathologically by tumor cells prior to invasion as tested by others (Fang et al., 2016). Byrne et al. suggest, remodeling of the bone is related to alteration of the tumor niche and reactivation of dormant tumor cells from breast and prostate cancer as well as multiple myeloma (Byrne et al., 2018). The constant ECM turnover as in the bone might also account for other niches of DTCs such as the stroma of liver, brain, lungs and skin, where melanoma cells could tend to stay cell cycle-arrested prior to escaping dormancy and forming metastases upon changes in composition and organization of their microenvironment.

This study outlines the complexity of tumor dormancy and how diverse the mechanisms of cancer cells to cope with cellular stress and a changing microenvironment are. It remains important to find all pieces of the puzzle but also to put all known facts together and thereby finally getting the whole picture. With its unique nature of provenance and development, melanoma will definitely play a role on this route. Once tumor dormancy is completely understood, definite cure from cancer will become tangible.

5 Abstract

Introduction Many years after removal of the primary tumor, melanoma patients can face a severe recurrence of the malignancy. The appearing metastases at different organ sites most likely arise by reawakening of “dormant” tumor cells. The survival of the latter is attributed to an induced reversible cell cycle arrest. Although cellular dormancy in tumor cells is already known for decades, *in vitro* models to investigate the cellular mechanisms of dormancy and late recurrence in melanoma remain to be established. This study aimed to elaborate an *in vitro* model for cellular dormancy in cutaneous melanoma, recapitulating the latency of recurrence. We hypothesized that Cisplatin induces a stable cell cycle arrest in a subgroup of cells in different melanoma cell lines and further assumed this cell cycle arrest as being reliably reversible upon the addition of a specific stimulus.

Methods The establishment of our *in vitro* model included the optimization of the experimental setting and scheme, the analysis for different cell cycle arrest associated characteristics in the surviving cells and exposure of the latter to putatively pro-proliferative stimuli such as conditioned media of proliferating melanoma cells, specific growth factors or components of the extracellular matrix.

Results A cell cycle arrest was induced by treatment with Cisplatin in combination with the reduction of fetal calf serum in the medium in three different melanoma cell lines but stability, homogeneity, and reproducibility in the arrest accounted only for SBCL2 cells, treated under specific conditions. One week after therapy removal, all three cell lines showed a G2/M-arrest in the majority of cells in cell cycle analysis by flow cytometry. In surviving SBCL2 cells, this arrest was largely maintained until day 17 of the scheme for short-term chemotherapy. Whereas PCNA expression analysis by immunofluorescence reaction supports the idea of a G2/M-arrest, β-galactosidase staining and morphological characteristics of surviving SBCL2 cells on day 18 of the scheme suggests a senescent phenotype which is commonly associated with a G1-arrest. Neither the application of putatively pro-proliferative stimuli nor the seeding on different components of the extracellular matrix triggered cell cycle-arrested SBCL2 cells into ready re-proliferation.

Discussion and Conclusion The established *in vitro* model enables for multifactorial investigation on cellular dormancy over several weeks, reflecting more closely than others the clinical reality of late recurrence. A potent pro-proliferative stimulus reversing Cisplatin-induced cell cycle arrest in our *in vitro* model remains to be found. Still, the diverse results of this study already encourage widening commonly accepted theories of cellular dormancy in cutaneous melanoma.

6 Zusammenfassung

Einleitung Jahre nach der Entfernung des Primärtumors können Melanompatienten einen schweren Rückfall der Erkrankung erleiden. Die sich bildenden Metastasen gehen vermutlich auf wiedererweckte Schläferzellen zurück. Das Überleben dieser wird auf einen induzierten reversiblen Zellzyklusarrest zurückgeführt. Obwohl die Existenz von Schläferzellen seit Jahrzenten bekannt ist, gibt es bisher keine *in vitro* Modelle, um die zellulären Mechanismen der Schläferzellen im Melanom und ihre Reaktivierung zu untersuchen.

Das Ziel dieser Studie war es, ein solches *in vitro* Modell für Zellschlaf beim kutanen Melanom zu entwickeln, welches zudem die klinische Latenz widerspiegelt. Wir vermuteten, dass Cisplatin in einer Untergruppe von verschiedenen Zelllinien des Melanoms einen stabilen Zellzyklusarrest induziert und gingen weiter davon aus, dass dieser Arrest reversibler Natur ist und bei Zugabe spezifischer Stimuli zuverlässig aufgehoben werden kann.

Methoden Die Etablierung unseres *in vitro* Models beinhaltete die Optimierung des experimentellen Versuchsaufbaus und -ablaufs, die Analyse verschiedener Zellzyklus assoziierter Eigenschaften der überlebenden Zellen und die Stimulation letzterer mit mutmaßlich pro-proliferativen Faktoren wie beispielsweise konditionierten Medien proliferierender Melanomzellen, spezifischer Wachstumsfaktoren und Komponenten der extrazellulären Matrix.

Ergebnisse Durch Behandlung mit Cisplatin in Kombination mit einer Reduktion des Fetalen Kälberserums im Nährmedium konnte in drei verschiedenen Melanomzelllinien ein Zellzyklusarrest induziert werden, jedoch war dieser

lediglich bei der SBCL2 Zelllinie und unter spezifischen Bedingungen stabil, homogen und reproduzierbar. Eine Woche nach Beendigung der Therapie zeigte die Zellzyklusanalyse in der Durchflusszytometrie einen Arrest in der G2/M-Phase bei der Mehrzahl der Zellen aller drei Zelllinien. In den überlebenden SBCL2 Zellen wurde dieser Arrest größtenteils bis Tag 17 des Schemas für „short-term chemotherapy“ aufrechterhalten. Während die PCNA-Expressions-analyse durch Immunfluoreszenz die Idee eines G2/M-Arrests unterstützt, deutet die β-Galactosidasefärbung der an Tag 18 des Schemas überlebenden SBCL2 Zellen in Richtung des seneszenten Phänotyps, welcher eher mit einem G1-Arrest assoziiert wird. Weder die Applikation mutmaßlich pro-proliferativer Stimuli noch die Aussaat auf verschiedenen Bestandteilen der extrazellulären Matrix konnten zellzyklusarretierte SBCL2 Zellen zur Re-Proliferation anstoßen.

Diskussion und Schlussfolgerung Das etablierte *in vitro* Model ermöglicht eine vielseitige Untersuchung von Schläferzellen über mehrere Wochen. Mehr als andere Modelle kann dies die klinische Realität später Rückfälle abbilden. Ein wirksamer Stimulus zur Reaktivierung des Cisplatin-induzierten Zellzyklusarrests bleibt zu entdecken. Dennoch regen die vielfältigen Ergebnisse dieser Arbeit bereits dazu an, die weithin akzeptierten Theorien zu Schläferzellen im kutanen Melanom zu überdenken.

7 Bibliography

Aguirre-Ghiso, J. A.: (2007) '**Models, mechanisms and clinical evidence for cancer dormancy**', In: *Nature Reviews Cancer*. NIH Public Access, 7(11), pp. 834–846. doi: 10.1038/nrc2256.

Altschuler, S. J. and Wu, L. F.: (2010) '**Cellular Heterogeneity: Do Differences Make a Difference?**', In: *Cell*, 141(4), pp. 559–563. doi: 10.1016/j.cell.2010.04.033.

American Cancer Society, A. E., Karnell, L. H. and Menck, H. R.: (1998) ***Cancer.*** Published for the American Cancer Society by Wiley Subscription Services. Available at: https://deepblue.lib.umich.edu/handle/2027.42/34348 (Accessed: 22 June 2019).

Apalla, Z., Lallas, A., Sotiriou, E., Lazaridou, E. and Ioannides, D.: (2017) '**Epidemiological trends in skin cancer**', In: *Dermatology Practical & Conceptual*. Derm101.com, 7(2), pp. 1–6. doi: 10.5826/dpc.0702a01.

Arlo J. Miller, M. C. M.: (2006) '**Melanoma**', In: *The New England Journal of Medicine*, 355(1), pp. 51–65. doi: 10.19744/j.cnki.11-1235/f.2006.09.027.

Barkan, D., Kleinman, H., Simmons, J. L., Asmussen, H., Kamaraju, A. K., Hoenorhoff, M. J., Liu, Z.-Y., Costes, S. V, Cho, E. H., Lockett, S., Khanna, C., Chambers, A. F. and Green, J. E.: (2008) '**Inhibition of Metastatic Outgrowth From Single Dormant Tumor Cells by Targeting the Cytoskeleton**', In: *Cancer Res*, 68(15), pp. 6241–6250. doi: 10.1158/0008-5472.CAN-07-6849.

Barnhill, R. L., Piepkorn, M. W., Cochran, A. J., Flynn, E., Karaoli, T. and Folkman, J.: (1998) '**Tumor vascularity, proliferation, and apoptosis in human melanoma micrometastases and macrometastases**', In: *Archives of Dermatology*, 134(8), pp. 991–994. doi: 10.1001/archderm.134.8.991.

Beauséjour, C. M., Krtolica, A., Galimi, F., Narita, M., Lowe, S. W., Yaswen, P. and Campisi, J.: (2003) '**Reversal of human cellular senescence: Roles of the p53 and p16 pathways**', In: *EMBO Journal*, 22(16), pp. 4212–4222. doi: 10.1093/emboj/cdg417.

Böhme, I. and Bosserhoff, A.: (2019) '**Extracellular acidosis triggers a senescence-like phenotype in human melanoma cells**', In: *Pigment Cell & Melanoma Research*, 00, pp. 1–11. doi: 10.1111/pcmr.12811.

Braumüller, H., Wieder, T., Brenner, E., Aßmann, S., Hahn, M., Alkhaled, M., Schilbach, K., Essmann, F., Kneilling, M., Griessinger, C., Ranta, F., Ullrich, S., Mocikat, R., Braungart, K., Mehra, T., Fehrenbacher, B., Berdel, J., Niessner, H., Meier, F., van den Broek, M., Häring, H., Handgretinger, R., Quintanilla-Martinez, L., Fend, F., Pesic, M., Bauer, J., Zender, L., Schaller, M., Schulze-

Osthoff, K., Röcken, M.: (2013) '**T helper-1 cell cytokines drive cancer into senescence**', In: *Nature*, 494, pp. 361–367. doi: 10.1038/nature11824.

Braun, S., Kentenich, C., Janni, W., Hepp, F., de Waal, J., Willgeroth, F., Sommer, H. and Pantel, K.: (2000) '**Lack of Effect of Adjuvant Chemotherapy on the Elimination of Single Dormant Tumor Cells in Bone Marrow of High-Risk Breast Cancer Patients**', In: *Journal of Clinical Oncology*, 18(1), pp. 80–80. doi: 10.1200/JCO.2000.18.1.80.

Byrne, N. M., Summers, M. A. and McDonald, M. M.: (2018) '**Tumor Cell Dormancy and Reactivation in Bone: Skeletal Biology and Therapeutic Opportunities.**', In: *JBMR plus*. Wiley-Blackwell, 3(3), pp. 1–8. doi: 10.1002/jbm4.10125.

Cameron, M. D., Schmidt, E. E., Kerkvliet, N., Nadkarni, K. V., Morris, V. L., Groom, A. C., Chambers, A. F. and MacDonald, I. C.: (2000) '**Temporal progression of metastasis in lung: Cell survival, dormancy, and location dependence of metastatic inefficiency**', In: *Cancer Research*, 60(9), pp. 2541–2546

Canman, C. E., Kikuchi, S., Heath, R., Evison, B. J., Hashimoto, H., Hishiki, A., Fujii, N., Inoue, A., Shao, Y. and Actis, M.: (2014) '**A Small Molecule Inhibitor of Monoubiquitinated Proliferating Cell Nuclear Antigen (PCNA) Inhibits Repair of Interstrand DNA Cross-link, Enhances DNA Double Strand Break, and Sensitizes Cancer Cells to Cisplatin**', In: *Journal of Biological Chemistry*, 289(10), pp. 7109–7120. doi: 10.1074/jbc.m113.520429.

Chernysheva, Markina, Demidov, Kupryshina, Chulkova, Palladina, Antipova and Tupitsyn: (2019) '**Bone Marrow Involvement in Melanoma. Potentials for Detection of Disseminated Tumor Cells and Characterization of Their Subsets by Flow Cytometry**', In: *Cells*, 8(627), p. 1-9, doi: 10.3390/cells8060627.

Clark, W. H., Elder, D. E., Guerry, D., Epstein, M. N., Greene, M. H. and Van Horn, M.: (1984) '**A study of tumor progression: The precursor lesions of superficial spreading and nodular melanoma**', In: *Human Pathology*, 15(12), pp. 1147–1165. doi: 10.1016/S0046-8177(84)80310-X.

Collin, G., Huna, A., Warnier, M., Flaman, J.-M. and Bernard, D.: (2018) '**Transcriptional repression of DNA repair genes is a hallmark and a cause of cellular senescence.**', In: *Cell death & disease*. Nature Publishing Group, 9(259), pp. 1-14. doi: 10.1038/s41419-018-0300-z.

Dimri, G. P., Rubelj, I., Linskens, M., Scott, G., Lee, X., Acosta, M., Basile, G., Pereira-Smith, O., Roskelley, C. and Medrano, E. E.: (2006) '**A biomarker that identifies senescent human cells in culture and in aging skin in vivo.**', In: *Proceedings of the National Academy of Sciences*, 92(20), pp. 9363–9367. doi:

10.1073/pnas.92.20.9363.

Domingues, B., Lopes, J., Soares, P. and Populo, H.: (2018) '**Melanoma treatment in review**', In: *ImmunoTargets and Therapy*, 7, pp. 35–49. doi: 10.2147/itt.s134842.

Eyles, J., Puaux, A. L., Wang, X., Toh, B., Prakash, C., Hong, M., Tan, T. G., Zheng, L., Ong, L. C., Jin, Y., Kato, M., Prévost-Blondel, A., Chow, P., Yang, H. and Abastado, J. P.: (2010) '**Tumor cells disseminate early, but immunosurveillance limits metastatic outgrowth, in a mouse model of melanoma**', In: *Journal of Clinical Investigation*, 120(6), pp. 2030–2039. doi: 10.1172/JCI42002.

Fang, J. Y., Tan, S. J., Wu, Y. C., Yang, Z., Hoang, B. X. and Han, B.: (2016) '**From competency to dormancy: A 3D model to study cancer cells and drug responsiveness**', In: *Journal of Translational Medicine*. BioMed Central, 14(1), pp. 1–13. doi: 10.1186/s12967-016-0798-8.

Fernández-Barral, A., Orgaz, J. L., Gomez, V., del Peso, L., Calzada, M. J. and Jiménez, B.: (2012) '**Hypoxia negatively regulates antimetastatic PEDF in melanoma cells by a hypoxia inducible factor-independent, autophagy dependent mechanism**', In: *PLoS ONE*, 7(3), pp. 1–14. doi: 10.1371/journal.pone.0032989.

Ferrara, G., Partenzi, A. and Filosa, A.: (2018) '**Sentinel Node Biopsy in Melanoma: A Short Update**', In: *Dermatopathology*, 5(1), pp. 21–25. doi: 10.1159/000484892.

Fidler, I. J.: (1975) '**Properties of Malignant Cells**', In: *Cancer Re*, 35, pp. 218–224. Available at: http://cancerres.aacrjournals.org/content/35/1/218.full-text.pdf (accessed on 11/10/2019).

Forschner, A., Eichner, F., Amaral, T., Keim, U., Garbe, C. and Eigentler, T. K.: (2017) '**Improvement of overall survival in stage IV melanoma patients during 2011–2014: analysis of real-world data in 441 patients of the German Central Malignant Melanoma Registry (CMMR)**', In: *Journal of Cancer Research and Clinical Oncology*, 143(3), pp. 533–540. doi: 10.1007/s00432-016-2309-y.

Franco-Barraza, J., Beacham, D. A., Amatangelo, M. D., Cukierman, E. and Chase, F.: (2017) '**Preparation of extracellular matrices produced by cultured and primary fibroblasts**', In: *Current Protocols in Cell Biology*, 71, pp. 1–44. doi: 10.1002/cpcb.2.

Frangos, J. E., Duncan, L. M., Piris, A., Nazarian, R. M., Mihm, M. C., Hoang, M. P., Gleason, B., Flotte, T. J., Byers, H. R., Barnhill, R. L. and Kimball, A. B.: (2012) '**Increased diagnosis of thin superficial spreading melanomas: A 20-year study.**', In: *Journal of the American Academy of Dermatology*, 67(3), pp. 387–

94. doi: 10.1016/j.jaad.2011.10.026.

Garbe, C., Peris, K., Hauschild, A., Saiag, P., Middleton, M., Bastholt, L., Grob, J. J., Malvehy, J., Newton-Bishop, J., Stratigos, A. J., Pehamberger, H. and Eggermont, A. M.: (2016) '**Diagnosis and treatment of melanoma. European consensus-based interdisciplinary guideline - Update 2016**', In: *European Journal of Cancer*, 63, pp. 201–217. doi: 10.1016/j.ejca.2016.05.005.

Ghajar, C. M.: (2015) '**Metastasis prevention by targeting the dormant niche**', In: *Nature*, 15(4), pp. 238–247. doi: 10.1038/nrc3910.

Gire, V. and Dulic, V.: (2015) '**Senescence from G2 arrest, revisited**', In: *Cell Cycle*, 14(3), pp. 297–304. doi: 10.1080/15384101.2014.1000134.

Gray-Schopfer, V. C., Cheong, S. C., Chong, H., Chow, J., Moss, T., Abdel-Malek, Z. A., Marais, R., Wynford-Thomas, D. and Bennett, D. C.: (2006) '**Cellular senescence in naevi and immortalisation in melanoma: A role for p16?**', In: *British Journal of Cancer*. Nature Publishing Group, 95(4), pp. 496–505. doi: 10.1038/sj.bjc.6603283.

Griessinger, C. M., Schmid, A. M., Sonanini, D., Schörg, B. F., Jarboui, M. A., Bukala, D., Mucha, N., Fehrenbacher, B., Steinhilber, J., Martella, M., Kohlhofer, U., Schaller, M., Zender, L., Rammensee, H.-G., Quintanilla-Martinez, L., Röcken, M., Kneilling, M. and Pichler, B. J.: (2018) '**The administration route of tumor-antigen-specific T-helper cells differentially modulates the tumor microenvironment and senescence**', In: *Carcinogenesis*, 40(2), pp. 289–302. doi: 10.1093/carcin/bgy161.

Grimm, J., Hufnagel, A., Wobser, M., Borst, A., Haferkamp, S., Houben, R. and Meierjohann, S.: (2018) '**BRAF inhibition causes resilience of melanoma cell lines by inducing the secretion of FGF1**', In: *Oncogenesis*. Springer US, 7(9), pp. 1–12. doi: 10.1038/s41389-018-0082-2.

Haferkamp, S., Borst, A., Adam, C., Becker, T. M., Motschenbacher, S., Windhövel, S., Hufnagel, A. L., Houben, R. and Meierjohann, S.: (2013) '**Vemurafenib induces senescence features in melanoma cells**', In: *Journal of Investigative Dermatology*, 133(6), pp. 1601–1609. doi: 10.1038/jid.2013.6.

Haferkamp, S., Scurr, L. L., Becker, T. M., Frausto, M., Kefford, R. F. and Rizos, H.: (2009) '**Oncogene-induced senescence does not require the p16(INK4a) or p14ARF melanoma tumor suppressors.**', In: *The Journal of investigative dermatology*. Elsevier, 129(8), pp. 1983–91. doi: 10.1038/jid.2009.5.

Henriet, P., Zhong, Z.-D., Brooks, P. C., Weinberg, K. I. and DeClerck, Y. A.: (2000) '**Contact with fibrillar collagen inhibits melanoma cell proliferation by up-regulating p27KIP1**', In: *Proceedings of the National Academy of Sciences*, 97(18), pp. 10026–10031. doi: 10.1073/pnas.170290997.

Hüsemann, Y., Geigl, J. B., Schubert, F., Musiani, P., Meyer, M., Burghart, E., Forni, G., Eils, R., Fehm, T., Riethmüller, G. and Klein, C. A.: (2008) '**Systemic Spread Is an Early Step in Breast Cancer**', In: *Cancer Cell*, 13(1), pp. 58–68. doi: 10.1016/j.ccr.2007.12.003.

Jain, D., Singh, T., Kumar, N. and Daga, M. K.: (2007) '**Metastatic malignant melanoma in bone marrow with occult primary site - A case report with review of literature**', In: *Diagnostic Pathology*, 2(1), pp. 1–4. doi: 10.1186/1746-1596-2-38.

Jayson, G. C., Kerbel, R., Ellis, L. M. and Harris, A. L.: (2016) '**Antiangiogenic therapy in oncology: current status and future directions**', In: *The Lancet*, 388, pp. 518–529. doi: 10.1016/S0140-6736(15)01088-0.

Kaur, A., Ecker, B. L., Douglass, S. M., Kugel, C. H., Webster, M. R., Almeida, F. V., Somasundaram, R., Hayden, J., Ban, E., Ahmadzadeh, H., Franco-Barraza, J., Shah, N., Mellis, I. A., Keeney, F., Kossenkov, A., Tang, H. Y., Yin, X., Liu, Q., Xu, X., Fane, M., Brafford, P., Herlyn, M., Speicher, D. W., Wargo, J. A., Tetzlaff, M. T., Haydu, L. E., Raj, A., Shenoy, V., Cukierman, E. and Weeraratna, A. T.: (2019) '**Remodeling of the collagen matrix in aging skin promotes melanoma metastasis and affects immune cell motility**', In: *Cancer Discovery*, 9(1), pp. 64–81. doi: 10.1158/2159-8290.CD-18-0193.

Klein, C. A.: (2009) '**Parallel progression of primary tumours and metastases**', In: *Nature*. Nature Publishing Group, 9, pp. 1279–1283. Available at: https://doi.org/10.1038/nrc2627

Kurki, P., Vanderlaan, M., Dolbeare, F., Gray, J. and Tan, E. M.: (1986) '**Expression of proliferating cell nuclear antigen (PCNA)/cyclin during the cell cycle**', In: *Experimental Cell Research*, 166, pp. 209-219. doi: 10.1016/0014-4827(86)90520-3.

Kwak, M., Farrow, N. E., Salama, A. K. S., Mosca, P. J., Hanks, B. A., Slingluff, C. L. and Beasley, G. M.: (2019) '**Updates in adjuvant systemic therapy for melanoma**', In: *Journal of Surgical Oncology*. John Wiley and Sons Inc., 11(9), pp. 222–231. doi: 10.1002/jso.25298.

Lasithiotakis, K. G., Sinnberg, T. W., Schittek, B., Flaherty, K. T., Kulms, D., MacZey, E., Garbe, C. and Meier, F. E.: (2008) '**Combined inhibition of MAPK and mTOR signaling inhibits growth, induces cell death, and abrogates invasive growth of melanoma cells**', In: *Journal of Investigative Dermatology*. Elsevier Masson SAS, 128(8), pp. 2013–2023. doi: 10.1038/jid.2008.44.

Lawson, M. A., McDonald, M. M., Kovacic, N., Khoo, W. H., Terry, R. L., Down, J., Kaplan, W., Paton-Hough, J., Fellows, C., Pettitt, J. A., Dear, T. N., Van Valckenborgh, E., Baldock, P. A., Rogers, M. J., Eaton, C. L., Vanderkerken, K., Pettit, A. R., Quinn, J. M. W., Zannettino, A. C. W., Giang Phan, T. and Croucher, P. I.: (2015) '**Osteoclasts control reactivation of dormant myeloma cells by**

remodelling the endosteal niche', In: *Nature Communications*, 6(8983), pp. 1–15. doi: 10.1038/ncomms9983.

Lee, S. and Schmitt, C. A.: (2019) '**The dynamic nature of senescence in cancer**', In: *Nature Cell Biology*, 21(1), pp. 94–101. doi: 10.1038/s41556-018-0249-2.

Li, L., Dragulev, B., Zigrino, P., Mauch, C. and Fox, J. W.: (2009) '**The invasive potential of human melanoma cell lines correlates with their ability to alter fibroblast gene expression in vitro and the stromal microenvironment in vivo**', In: *International Journal of Cancer*, 125(8), pp. 1796–1804. doi: 10.1002/ijc.24463.

Li, S., Kennedy, M., Payne, S., Kennedy, K., Seewaldt, V. L., Pizzo, S. V. and Bachelder, R. E.: (2014) '**Model of tumor dormancy/recurrence after short-term chemotherapy**', In: *PLoS ONE*, 9(5), pp. 1–8. doi: 10.1371/journal.pone.0098021.

Luke, J. J., Flaherty, K. T., Ribas, A. and Long, G. V.: (2017) '**Targeted agents and immunotherapies: Optimizing outcomes in melanoma**', In: *Nature Reviews Clinical Oncology*. Nature Publishing Group, 24(8), pp. 463–482. doi: 10.1038/nrclinonc.2017.43.

Luzzi, K. J., MacDonald, I. C., Schmidt, E. E., Kerkvliet, N., Morris, V. L., Chambers, A. F. and Groom, A. C.: (1998) '**Multistep Nature of Metastatic Inefficiency**', In: *The American Journal of Pathology*, 153(3), pp. 865–873. doi: 10.1016/s0002-9440(10)65628-3.

MacKie, R. M., Reid, R. and Junor, B.: (2003) '**Fatal Melanoma Transferred in a Donated Kidney 16 Years after Melanoma Surgery**', In: *New England Journal of Medicine*. Massachusetts Medical Society , 348(6), pp. 567–568. doi: 10.1056/NEJM200302063480620.

Makino, E., Gutmann, V., Kosnopfel, C., Niessner, H., Forschner, A., Garbe, C., Sinnberg, T. and Schittek, B.: (2018) '**Melanoma cells resistant towards MAPK inhibitors exhibit reduced TAp73 expression mediating enhanced sensitivity to platinum-based drugs**', In: *Cell Death and Disease*. Nature Publishing Group, 9(930), pp. 1-13. doi: 10.1038/s41419-018-0952-8.

Marlow, R., Honeth, G., Lombardi, S., Cariati, M., Hessey, S., Pipili, A., Mariotti, V., Buchupalli, B., Foster, K., Bonnet, D., Grigoriadis, A., Rameshwar, P., Purushotham, A., Tutt, A. and Dontu, G.: (2013) '**A novel model of dormancy for bone metastatic breast cancer cells**', In: *Cancer Research*, 73(23), pp. 6886–6899. doi: 10.1158/0008-5472.CAN-13-0991.

Martinez, D., Li, Y., Carpenter, E. L., Attiyeh, E. F., Diskin, S. J., Kim, S., Parasuraman, S., Caponigro, G., Schnepp, R. W., Wood, C., Pawel, B., Cole, K. A. and Maris, J. M.: (2013) '**Dual CDK4/CDK6 Inhibition Induces Cell Cycle**

Arrest and Senescence in Neuroblastoma', In: *Clinical Cancer Research*, 19(22), pp. 1–16. doi: 10.1158/1078-0432.CCR-13-1675.Dual.

Matthews, N. H., Li, W.-Q., Qureshi, A. A., Weinstock, M. A. and Cho, E.: (2017) '**Epidemiology of melanoma**', in Ward, W. H. and Farma, J. M. (eds) In: *Cutaneous Melanoma: Etiology and Therapy*. Brisbane, Australia: Codon Publications, pp. 3–22. Available at: http://link.springer.com/10.1007/978-3-540-35106-1_28 (Accessed: 27 July 2019).

Meyer, T., Koch, A., Ebert, E. V., Czech, B., Mueller, M., Bosserhoff, A., Lang, S. A. and Hellerbrand, C.: (2017) '**Effect of melanoma cells on proliferation and migration of activated hepatic stellate cells in vitro**', In: *Pathology Research and Practice*, 213(4), pp. 400–404. doi: 10.1016/j.prp.2016.12.014.

Michaloglou, C., Vredeveld, L. C. W., Soengas, M. S., Denoyelle, C., Kuilman, T., Van Der Horst, C. M. A. M., Majoor, D. M., Shay, J. W., Mooi, W. J. and Peeper, D. S.: (2005) '**BRAFE600-associated senescence-like cell cycle arrest of human naevi**', In: *Nature*, 436(7051), pp. 720–724. doi: 10.1038/nature03890.

Morris, V. L., Percy, D. B., Lizardo, M. M., Chambers, A. F. and MacDonald, I. C.: (2013) '**Dormancy and metastasis of melanoma cells to lymph nodes, lung and liver**', In: *Tumor Dormancy, Quiescence, and Senescence: Aging, Cancer, and Noncancer Pathologies*. Springer Netherlands, pp. 63–78. doi: 10.1007/978-94-007-5958-9_6.

Muñoz-Couselo, E., Adelantado, E. Z., Ortiz, C., García, J. S. and Perez-Garcia, J.: (2017) '**NRAS-mutant melanoma: Current challenges and future prospect**', In: *OncoTargets and Therapy*, 10, pp. 3941–3947. doi: 10.2147/OTT.S117121.

Naumov, G. N., Akslen, L. A. and Folkman, J.: (2006) '**Role of angiogenesis in human tumor dormancy: Animal models of the angiogenic switch**', In: *Cell Cycle*, 5(16), pp. 1779–1787. doi: 10.4161/cc.5.16.3018.

Ossowski, L. and Aguirre-Ghiso, J. A.: (2010) '**Dormancy of metastatic melanoma**', In: *Pigment Cell and Melanoma Research*, 23(1), pp. 41–56. doi: 10.1111/j.1755-148X.2009.00647.x.

Parkin, D. M., Mesher, D. and Sasieni, P.: (2011) '**Cancers attributable to solar (ultraviolet) radiation exposure in the UK in 2010**', In: *British Journal of Cancer*, 105, pp. S66–S69. doi: 10.1038/bjc.2011.486.

Peppicelli, S., Andreucci, E., Ruzzolini, J., Laurenzana, A., Margheri, F., Fibbi, G., Del Rosso, M., Bianchini, F. and Calorini, L.: (2017) '**The acidic microenvironment as a possible niche of dormant tumor cells**', In: *Cellular and Molecular Life Sciences*, 74(15), pp. 2761–2771. doi: 10.1007/s00018-017-2496-y.

Qian, Y. and Chen, X.: (2013) '**Senescence Regulation by the p53 Protein Family**', In: *Methods in Molecular Biology*, 965, pp. 37–61. doi: 10.1007/978-1-62703-239-1_3.

Röcken, M.: (2010) '**Early tumor dissemination, but late metastasis: insights into tumor dormancy**', In: *Journal of Clinical Investigation*, 120(6), pp. 1800–1803. doi: 10.1172/JCI43424.

Saleh, T., Tyutyunyk-Massey, L., Murray, G. F., Alotaibi, M. R., Kawale, A. S., Elsayed, Z., Henderson, S. C., Yakovlev, V., Elmore, L. W., Toor, A., Harada, H., Reed, J., Landry, J. W. and Gewirtz, D. A.: (2019) '**Tumor cell escape from therapy-induced senescence**', In: *Biochemical Pharmacology*. Elsevier Inc., 162, pp. 202–212. doi: 10.1016/j.bcp.2018.12.013.

Schardt, J. A., Meyer, M., Hartmann, C. H., Schubert, F., Schmidt-Kittler, O., Fuhrmann, C., Polzer, B., Petronio, M., Eils, R. and Klein, C. A.: (2005) '**Genomic analysis of single cytokeratin-positive cells from bone marrow reveals early mutational events in breast cancer**', In: *Cancer Cell*, 8(3), pp. 227–239. doi: 10.1016/j.ccr.2005.08.003.

Senft, D. and Ronai, Z. A.: (2016) '**Immunogenic, cellular, and angiogenic drivers of tumor dormancy-a melanoma view**', In: *Pigment Cell and Melanoma Research*, 29(1), pp. 27–42. doi: 10.1111/pcmr.12432.

Shirmanova, M. V., Druzhkova, I. N., Lukina, M. M., Dudenkova, V. V., Ignatova, N. I., Snopova, L. B., Shcheslavskiy, V. I., Belousov, V. V. and Zagaynova, E. V.: (2017) '**Chemotherapy with cisplatin: Insights into intracellular pH and metabolic landscape of cancer cells in vitro and in vivo**', In: *Scientific Reports*. Nature Publishing Group, 7(8911), pp. 1–13. doi: 10.1038/s41598-017-09426-4.

Sini, M. C., Doneddu, V., Paliogiannis, P., Casula, M., Colombino, M., Manca, A., Botti, G., Ascierto, P. A., Lissia, A., Cossu, A. and Palmieri, G.: (2018) '**Genetic alterations in main candidate genes during melanoma progression**', In: *Oncotarget*, 9(9), pp. 8531–8541. doi: 10.18632/oncotarget.23989.

Sinnberg, T., Lasithiotakis, K., Niessner, H., Schittek, B., Flaherty, K. T., Kulms, D., MacZey, E., Campos, M., Gogel, J., Garbe, C. and Meier, F.: (2009) '**Inhibition of PI3K-AKT-mTOR signaling sensitizes melanoma cells to cisplatin and temozolomide**', In: *Journal of Investigative Dermatology*, 129, pp. 1500–1515. doi: 10.1038/jid.2008.379.

Sinnberg, T., Wang, J., Sauer, B. and Schittek, B.: (2016) '**Casein kinase 1α has a non-redundant and dominant role within the CK1 family in melanoma progression**', In: *BMC Cancer*. BioMed Central, 16(594), pp. 1–15. doi: 10.1186/s12885-016-2643-0.

Sosa, M. S., Bragado, P. and Aguirre-Ghiso, J. A.: (2014) '**Mechanisms of disseminated cancer cell dormancy: An awakening field**', In: *Nature Reviews Cancer*, 14(9), pp. 611–622. doi: 10.1038/nrc3793.

Strauss, D. C. and Thomas, J. M.: (2010) '**Transmission of donor melanoma by organ transplantation.**', In: *The Lancet. Oncology*, 11(8), pp. 790–6. doi: 10.1016/S1470-2045(10)70024-3.

Sullivan, R. J., Atkins, M. B., Kirkwood, J. M., Agarwala, S. S., Clark, J. I., Ernstoff, M. S., Fecher, L., Gajewski, T. F., Gastman, B., Lawson, D. H., Lutzky, J., McDermott, D. F., Margolin, K. A., Mehnert, J. M., Pavlick, A. C., Richards, J. M., Rubin, K. M., Sharfman, W., Silverstein, S., Slingluff, C. L., Sondak, V. K., Tarhini, A. A., Thompson, J. A., Urba, W. J., White, R. L., Whitman, E. D., Hodi, F. S and Kaufman, H. L.: (2018) '**An update on the Society for Immunotherapy of Cancer consensus statement on tumor immunotherapy for the treatment of cutaneous melanoma: Version 2.0**', In: *Journal for ImmunoTherapy of Cancer*. BioMed Central Ltd., 6(44), pp. 1–23. doi: 10.1186/s40425-018-0362-6.

Sun, X., Shi, B., Zheng, H., Min, L., Yang, J., Li, X., Liao, X., Huang, W., Zhang, M., Xu, S., Zhu, Z., Cui, H. and Liu, X.: (2018) '**Senescence-associated secretory factors induced by cisplatin in melanoma cells promote non-senescent melanoma cell growth through activation of the ERK1/2-RSK1 pathway article**', In: *Cell Death and Disease*, 9(260), pp. 1–15. doi: 10.1038/s41419-018-0303-9.

Tao, Y. F., Wang, N. N., Xu, L. X., Li, Z. H., Li, X. L., Xu, Y. Y., Fang, F., Li, M., Qian, G. H., Li, Y. H., Li, Y. P., Wu, Y., Ren, J. L., Du, W. W., Lu, J., Feng, X., Wang, J., He, W. Q., Hu, S. Y. and Pan, J..: (2017) '**Molecular mechanism of G 1 arrest and cellular senescence induced by LEE011, a novel CDK4/CDK6 inhibitor, in leukemia cells**', In: *Cancer Cell International*, 17(1), pp. 1–17. doi: 10.1186/s12935-017-0405-y.

Tivari, S., Korah, R., Lindy, M. and Wieder, R.: (2015) '**An in vitro dormancy model of estrogen-sensitive breast cancer in the bone marrow: A tool for molecular mechanism studies and hypothesis generation**', In: *Journal of Visualized Experiments*. Journal of Visualized Experiments, 2015(100), pp. 1–10. doi: 10.3791/52672.

Tivari, S., Lu, H., Dasgupta, T., De Lorenzo, M. S. and Wieder, R.: (2018) '**Reawakening of dormant estrogen-dependent human breast cancer cells by bone marrow stroma secretory senescence**', In: *Cell Communication and Signaling*, 16(48), pp. 1–18. doi: 10.1186/s12964-018-0259-5.

Townson, J. L., Ramadan, S. S., Simedrea, C., Rutt, B. K., MacDonald, I. C., Foster, P. J. and Chambers, A. F.: (2009) '**Three-dimensional imaging and quantification of both solitary cells and metastases in whole mouse liver by magnetic resonance imaging**', In: *Cancer Research*. American Association for Cancer Research, 69(21), pp. 8326–8331. doi: 10.1158/0008-5472.CAN-09-

1496.

Ulmer, A., Fischer, J. R., Schanz, S., Sotlar, K., Breuninger, H., Dietz, K., Fierlbeck, G. and Klein, C. A.: (2005) '**Detection of Melanoma Cells Displaying Multiple Genomic Changes in Histopathologically Negative Sentinel Lymph Nodes**', In: *Clinical Cancer Research*. American Association for Cancer Research, 11(15), pp. 5425–5432. doi: 10.1158/1078-0432.CCR-04-1995.

Wang, E.: (1995) '**Senescent human fibroblasts resist programmed cell death, and failure to suppress bcl2 is involved.**', In: *Cancer research*, 55(11), pp. 2284–92. Available at: http://www.ncbi.nlm.nih.gov/pubmed/7757977 (Accessed: 5 July 2019).

Weidenfeld, K. and Barkan, D.: (2018) '**EMT and Stemness in Tumor Dormancy and Outgrowth: Are They Intertwined Processes?**', In: *Frontiers in Oncology*, 8(381), pp. 1–6. doi: 10.3389/fonc.2018.00381.

Werner-Klein, M., Scheitler, S., Hoffmann, M., Hodak, I., Dietz, K., Lehnert, P., Naimer, V., Polzer, B., Treitschke, S., Werno, C., Markiewicz, A., Weidele, K., Czyz, Z., Hohenleutner, U., Hafner, C., Haferkamp, S., Berneburg, M., Rümmele, P., Ulmer, A. and Klein, C. A.: (2018) '**Genetic alterations driving metastatic colony formation are acquired outside of the primary tumour in melanoma**', In: *Nature communications*, 9(595), pp. 1–17. doi: 10.1038/s41467-017-02674-y.

Winder, M. and Virós, A.: (2018) '**Mechanisms of Drug Resistance in Melanoma**', pp. 91-108, In: Mandalá, M. and Romano, E. (eds) *Mechanisms of Drug Resistance in Cancer Therapy. Handbook of Experimental Pharmacology Volume 249*. Springer, Cham, doi: 10.1007/164_2017_17.

Wu, F.-H., Mu, L., Li, X.-L., Hu, Y.-B., Liu, H., Han, L.-T. and Gong, J.-P.: (2017) '**Characterization and functional analysis of a slow-cycling subpopulation in colorectal cancer enriched by cell cycle inducer combined chemotherapy**', In: *Oncotarget*, 8(45), pp. 78466-78479. doi: 10.18632/oncotarget.19638.

Yang, L., Fang, J. and Chen, J.: (2017) '**Tumor cell senescence response produces aggressive variants**', In: *Cell Death Discovery*, 3(1), pp. 1–11. doi: 10.1038/cddiscovery.2017.49.

Yang, X., Liang, X., Zheng, M. and Tang, Y.: (2018) '**Cellular Phenotype Plasticity in Cancer Dormancy and Metastasis**', In: *Frontiers in Oncology*, 8(505), pp. 1–12. doi: 10.3389/fonc.2018.00505.

Yeh, A. C. and Ramaswamy, S.: (2015) '**Mechanisms of cancer cell dormancy-another hallmark of cancer?**', In: *Cancer Research*, 75(23), pp. 5014–5022. doi: 10.1158/0008-5472.CAN-15-1370.

Zhao, J., Fuhrmann-Stroissnigg, H., Gurkar, A. U., Flores, R. R., Dorronsoro, A.,

Stolz, D. B., St. Croix, C. M., Niedernhofer, L. J. and Robbins, P. D.: (2017) '**Quantitative analysis of cellular senescence in culture and in Vivo**', In: *Current Protocols in Cytometry*, 79, pp. 9.51.1-9.51.25. doi: 10.1002/cpcy.16.

8 Erklärung zum Eigenanteil

Die Arbeit wurde in der Sektion für Dermatologische Onkologie der Universitäts-Hautklinik Tübingen unter Betreuung von Prof. Dr. rer. nat. Birgit Schittek durchgeführt, durch welche zudem die Konzeption der Studie erfolgte.

Sämtliche Versuche wurden nach Einarbeitung durch Birgit Sauer und teilweise nach Rücksprache mit Dr. rer. nat. Corinna Kosnopfel und/oder Birgit Sauer von mir eigenständig durchgeführt.

Die statistische Auswertung erfolgte, ebenfalls nach Rücksprache mit Dr. rer. nat. Corinna Kosnopfel, eigenständig durch mich.

Die primären Fibroblasten (siehe Tabelle 2.1.8) wurden freundlicherweise durch Birgit Sauer isoliert und bereitgestellt.

Die Aufnahme und Bereitstellung ausgewählter Ausschnitte der Fluoreszenz-mikroskopie (siehe Abbildungen 3.2.1-2, 3.2.3-1 und 3.2.3-2) erfolgte durch Birgit Fehrenbacher.

Eine Vorlage zur Regressionskurvenberechnung für die Proteinkonzentrations-bestimmung (siehe Abschnitt 2.2.5.3) wurde mir freundlicherweise durch Dr. rer. nat. Elena Makino bereitgestellt.

Ich versichere, das Manuskript selbständig verfasst zu haben und keine weiteren als die von mir angegebenen Quellen verwendet zu haben.

Tübingen, den

Emanuel Böhlert

9 Danksagung

Zuallererst möchte ich Frau Prof. Dr. rer. nat. Birgit Schittek danken für die durchgehende Betreuung, die Bereitstellung der Laborarbeitsplätze und des hochinteressanten und aktuellen Themas. Dankbar hervorheben möchte ich insbesondere die offene und aktive Unterstützung, meinen Wunsch zu verwirklichen, von meinem bisherigen Studienort nach Tübingen zu wechseln, die maßgebliche Hilfe bei der finanziellen Ermöglichung des Projekts sowie die Einladung und Einbindung in alle wissenschaftlichen und geselligen Veranstaltungen der Arbeitsgruppe.

Ein besonders großer Dank geht an Dr. rer. nat. Corinna Kosnopfel, welche mir - neben ihren eigenen zeitintensiven Projekten - als Mentorin in methodischen und wissenschaftlichen Fragen zur Seite stand und in vielen Situationen weitergeholfen hat.

Während meiner Zeit im Labor hatte ich auch enorme Unterstützung durch alle weiteren KollegInnen der Arbeitsgruppe: Francisco, Bibo, Elena, Heike und Tobias – ihr habt mir das gute Gefühl gegeben, Teil der Gemeinschaft zu sein, mich auf die Kongresse und Events mitgenommen, Vorschläge zur Methodik gemacht, aber vor allem, und zum Glück, auch meine Projektideen und Ergebnisse kritisch hinterfragt. Immer wieder haben mir die verschiedensten Leute in Labor und Klinik geholfen oder einfach die Atmosphäre im oft stressigen Arbeitsalltag beim gemeinsamen Kaffee aufgelockert – auch bei euch möchte ich mich bedanken!

Die finanzielle und ideelle Förderung durch das Mildred-Scheel-Doktorandenprogramm der Deutschen Krebshilfe sowie das IZKF-Promotionskolleg der Universität Tübingen haben mir die Arbeit im Labor und an der Dissertation maßgeblich erleichtert, vielen Dank allen Entscheidungsträgern und Förderern für die Aufnahme meines Projektes in das jeweilige Programm.

Zu großem Dank verpflichtet bin ich meiner Familie: meinen Eltern und Geschwistern, meiner Tochter Anouk Magdalena und der Familie Ellner, die in Gesprächen und gemeinsam verbrachter Zeit einen wichtigen Ausgleich geschaffen und mich in jeder Lebenslage unterstützt haben.